STRENGTH OF SENSITIVE CLAY UNDER CYCLIC LOADING

KHALID JAVED

A Thesis

In

THE DEPARTMENT OF BUILDING, CIVIL AND ENVIRONMENTAL ENGINEERING

Presented in Partial Fulfillment of the Requirements

For the Degree of Master in Applied Science

CONCORDIA UNIVERSITY

Montreal, Quebec, Canada

August 2002

Khalid Javed, 2002

National Library of Canada
Acquisitions and Bibliographic Services
395 Wellington Street
Ottawa ON K1A 0N4
Canada

Bibliothèque nationale du Canada
Acquisitions et services bibliographiques
395, rue Wellington
Ottawa ON K1A 0N4
Canada

Your file Votre référence

Our file Notre référence

The author has granted a non-exclusive licence allowing the National Library of Canada to reproduce, loan, distribute or sell copies of this thesis in microform, paper or electronic formats.

L'auteur a accordé une licence non exclusive permettant à la Bibliothèque nationale du Canada de reproduire, prêter, distribuer ou vendre des copies de cette thèse sous la forme de microfiche/film, de reproduction sur papier ou sur format électronique.

The author retains ownership of the copyright in this thesis. Neither the thesis nor substantial extracts from it may be printed or otherwise reproduced without the author's permission.

L'auteur conserve la propriété du droit d'auteur qui protège cette thèse. Ni la thèse ni des extraits substantiels de celle-ci ne doivent être imprimés ou autrement reproduits sans son autorisation.

0-612-82659-7

Canada

ABSTRACT

Sensitive clay is a kind of clay, which loses its shear strength when it is subjected to cyclic loading. High-rise buildings, towers, bridges etc., founded on sensitive clays usually suffer from reduction of the safety factor during its life span. Cyclic loading on foundation of sensitive clay during the undrained period may lead to quick clay condition and a catastrophic failure of the structure. In the literature, governing parameters such as cyclic deviator stress, pore water pressure, axial strain, pre-consolidation pressure, confining stress, initial degree of saturation, water content, liquidity index and the number of cycles are divided into two categories and then presented as a function of sensitivity. Nevertheless the limited data available has restricted the use of empirical formulae. It is of interest to note that sensitive clay's shear strength increases due to consolidation and decreases due to cyclic load. In this case, the pre-consolidation pressure plays the role of governing parameter. In this investigation, the experimental results available at Concordia University as well as the data available in literature will be used to evaluate the empirical formulae and models. The governing parameters will be evaluated on this basis. Based on this analysis, a procedure to assist practicing engineers in designing foundation on sensitive clay is proposed.

Acknowledgement

I owe my most sincere gratitude to Al-mighty Allah who has been the source of my entire initiative and accomplishment required to fulfill this stupendous task.

My most fervent thanks are due to my mother whose prayers enabled me to see this day.

I pray to Allah for my late father Abdul Shakur to grant him paradise and elevate his level in the life hereafter. He was a competent civil engineer and a man-of-peace. Whatever achievements I have in my life are the result of his training.

The entire credit of the accomplishment of this research goes to Prof. Dr. Adel Hanna, my thesis director, whose technical guidance and deep involvement, personal interest and untiring assistance enabled me to present this work today.

My acknowledgement would not be complete unless I mention here the services and financial assistance provided to me by Concordia University, which enabled me to finish this work without any worries.

I am also thankful to my wife and kids for unexhausted support and encouragement.

TABLE OF CONTENTS

LIST OF TABLES

LIST OF FIGURES

Page No.

LIST OF SYMBOLS

$(T_{fc})_N$	Strength Ratio at the Given number of Cycles
A and B	Skempton Pore Water Pressure Parameters
a	Attraction
a	Hyodo's Model Constant
c_L	Shear Strength at Liquid Limit
c_p	Shear Strength at Plastic Limit
c_u'	Modified Undrained Static Shear Strength
c_u	Undrained Static Shear Strength
c_u	Undrained Undisturbed Shear Strength
c_{ur}	Undrained Remolded Shear Strength
c_v	Co-efficient of Consolidation
e	Deviatoric Strain Tensor in Modified Cam Clay Model
e	Void Ratio
e_f	Final Void Ratio
e_o	Initial Void Ratio
F	Factor of Safety
f	Frequency in Hz
G	Shear Modulus
G_s	Specific Gravity of Soil Particles
H	Length of Drainage

h	Hour
I_L	Liquidity Index
I_p	Plasticity Index
k	Constant for Describing Variation in Sensitivity
k	Fatigue Parameter
k	Material Constant
LL	Liquid Limit
M	Clay Parameter
m	Slope of the Pore Pressure Line
N	Number of Cycles
N_y	Number of Cycles to Yield
P	Effective Pressure
p	Material Constant
p'	Mean Effective Normal Stress
p_c	Consolidation Pressure (at the start of the test)
p_f	Final Effective Stress
PI	Plasticity Index
PL	Plastic Limit
p_o	Drained Virgin Pressure
p_o	Undrained Virgin Pressure
p_u	Undrained Virgin Pressure
q	Deviator Stress
q_f	Final Deviator Stress

R	Ratio between c_p and c_L
S	Degree of Saturation
s	Deviatoric Stress Tensor in Cam Clay Model
S	Shear Stress Level
S_t	Sensitivity
T	Dimensionless Time Factor ($T = T_{50}$)
T	Peak Cyclic Strength Ratio
T_{fc}	Strength at the End of Cyclic Loading
t	Time Corresponding to the Particular Degree of Consolidation
u	Pore Water Pressure
u^+	Pore Water Pressure generated by Cyclic loading
u_p	Permanent pore Water Pressure
u_{st}	Static Pore Water Pressure
w	Natural Water Content
w.c	Natural Water Content
w_L	Liquid Limit
w_n	Natural Water Content
w_p	Plastic Limit
Δe	Change in Void Ratio
ΔH	Change in the Height of a Soil Sample During Consolidation Test
Δu	Change in Pore Pressure
ϑ	Lode Angle
Λ	Parameter of the Cam Clay Model

α	A parameter of the Modified Cam Clay Model
ε	Axial Strain
ε	Strain Tensor
ε_p	Peak Axial Strain
ϕ	Angle of Friction
γ	Maximum Single Amplitude Shear Strain
γ_{st}	Shear Strain due to Initial Static Shear Stress
γ_y	Maximum Single Amplitude Shear Strain at Failure
η	Stress Ratio
η^*	Relative Effective Stress Ratio
η_f	Final Effective Stress Ratio
η_p	Peak Effective Stress Ratio
η_s	Initial Effective Stress Ratio
κ	Gradient of Swelling Line
λ	Gradient of Virgin Consolidation Line
σ'	Effective Stress
σ'	Pre-consolidation Pressure
σ^*	Equivalent Vertical Effective Stress
σ_c'	Effective Confining Pressure
σ_d	Deviator Stress
σ'_{vc}	Vertical Effective Stress Pressure
$\sigma_1, \sigma_2, \sigma_3$	Principal Stresses

τ	Cyclic Shear strength
τ_c	Cyclic Shear Strength
τ_{cyc}	Cyclic Shear Stress
τ_f	Maximum Cyclic Shear Strength
τ_{st}	Static Shear Strength
τ_{tot}	Total Shear Strength
υ	Specific Volume
υ_1	Virgin Volume at Unit Pressure
υ_l	Virgin Line Volume
υ_s	Volume for a Specific Swelling Line

CHAPTER 1

INTRODUCTION

1.1 Preface

Sensitive clay is a type of clay, which displays a considerable decrease in shear strength when it is remolded. This property of clays is called sensitivity. Terzaghi (1944) was the first who gave the quantitative measure of the sensitivity as a ratio of peak undisturbed shear strength to remolded shear strength. The sensitivity for normal clays is usually between 1 to 4. Clays with sensitivities between 4 and 8 are referred to as sensitive and those with sensitivities between 8 and 16 are defined as highly sensitive. Clays having sensitivities greater than 16 are called quick clays (Craig, 1978). Sensitive clays occur in many parts of the world such as eastern Canada, Norway, Sweden, the coastal region of India and south East Asia. It challenges geo-technical engineers with specific problems concerning stability, settlement, and the predictions of soil response behavior. High rise buildings, towers, bridges etc., founded on sensitive clays usually suffer from reduction of the safety factor during its life span. Cyclic loading of wind, waves, ice and snow accumulation, earthquakes and other live loads cause cyclic stresses in the foundations of structures, which may lead to quick clay condition and catastrophic failure. Tall flexible structures such as chimneys and long-span bridges are usually subjected to dynamic oscillations under wind loading which amplify the static wind forces. Structures supporting traveling machinery such as radar antenna, cranes and large telescopes, etc. transmit significant cyclic loads to their foundations. Storage facilities such as: silos and

oil tanks transmit very high foundation stresses when full and much lower stresses when empty.

Cyclic loading causes a remolding action that helps the available water in the soil to dissolve away the salts, which results in the change of soil structure and compaction. Figure 1.1 shows how a sensitive clay structure, which is called a house of cards, changes after this remolding action. Hence, this causes a loss in shear strength of the soil and results in slippage, down-slope or liquefaction.

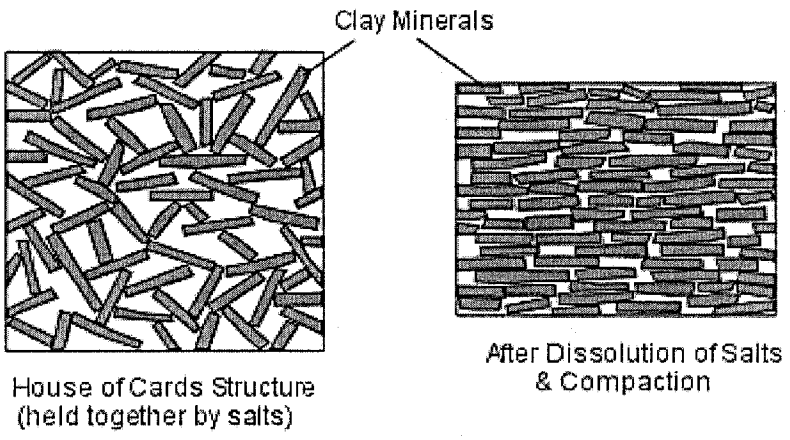

Figure 1.1 Sensitive Clay Structure before and after Remolding

Due to cyclic loading the pore water pressure increases until quick clay conditions. This increase in pore water pressure under cyclic loading usually depends on the initial state of stress, the cyclic stress level, and the magnitude of the cyclic stress increment. The work of Lebuis et al (1983), Locat (1997) and Leroueil and Locat (1998) clearly relates the liquidity index to cyclic mobility of sensitive clays and hence, indicating that the liquidity index as a good predictor of the rheological properties such as the yield strength and the viscosity for these clays.

In the present investigation, the experimental results available at Concordia University as well as the data available in literature will be used to evaluate the empirical

formulae, models and governing parameters. Based on this analysis, a design procedure to assist practicing engineers in designing foundations on sensitive clay is proposed.

1.2 Brief Background of Sensitive Clays

Observations about the distribution of the so-called "sensitive clays" indicate that they are mostly made of material which consist of rock flour eroded from metamorphic terrain. For example, at the St. Lawrence Lowlands, the Champlain Sea clays are found over a wide area. This basin is limited to the south by the Appalachian Mountains and to the north by the Laurentian Plateau. Most of the highly sensitive clays' behavior (i.e. typical mudflow) is found along the foothills of the Laurentian Plateau (see Figure 1.2).

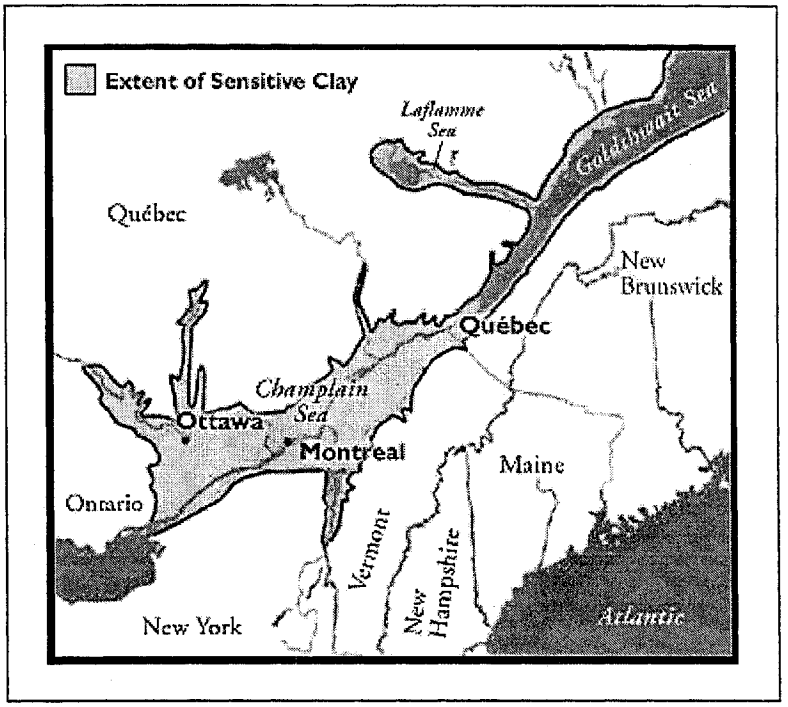

Figure 1.2: Extent of Sensitive Clay Soils: Ottawa and St. Lawrence River Lowlands (Loacat, J., 1995)

Champlain clay deposits are nearly or completely saturated with natural moisture contents close to or in excess of their respective liquid limits. High initial moisture contents are considered to result from the marine depositional environment and it is generally accepted that the existence of some forms of chemical bonding explain the existence of high void ratios in combination with high apparent pre-consolidation pressures. These Champlain clays have sensitivities varying from 6 to even more than 30 and might be considered susceptible to remolding under repeated loading. Hence these deposits prove to be excellent for studying the cyclic loading behavior of clays with varying sensitivities. From the work of Quigley (1980), Torrance (1983) and Locat (1995) it is clear that the conditions for this high level of sensitivity are due to processes like meta-stable fabric, cementation, weathering, thixotropic hardening, formation or addition of dispersing agents, leaching, ion exchange and changes in monovalent/divalent cation ratio. The geo-technical properties of these sensitive clays are the result of these processes.

CHAPTER 2

LITERATURE REVIEW

Early investigations on sensitive clays were focused on conducting experimental work, the triaxial tests on undisturbed and remolded clay for the purpose of developing relationship between cyclic stress-strain and pore water pressure (Seed and Chan 1966, Theirs and Seed (1968, 1969), Sangrey 1968, Sangrey et al 1969, France and Sangrey 1977 and Sangrey et al 1978). Their study established the fact that cyclic loading increases the pore water pressure under undrained conditions up to a number of cycle, which defined as a critical level beyond which the failure will occur. Nevertheless the results are limited to the conditions of the experimental work, and accordingly, the validity of the empirical formulae is questionable. Mitchell and King (1977) have conducted similar investigations. However, in addition to the above, they have reported that the higher the initial confining stress and over-consolidation pressure, the higher the number of cycles needed to reach failure.

Iwaski et al. (1978) conducted the experimental studies and showed that each load cycle is accompanied by a change in shear strain, some of which is partly recoverable. The magnitude of recoverable strain remains fairly constant during each cycle, while the irrecoverable or plastic strain developed during each successive cycle tends to reduce with an increase of the number of cycles. Eventually, the soil attains a form of equilibrium for that particular loading pattern, and the magnitude of the recoverable strain experienced during any cycle greatly exceeds the plastic strain increment for that cycle, hence, defining quasi-elastic or resilient state. The study also

established that the resilient stiffness of soil is stress level dependent and is also dependent on the magnitude of resilient shear strain.

Eekelen and Potts, (1978) performed static tests on Drammen clay samples. They used a modified Cam Clay Model not only to determine the static strength of the clay but also to determine the reduction in strength at the end of a given number of cyclic loading. A summary of the Modified Cam Clay Model used by them is given in the following section.

For an element of clay which is subjected to slow, perfectly drained hydrostatic compression, moves along a trajectory in υ–ln p plane which consists of two straight lines (Figure 2.1). The equation for swelling line (SL) and virgin consolidation line (VCL) are given as:

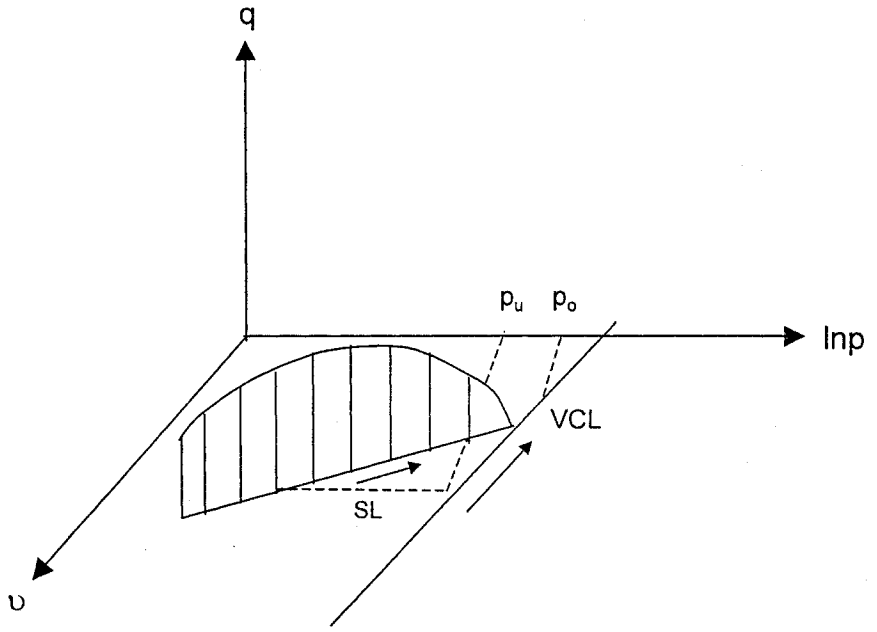

Figure 2.1: Consolidation and Yield of Modified Cam Clay

Eekelen and Potts, (1978)

$$\upsilon + \kappa \ lnp = \upsilon_s \text{ (swelling line, SL)} \qquad 2.1$$

$$\upsilon + \lambda \ lnp = \upsilon_l \text{ (virgin consolidation line, VCL)} \qquad 2.2$$

Where: υ = specific volume, κ = gradient of swelling lines, υ_s = volume for each swelling line (SL), λ = gradient of VCL, υ_l= virgin volume at unit pressure, p = effective hydrostatic static stress and q = deviator stress. For a stable state boundary surface (SSBS) the model gives the following relationship:

$$q^2 - M^2 p^2 (\frac{p_o}{p} - 1) = 0 \qquad 2.3$$

where M is a clay parameter, and p_o is the drained virgin pressure or pre-consolidation pressure (see Figure 2.1). For critical or failure state the following equation is used in the Modified Cam Clay Model:

$$p_f = \frac{1}{2^{\Lambda}} p_u = \left(\frac{1}{2} p_o\right)^{\Lambda} (p_c)^{1-\Lambda} \qquad 2.4$$

where p_f is the consolidation pressure at failure, p_u is the undrained pressure, p_o the preconsolidation pressure, and p_c the consolidation pressure at the start of the static test. Eekelen and Potts (1978), proposed an attraction factor 'a' and replaced p and p_u by $(p+ a)$ and $(p_u+ a)$, and gave the following equation for critical state as:

$$p_f + a = \left(1 - \frac{1}{2\Lambda}\right)^{\Lambda} (p_u + a) = \left(1 - \frac{1}{2\Lambda_o}\right)^{\Lambda} \left[(p_o)^{\Lambda} (p_c)^{1-\Lambda} + a\right) \qquad 2.5$$

which gives lower values of p and q at failure than equation 2.4. For the relationship between the strain-hardening parameter (S) and the plastic shear strain (ε^{pl}) Eekelen and Potts (1978) gave the following relationship:

$$\varepsilon^{pl}\sqrt{3} = \alpha \frac{S}{1-S} \qquad 2.6$$

where α is constant. For general static loading they gave the following equation:

$$S = \frac{M(p+a)}{(2+M/3)\cos\vartheta + (M/\sqrt{3})\sin\vartheta} \qquad 2.7$$

where ϑ is the lode angle, for which the value in triaxial compression is -30°. In the three dimensional principal stress space the surface $S=1$ is a hexagonal cone (see Figure 2.2), the locus of the points which satisfy the 'Mohr-Coulomb criterion. For maximum shear stress (τ_f) the relationship is given as:

$$\frac{\tau_f}{s+a} = \frac{M}{2+M/3} \equiv \sin\phi \qquad 2.8$$

where $\tau_f = \frac{1}{2}(\sigma_1 - \sigma_3)$ is the maximum shear stress, and $s = \frac{1}{2}(\sigma_1 + \sigma_3)$ is the mean of the largest and the smallest principal stress. The hexagonal cone $S=1$ is called the Mohr-Coulomb or MC cone. Cone and cap intersect along the hexagon with $p=p_f$ given by equation 2.13, illustrated in Figure 2.2 for a particular value of specific volume (υ). For static strength (T_f) the model gives the following equation:

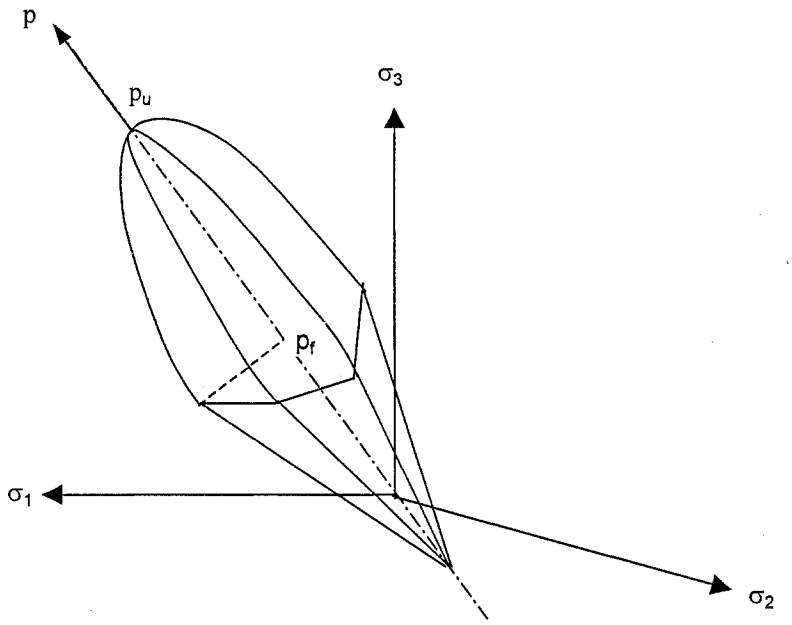

Figure: 2.2 Stable State Boundary Surface (SSBS) in Three Dimensions for One Particular Value of Specific Volume (υ)

Eekelen and Potts, (1978)

$$T_f = b(\, p_u + a) = b(\, p_o^{\Lambda} p_c^{1-\Lambda} + a) \qquad 2.9$$

where;

$$b = \left(1 - \frac{1}{2\Lambda}\right)^{\Lambda} \frac{M}{(2 + M/3)\cos\vartheta + (M/\sqrt{3})\sin\vartheta} \qquad 2.10$$

The angle ϑ in b is the Lode angle at failure, which is -30° for triaxial compression, $+30^{\circ}$ for triaxial extension, and 0° for simple shear. Eekelen and Potts (1978) incorporated the concept given by Eekelen (1977) in terms of one single state parameter called 'fatigue' in order to give the relationship of cyclic shear strength (T_{fc}) at the end of cyclic loading as:

$$T_{fc} = b\left[p_u (1 - \frac{u^+}{p_c})^{\kappa/\lambda} + a \right] \qquad 2.11$$

where u^+ is the pore water pressure generated at the end of cyclic loading.

Chagnon et al (1979) conducted field and laboratory investigations about the sensitive clays in eastern areas of Canada, i.e., in the province of Quebec. They suggested solutions for various engineering geology problems related to these clays in light of these field and laboratory investigations. Table 2.1 gives the summary of their investigations.

Table 2.1 Summary of Field and Laboratory Investigations (Chagnon et al 1979)

Group No.	Water content w (%)	Liquid limit L.L (%)	Plastic Limit P.L (%)	Undrained Shear Strength Remolded $(cu)_r$ kPa	Sensitivity S_t	Salt (g/l)
1	72.5-70	71-67	45-42.5	2.3-1.5	8.5-5.5	-
2	47-10	32-9.9	22-2.9	0.19-0.11	310-140	0.43-0.24
3	57-9.7	42-11	24-3.3	0.87-0.57	59-27	0.57-0.54
4	57-14.8	53-13.9	26-4.3	3.6-3.1	12-4.2	0.73-0.13
5	57-11.2	52-15.5	27-4	5.5-0.35	11-6.2	17-9.20

Shaw (1980) conducted a study on the same lines as by Iwaski et al (1978). His study shows that during cyclic triaxial testing on uniform crushed limestone, a small negligible permanent strain occurs during each individual cycle; but over a large number of load

permanent strain occurs during each individual cycle; but over a large number of load applications, the magnitude of accumulated permanent strain may be quite significant.

Houstan and Hermann (1980) conducted an experimental investigation on seven marine soils namely: Atlantic Calcareous Ooze, Reconstitute Atlantic Calcareous Ooze, Pacific Calcarreous Ooze, Pacific Hemi Pelagic, Atlantic Hemi Pelagic, Pacific Pelagic Clay and San Francisco Bay Mud. The object of their study was to quantify the undrained response of seafloor soils to various combinations of static and cyclic loading. The average sensitivity (S_t) of all the clays tested was 3 or less than 3 except for San Francisco Bay Mud, which had 8, the highest of all. Figure 2.3 shows the cyclic failure data of the Bay Mud for 0% static bias (percentage of initial deviator stress) and 40% static bias. In comparison to the other soils, the cyclic failure data of bay Mud shows highest resistance to cyclic loading. The results of Figure 2.3 were cross plotted to obtain cyclic strength contours shown in Figure 2.4. The width of the zone indicates the range of uncertainty associated with the cross-plotting operation.

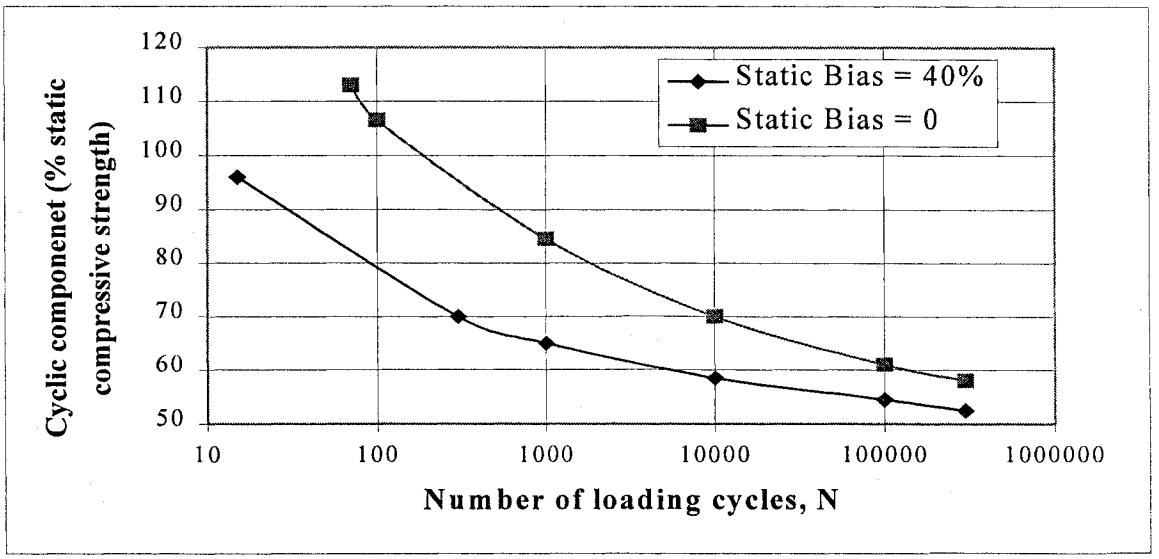

Figure 2.3: Cyclic Failure Data for San Francisco Bay Mud (Houstan and Hermann, 1979)

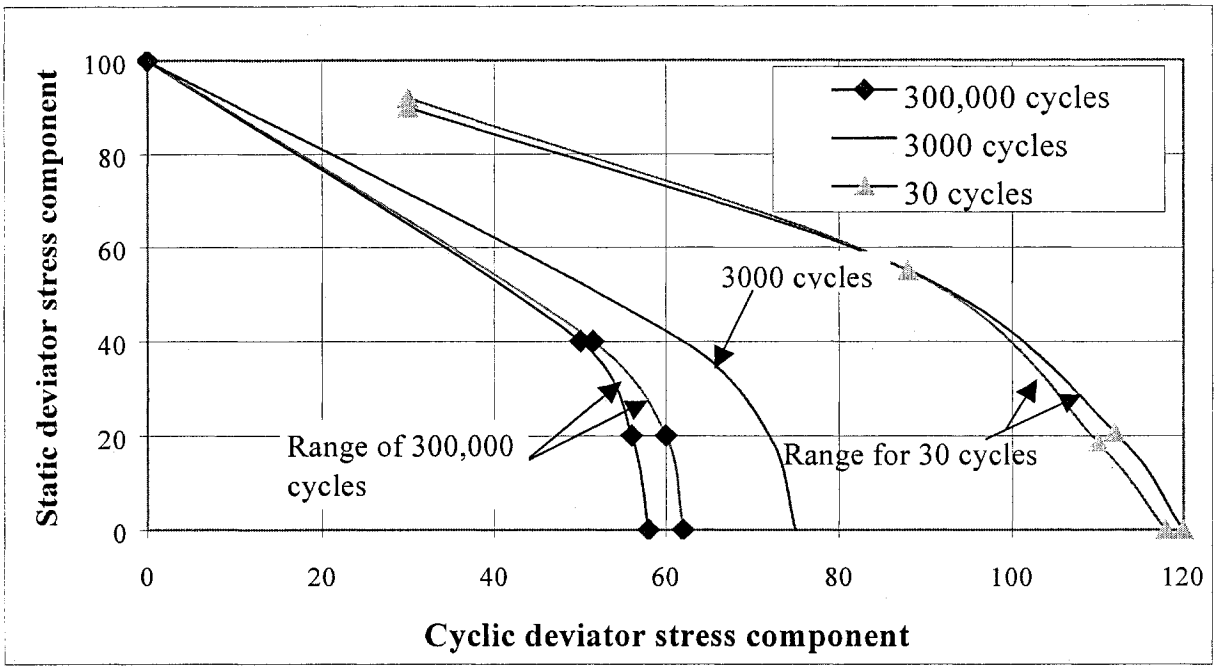

Figure 2.4: Cyclic Strength Contours for San Francisco Bay Mud (Houstan & Hermann, 1979)

Table 2.2 Cyclic Strength as Function of Plasticity (Houstan and Hermann, 1979)

Cyclic Component for 3,000-Cycle Contour					
	At pure stress reversal (Static Bias = 0)		At boundary between stress reversal and no stress reversal		Plasticity index (%)
Soil	Static Compressive strength (%)	Absolute value, in kg/sq.cm	Static Compressive strength (%)	Absolute value, in kg/sq.cm	
Atlantic Calcareous Ooze c_u = 0.493 –0.629 kg/sq. cm Sensitivity (S_t) <=3	5	0.056	22	0.25	Non-plastic

Table 2.2 continued

Reconstitute Atlantic Calcareous Ooze c_u = 0.115 –0.124 kg/sq. cm Sensitivity (S_t) <=3	12	0.029	22	0.053	Non-plastic
Pacific Calcareous Ooze c_u = 0.196 kg/sq. cm Sensitivity (S_t) <=3	22	0.086	30	0.12	Non-plastic
Pacific Hemi-Pelagic c_u = 0.133 –0.158 kg/sq. cm Sensitivity (S_t) <=3	38	0.116	45	0.14	20-32
Atlantic Hemi-Pelagic c_u = 0.152 –0..154 kg/sq. cm Sensitivity (S_t) <=3	46	0.134	-	-	16-37
Pacific Pelagic-Clay c_u = 0.127 –0..128 kg/sq. cm Sensitivity (S_t) <=3	74	0.188	58	0.15	42-74
San Franciso Bay Mud c_u = 0.111 –0.134 kg/sq. cm Sensitivity (S_t) >=8	75	0.184	51	0.125	45-58

Three contours were established for this soil, the combination of static and cyclic stresses required to cause failure at 30 cycles, 3,000 cycles and 300,000 cycles of loading. Based on this cyclic strength contour analysis, Houstan and Hermann (1980) showed that cyclic strength of clays can be expressed as a function of plasticity. The important thing is that study is based on static, cyclic loading and also on the combination of static and cyclic loading which usually happens in practical problems. Except in a few cases, all other foundations of civil engineering structures are based on the combination of static and cyclic loading. Furthermore, the study confirms the quasi-elastic resilient state defined by Iwaski et al (1978). The most interesting part of the study is that it established an interesting relationship between cyclic strength and plasticity index, and in Table 2.1 it is shown that the cyclic strength is a function of plasticity. The close comparison of Pacific pelagic Clay and San Francisco Bay Mud reveals some important clues related to the present study. Although the Pacific Pelagic Clay may have slightly higher average plasticity, the Bay Mud has the higher sensitivity (S_t =8) and has maximum static compressive strength at pure stress reversal. On the other hand sensitivity can not be used instead of plasticity. Literature review shows that in the case of Norwegian quick clays, the leaching process that is believed to make the clays quick (Chapter-1) also reduces the plasticity.

Matsui et al (1980) conducted experimental study on the shear characteristics of clays with respect to cyclic stress-strain history and its corresponding pore pressures. A Senri clay remolded specimen was used in the study, having water content greater than the liquid limit. Results of the study clarified the effect of loading frequency, effective confining pressure, cyclic stress level and over-consolidation ratio on the excess pore pressure during cyclic loading. The study indicated that over-consolidation clay due to cyclic stress-strain history is similar in

strength to an ordinary over-consolidation history and that, in spite of the temporary loss in shear strength and deformation modulus immediately after cyclic loading, the dissipation of pore pressure leads to higher strength than the initial strength.

Seed and Idris (1982) studied the effects of cyclic frequency. They concluded that the faster the rate of cycling the more the situation resembles undrained conditions. The study also pointed out the situation, which arises when pore pressures simultaneously accumulate as a result of continued cyclic loading and dissipate along the gradients of excessive pore pressures.

Procter and Khaffaf (1984) studied the weakening behavior of undrained saturated remolded samples of Derwent Clay subjected to cyclic loading. They used the study of Craig (1982) "Strain Rate and Viscous Effects in Physical Models" to compare the frequency response of cyclic shear stress ratio (τ/c_u) to frequency response of modified cyclic shear stress ratio (τ/c^-_u) causing 5% double amplitude strain. Figure 2.5 shows the ratio of static shear strengths (c^-_u/c_u) versus strain rate from which the modified shear strength (c^-_u) relevant to a given load controlled cyclic strain contour is determined on the basis of a mean strain rate equal to $2 * \varepsilon_{da} * f$, where ε_{da} is mean double amplitude axial strain peak to peak and f is the frequency of cyclic loading in hertz (Hz). Figure 2.6(a) and 2.6(b) show the frequency response of cyclic shear stress ratio (τ/c_u) and frequency response of modified cyclic stress ratio (τ/c^-_u) causing 5% double amplitude strain. Figure 2.6(a) shows that a frequency change from 1/120 Hz to 1 Hz causes approximately a 30% increase in cyclic stress ratio (τ/c_u) within the limit $10 \leq N \leq 5000$, where N = number of cycles. Figure 2.6(b) shows the reanalyzed data of Figure 2.6(a) by using a modified shear stress ratio (τ/c^-_u), where the modified shear strength ratio (c^-_u) is obtained by using Figure 2.5. The Figure

2.6(b) gives an idea that the final weakened conditions of all the samples tested were similar and independent of frequency variation.

The study of Procter and Khaffaf (1984) gives an idea that if data from load controlled tests are reanalyzed to account for rate effects on shear strength, then a constant value independent of frequency is obtained as shown in Figure 2.6(b). Furthermore, the fully weakened state for the soil tested can be achieved in a single displacement controlled test provided that 10,000 cycles at mean double amplitude strain of at least 5% are applied. Figures 2.6(a) and 2.6(b) show that irrespective of data reanalysis, the minimum cyclic stress ratio measured in single amplitude is constant for frequencies less than 1/5 Hz.

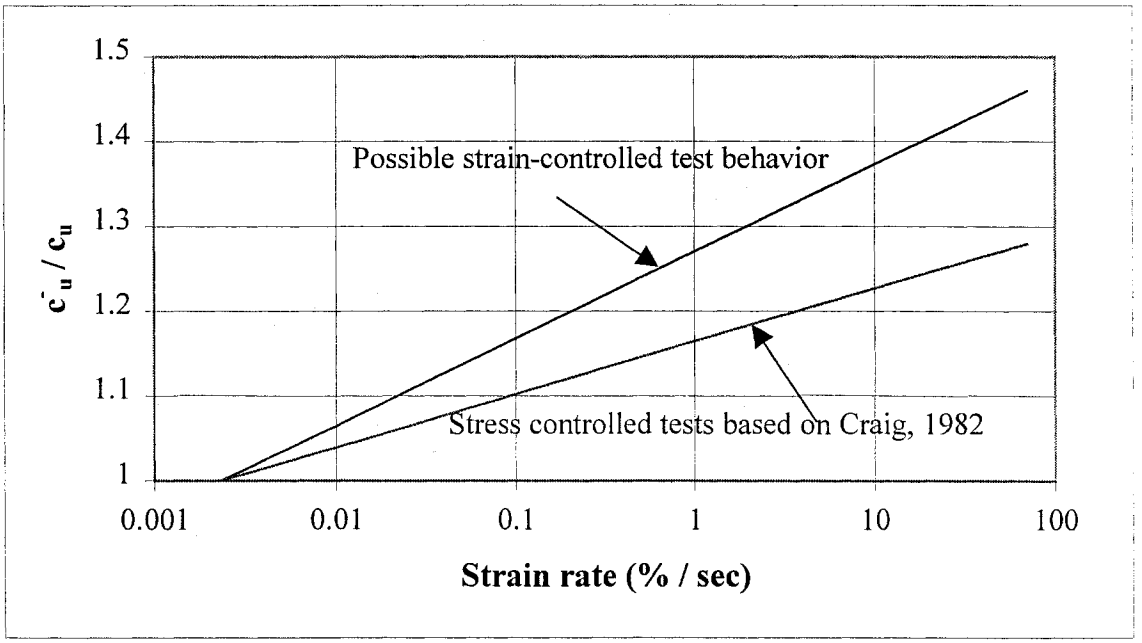

Figure 2.5: Ratio of Modified to Static Shear Strengths Versus Strain Rate (Procter and Khaffaf, 1984)

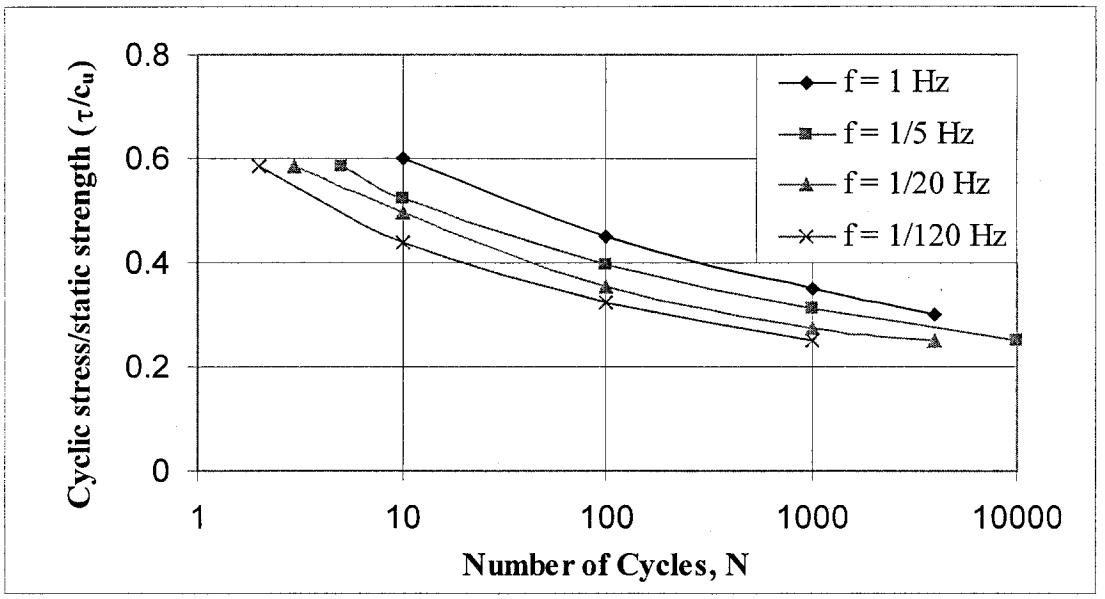

Figure 2.6(a): Frequency Response of Cyclic Stress Ratio (τ/c_u)

(Procter and Khaffaf, 1984)

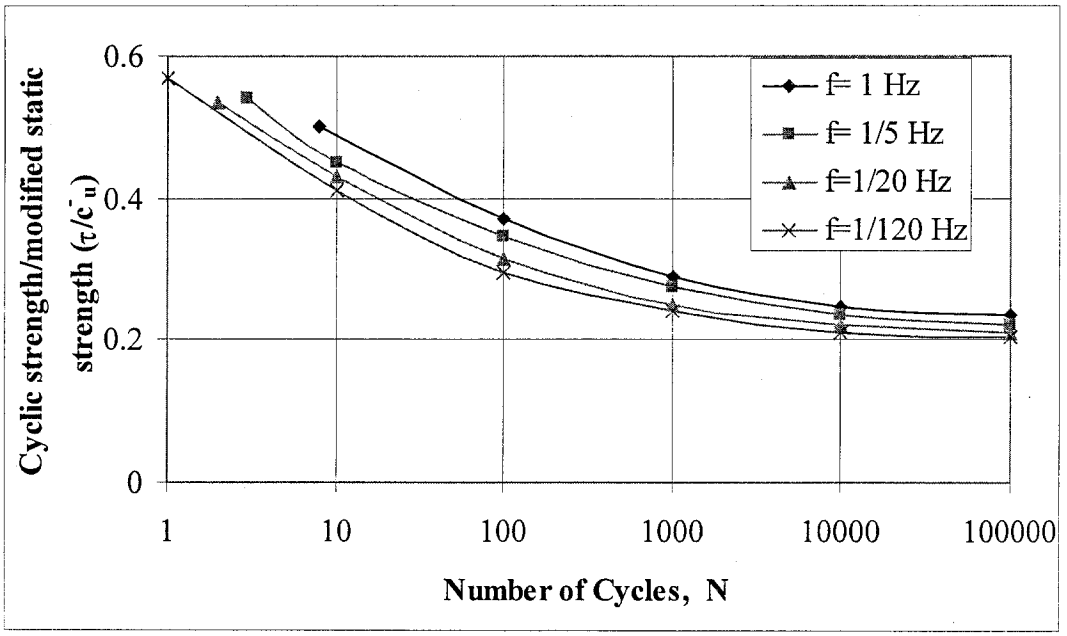

Figure 2.6(b): Frequency Response of Modified Cyclic Stress Ratio (τ/c^-_u)

(Procter and Khaffaf, 1984)

Lefebyre and leBoeuf (1987) conducted a series of monotonic and cyclic triaxial tests to study the influence of the rate of strain and load cycles on the undrained shear strength of three undisturbed sensitive clays from Eastern Canada. These tests were carried out at the Universite' de Sherbrooke, Quebec, Canada. Table 2.3 shows the general properties of these investigated soils. For each clay, two distinct series of tests were carried out, one on naturally over-consolidated clays or undisturbed samples and the other on remolded specimens. Results show that for structured clay, strain rate as high as 15% can be used for degree of pore pressure equalization of about 95% due to a very low compressibility. On the other hand, for the same degree of equalization, the calculated strain rate of remolded clay is about 1%/h. Figure 2.7 shows the undrained shear strength measured for the undisturbed and remolded specimens at different strain rates, normalized by the undrained shear strength measured at a strain rate of 1%/h and plotted against the log of the strain rate.

Table 2.3: General Properties of Investigated Soils

(Lefebyre and leBoeuf 1987)

Location	Depth (m)	Natural water content w (%)	Liquid limit w_l	Plastic limit w_p	Plasticity Index I_p	Liquidity Index I_l	< 2μm	Sensitivity S_t	Pre-consolidation pressure σ'_p
Dyke-12	-	54-65	33.5	21.8	11.7	2.84	59	>300	112
Dyke-39	-	35-52	27	20.0	7.0	2.85	45	500	190
Olga	4	90-93	68	28	40	1.55	90	-	78
B6	6.8	50	38	24	14	1.80	76	100	145
B6	10.1	48	32.5	22.3	10.1	2.47	75.7	450	175
St. Jean	-	42	36	20	16	1.38	50	100	940

The data shown in Figure 2.7 shows that there is a very narrow boundary, which indicates a linear relationship between the normalized shear strength ratio and the strain rate. Furthermore, the study indicated that the strain rate effect on undrained shear strength ratio appears to be the same for both undisturbed and remolded specimens. Based on all test analyses the study concludes that for naturally consolidated clays, pore pressure generated at a given deviator stress are essentially independent of the strain rate, while the peak shear strength envelope is lowered as the strain rate is decreased.

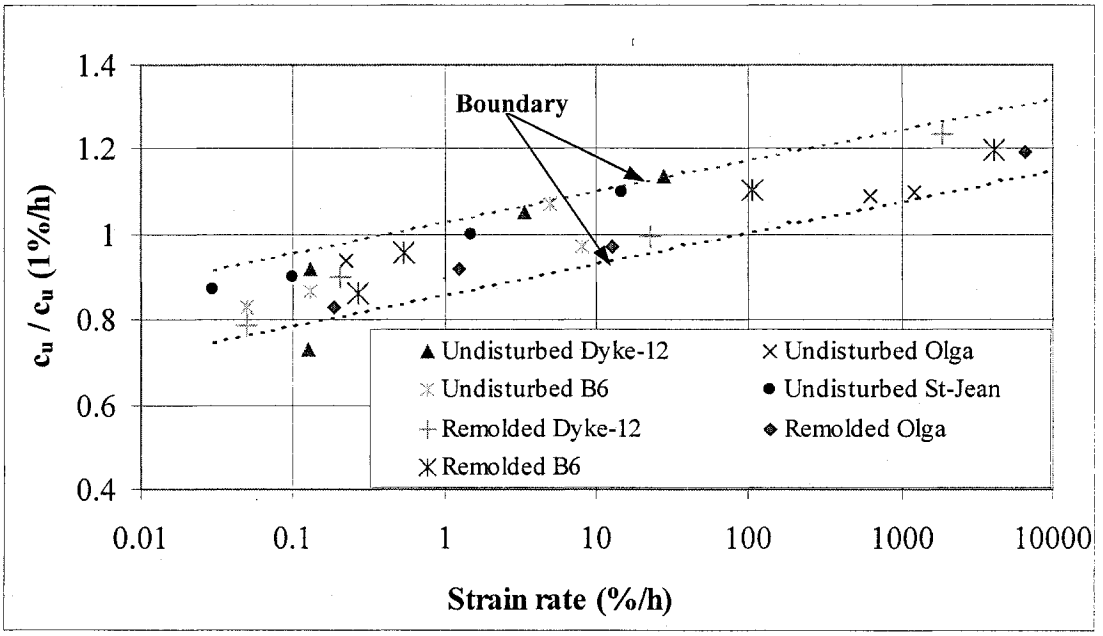

Figure 2.7: Change of Undrained Strength Ratio, Normalized to Undrained Strength Ratio at Strain Rate for all Investigated Clays (Lefebyre and LeBoeuf, 1987)

For normally consolidated clay, a lower strain rate results in an increase in pore pressure generation during shearing due to the tendency of the clay skeleton to creep, while the peak shear strength envelope remains the same. It should be noted that the clays tested in this study were

highly sensitive, suggesting that there is no big difference in the shear stress ratio if these clays are tested at a consolidation pressure greater or less than the historical pre-consolidation pressure (see table 2.3)

Ansal and Erken (1989) made an experimental investigation on the cyclic behavior of normally consolidated clays by using cyclic simple shear tests on one-dimensionally and isotropically consolidated kaolinite samples. As a result of their investigation, they developed an empirical model to estimate the response of a soil element subjected to cyclic shear stresses for a given number of cycles. Figure 2.8 shows the results of variation of cyclic shear stress ratio $(\tau/\tau_f)_y$ with respect to the number of cycles, N.

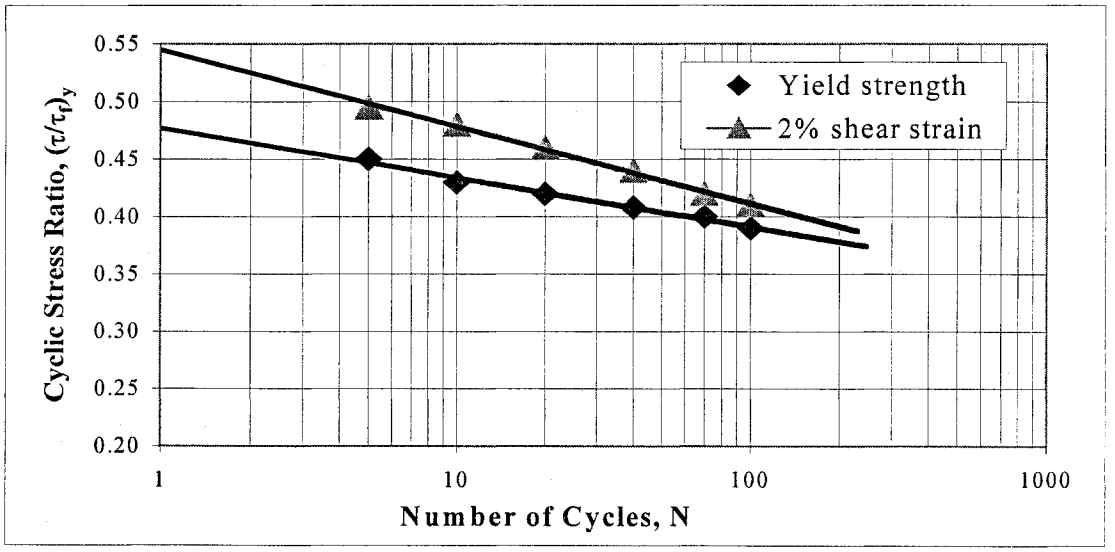

Figure 2.8: Cyclic Yield Strength Versus Number of Cycles (Ansal and Erken, 1989)

The linear relationship between the cyclic shear stress ratio $(\tau/\tau_f)_y$ and the number of cycles (N) shown in Figure 2.8 is as follows:

$$\left(\frac{\tau}{\tau_f}\right)_y = a - b \log N \qquad 2.12$$

where $(\tau/\tau_f)_y$ = cyclic shear strength ratio; N = the number of cycles; and a and b = material constants obtained from linear regression analysis. The figure also shows that, for any specified cyclic shear strain amplitude (2%) taken as the upper allowable limit for a specific design purpose, the same approach can be used. The results of the study also indicated that for normally consolidated clays there is a critical shear stress ratio level or a threshold cyclic shear stress ratio below, which no pore pressure will develop, as shown in Figure 2.9.

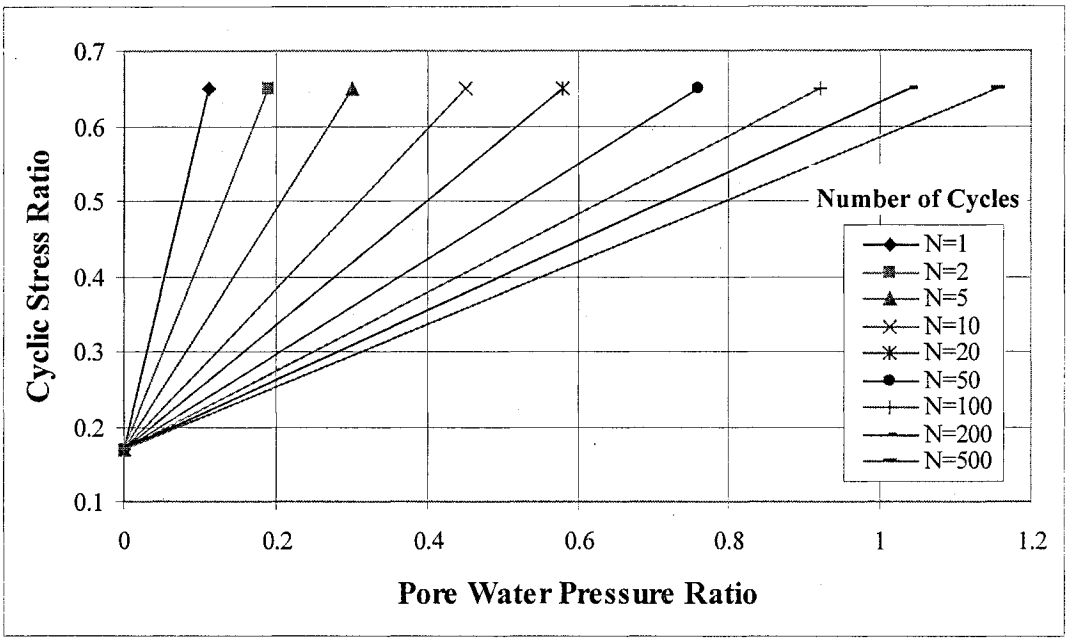

Figure 2.9: Cyclic Stress Ratio-Pore Pressure Relationship for Different Number of Cycles (Ansal and Erken, 1989)

The study also defines the variation of the slope of the pore pressure lines with respect to the number of cycles. Figure 2.10 gives a relationship between the slope of pore water pressure lines and the number of cycles as follows:

$$u = \left[\frac{\tau}{\tau_f} - (S.R)_t \right] m \qquad 2.13$$

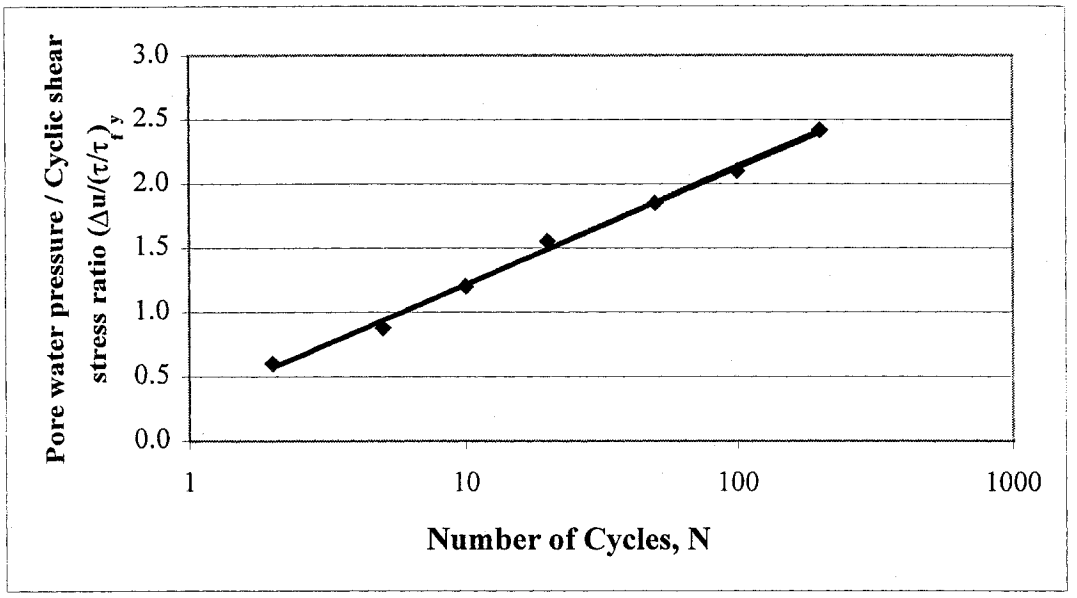

Figure 2.10: Slope of Pore Water pressure lines Versus Number of Cycles (Ansal and Erken, 1989)

$$m = k + p \log N \qquad 2.14$$

where m = the slope of the pore pressure line $\Delta u/\Delta(\tau/\tau_f)$; N = the number of cycles; k and p = material constants obtained from the regression analysis; and $(S.R)_t$ is the threshold cyclic shear stress ratio. Based on their experimental study, Ansal and Erken also found that the influence of frequency can be neglected in problems such as offshore platforms where the number of cycles

with respect to wave action will be large. The study also indicates that cyclic behavior of normally consolidated clay, as in the case of natural deposits, is similar to those for completely remolded clay samples. Tests show that remolded samples appear to be more resistant to cyclic shear stresses; cyclic shear strain amplitude developed in these tests (remolded samples) are smaller in comparison to cyclic shear strains measured in one-dimensionally consolidated samples. However, the pore pressure is higher in the case of remolded samples. Figure 2.11(a) and Figure 2.11(b) show the comparison of the shear strain and the pore water pressure behavior of one–dimensionally consolidated and remolded samples.

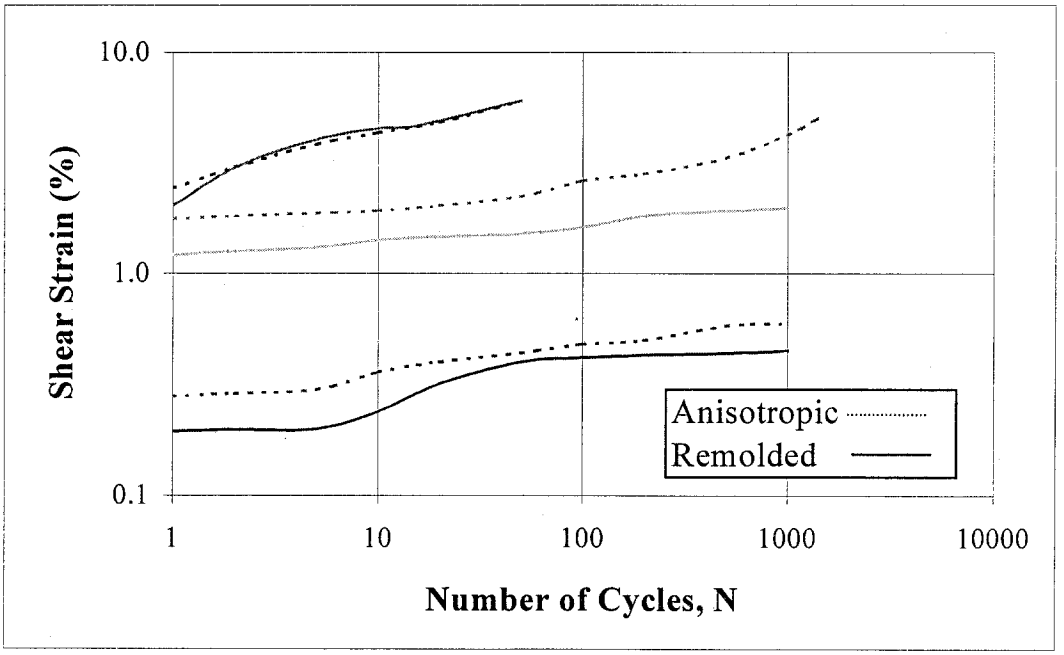

2.11(a): Comparison of Figure Shear Strain of One-Dimensionally Consolidated and Remolded Samples (Ansal and Erken, 1989)

The results of this study confirm the early studies done by Sangrey et al. (1969) except that the pore pressure accumulation behavior observed by Ansal and Erken (1989) for normally consolidated clay. The clay, as observed by Ansal and Erken (1989), is a bit different; however.

The results correlate with the study of Matsui et al (1980), where a similar threshold cyclic shear stress level was observed. Furthermore, based on their experimental results, Ansal and Erken (1989) give a three equation empirical model. Although the model seems to be simple and useful in predicting shear stress ratio corresponding to a specific strain, it is based on only a simple shear test and on only one type of one-dimensionally and isotropically consolidated kaolinite clay.

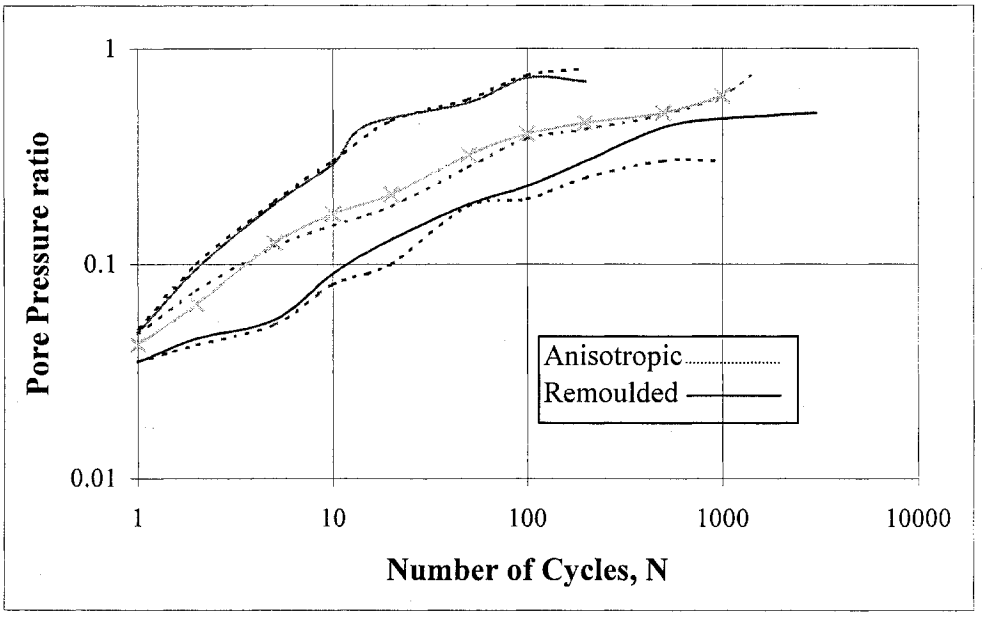

Figure 2.11(b): Comparison of Pore Water Pressure of One-Dimensionally Consolidated and Remolded Samples (Ansal and Erken, 1989)

Wood (1990) analyzed the data collected by Skempton and Northey (1953) for studying the effect of liquidity index on the undrained shear strength of sensitive clays from various parts of the world. His study shows a clear trend of increasing sensitivity with increasing liquidity index (I_L) as shown in Figure 2.12. He used the relationship given by Bejerrum (1954) for the

Norwegian clays as follows:

$$S_t = exp(kI_L) \qquad 2.15$$

where k is a constant describing variation in sensitivity with liquidity. A value of $k \sim 2$ provides a reasonable fit. This implies a sensitivity $S_t \sim 7.4$ for a clay approximately at its liquid limit ($w = w_L$, $I_L = 1$). Based on his analysis, he established the relationship between the liquidity index and the undrained shear strength of the sensitive clays as shown in Figure 2.13. He assigned strengths of 2 kPa and 200 kPa for the shear strength of the soils at their liquid and plastic limits respectively, (see Figure 2.13) and gave a relationship between the remolded strength of the soils solely based on the liquidity index:

$$c_u = c_L R exp[(k - lnR)I_L] \qquad 2.16$$

where c_u = undrained shear strength, c_L = shear strength at liquid limit, R= ratio between shear strength at plastic limit (c_P) and shear strength at liquid limit (c_L), I_L = liquidity index and k = constant describing the variation in sensitivity.

Furthermore, he found that, in the case of undrained shear strength, the Mohr circle of effective stress at failure point F (Figure 2.14) can be associated with an infinite number of possible stress circles ($T_1, T_2, \ldots\ldots$) displaced along the normal stress axis by an amount equal to the pore pressure. The pore pressure does not affect the differences of the stresses or shear stresses, so all stress circles must have the same size especially in case of clay soils, which are usually loaded fast to avoid the drainage of shear-induced pore pressures.

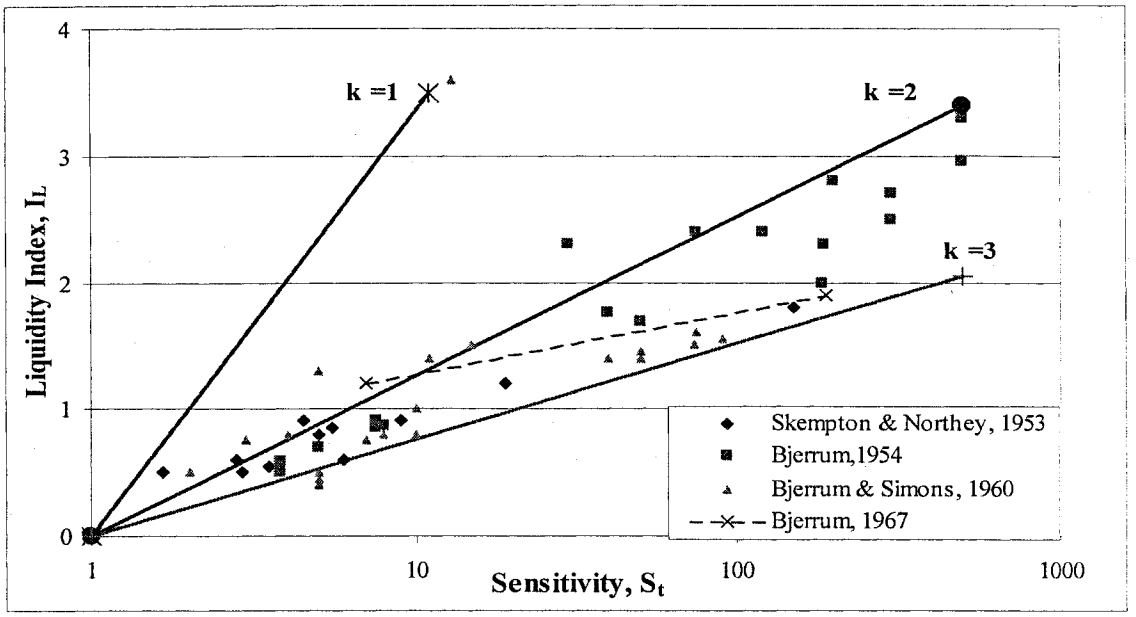

Figure 2.12: Interrelationship between Sensitivity and Liquidity Index for Natural Clays (Wood, 1990)

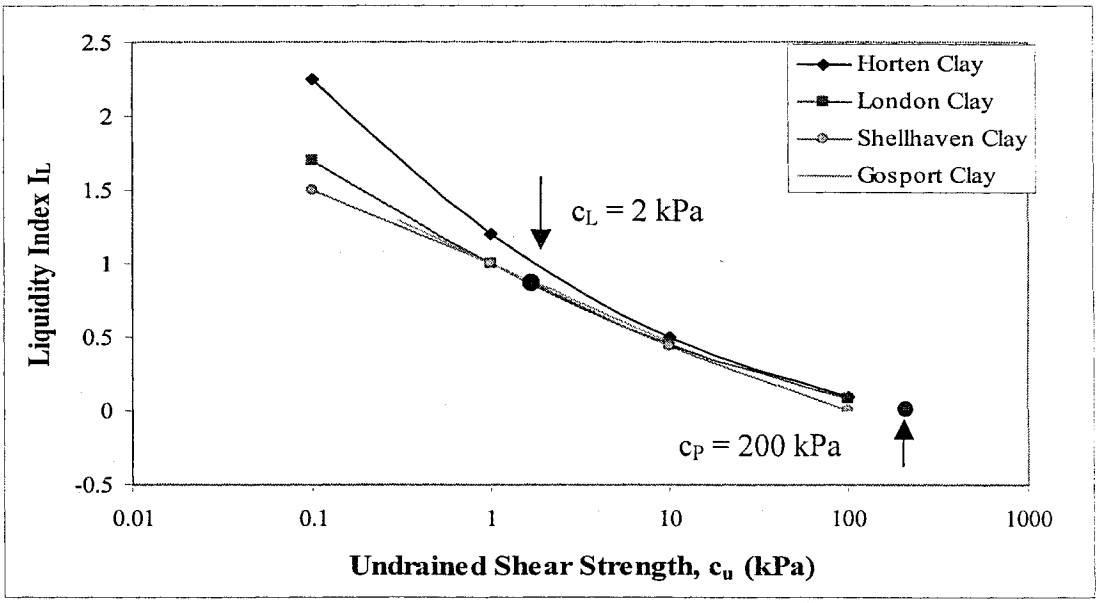

Figure 2.13: Variation of Remolded Undrained Strength c_u with Liquidity Index I_L (Wood, 1990)

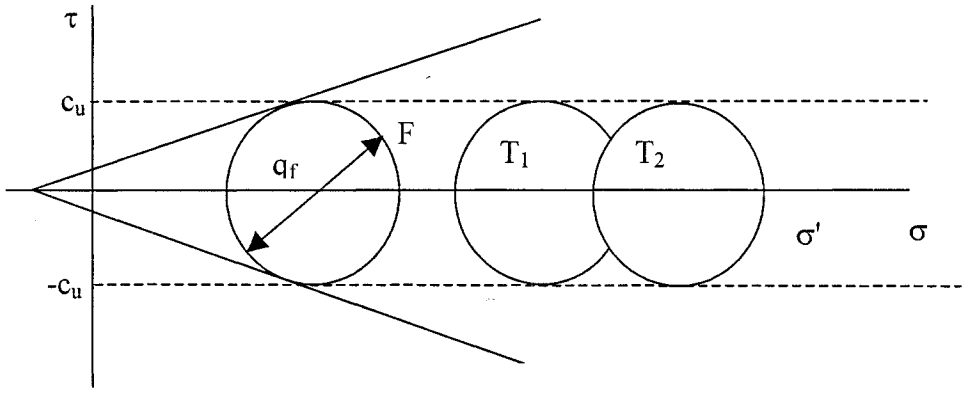

Figure 2.14: Mohr's Circles of Total Stress and Effective Stress

Wood (1990) proposed that it is more desirable to mention maximum shear stress (τ_f) in terms of undrained shear strength (c_u), which is the radius of all the Mohr circles in Figure 2.14. Therefore, the maximum shear stress that a clay soil can withstand and the failure criterion for undrained conditions becomes:

$$\tau_f = \pm c_u \qquad 2.17$$

O' Reilly et al (1991) presented a soil model which takes into account the complexity of stress conditions in the soil beneath structures subjected to a combination of static and cyclic loads. Figure 2.15 shows the model's simplified stress conditions for some soil elements (1, 2, 3 and 4) along a potential failure surface.

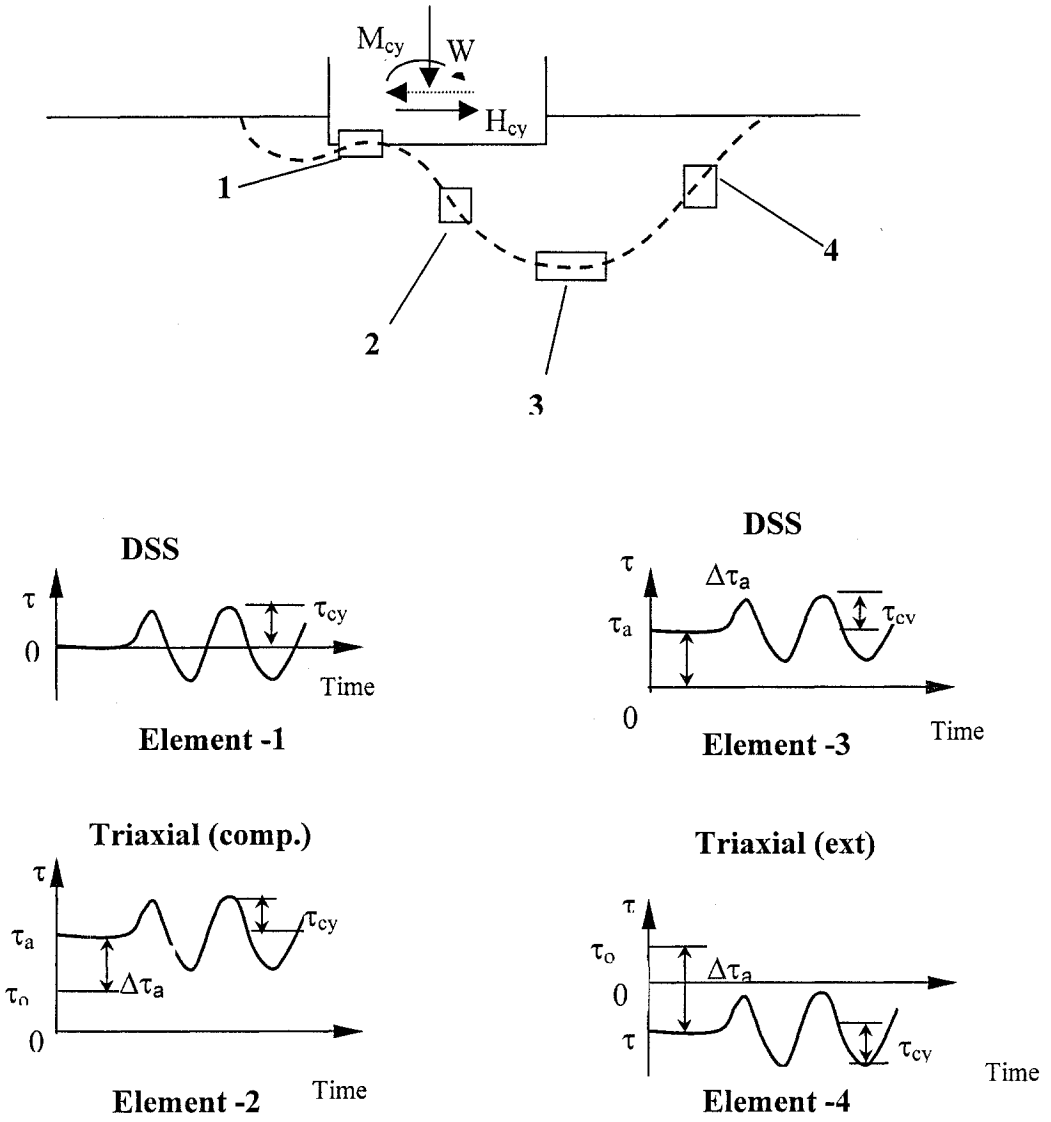

Figure 2.15: Simplified Stress Conditions for some Elements along a Potential Failure Surface (Reilly and Brown, 1991)

In the Figure, W= weight of the platform, H_{cy} = horizontal shear stress, M_{cy} = stresses due to wind load or other cyclic loading., DSS = direct simple shear test, τ = shear stress, τ_{cy} = cyclic shear stress, τ_a = average shear stress, τ_o = initial shear stress prior to the installation of platform and $\Delta\tau_a$ = additional shear stress induced by the submerged weight of the platform. The model stated that these elements (1,2,3 and 4) follow various stress paths which may be approximated to a triaxial or a direct shear type of loading, and they are subjected to various combinations of average shear stresses (τ_a) and cyclic shear stresses (τ_{cy}). The average shear stress (τ_a) is composed of the initial shear stress (τ_o) and additional shear stress ($\Delta\tau_a$). The model shows that in the case of element 2, the weight of the platform a gives a higher vertical than horizontal static normal stress hence, during cyclic loading, element 2 will tend to compress vertically. Element 4 is in the passive zone, and the weight of the platform causes a higher horizontal than vertical static normal stress, element 4 will, therefore, tend to compress horizontally and extend vertically during the application of cyclic loading. Consequently, element 2 is best represented by a triaxial compression test and element 4 by a triaxial extension test. The model also shows that for elements 1 and 3 the shear surface will be horizontal. Therefore, these elements are best represented by direct simple shear (DSS) tests, and these tests should be run to establish the shear strength on the horizontal plane, i.e., the horizontal shear stress at failure. Hence, the study emphasizes that since both the shear strength and the deformation properties of soils under cyclic loading are anisotropic, therefore, the triaxial compression, the triaxial extension and the DSS tests should be included in the laboratory test program for gravity structure of some importance. It should also be noted that the model depicts the importance of the actual conditions of stresses in the field, which are usually the combination of static and cyclic loading.

Liang and Ma (1992) developed and verified a constitutive model for the stress strain-pore pressure behavior of fluid-saturated cohesive soils. The model adopts the joint invariant of the second order stress tensor and clay fabric tensor as a formalism to account for material anisotropy. The model includes three internal variables: the density hardening variable representing changes in void ratio; the rotational hardening variable depicting fabric ellipsoid changes; and finally, the distortional hardening variable controlling the shape of the bounding surface. The concept of quasi-pre-consolidation pressure was used in formulating an internal variable for the isotropic density hardening. For evolutionary laws based on micro-mechanics and phenomenological observations, Liang and Ma (1992) constitutive model gives the relationships for isotropic density hardening and anisotropic or rotational hardening in drained conditions. The model considers two counter part mechanisms for the evolution of distortional hardening (R). One mechanism is that the bounding surface will widen along with the clay fabric moving to preferred orientations, meaning that a smaller value of R permits lower pore water pressure response. The other one is that the bounding surface will flatten along with the loading involving the principal stress rotation, meaning a larger value for R causes a sharper pore water pressure response. For un-drained conditions the model assumes that both water and clay particles are compressible which means a zero volumetric strain. The predictive capability of the model is tested on a database created from the available literature. The results show that the model is quite capable of predicting the behavior of saturated clays subjected to undrained cyclic loading, such as degradation of undrained strength and stiffness, accumulation of permanent strain and pore pressure, influence of initial consolidation conditions, and the effect of rotation of principal stress direction.

Wathugala and Desai (1993) modified hierarchical single surface (HiSS) models into a modified series of models (termed as δ^*) which could capture the behavior of cohesive soils. These models consider monotonic loading as virgin loading and unloading and reloading as non-virgin loading. An associated (δ_o) model of the series was found to be sufficient for predicting the cyclic behavior of clays. The model defines a new hardening function based on that the normally consolidated (NC) clays that do not dilate; and instead they show a contractive response under monotonic loading. The model considers the unloading phase as elastic and reloading similar to virgin loading with some modification like a plastic modulus for virgin loading is replaced by a plastic modulus of reloading and a unit normal tensor is replaced by a unit normal tensor for a reference surface (R) which passes through the current stress point in the stress space. The results show that the model is capable of capturing the undrained shear behavior of normally consolidated clay, slightly over-consolidated clay behavior and drained behavior during hydrostatic compression tests and stress-strain behavior during cyclic loadings.

Hydo et al (1993) proposed a semi-empirical model for the evaluation of developing residual shear strain during cyclic loading. The model considers 10% peak axial strain as a failure criterion in both reversal and non-reversal regions and gives a relationship between the cyclic deviator stress ratio and the number of cycles required to cause failure for each initial static deviator stress (q_s). The unified cyclic shear strength is given by:

$$R_f = \left\{(q_{cyc} + q_s)/p_c\right\}_f = \kappa N^{\beta} \qquad 2.18$$

where R_f = cyclic strength ratio; q_{cyc} = cyclic deviator stress; q_s = initial deviator stress; p_c = constant mean principal stress; N = number of cycles; $\kappa = 1.0+1.5q_s/q_c$ and $\beta = -0.088$.

The peak axial strains ε_p from all tests were related using an effective stress ratio:

$$\varepsilon_p = \eta_p/(2.0-\eta_p) \qquad 2.19$$

where η_p = peak deviator stress divided by mean effective principal stress of each peak to peak cyclic stress (q_s / p).

In order to introduce the undrained cyclic behavior of clay, two parameters were introduced in the model. The first parameter defined is an index (R/R_f) showing the possibility of cyclic failure, which is the ratio of peak cyclic deviator stress ($R = q_s + q_{cyc}$) to cyclic shear strength (R_f) in a given number of cycles. R/R_f is termed as a cyclic shear strength ratio and is equivalent to a reciprocal of the safety factor against cyclic failure. When the magnitude of R is constant, R/R_f increases with the increasing number of cycles and carries from zero at non-loading to unity at failure. The second parameter in the model is defined as:

$$\eta^* = (\eta_p - \eta_s)/(\eta_f - \eta_s) \qquad 2.20$$

where η_p is an effective stress ratio at the peak cyclic stress in each cycle, η_s is the effective stress ratio of initially consolidated condition, η_f = effective stress ratio at the failure, and η^* = the relative effective stress ratio between initial point and final point in p-q space as shown in Figure 2.16.

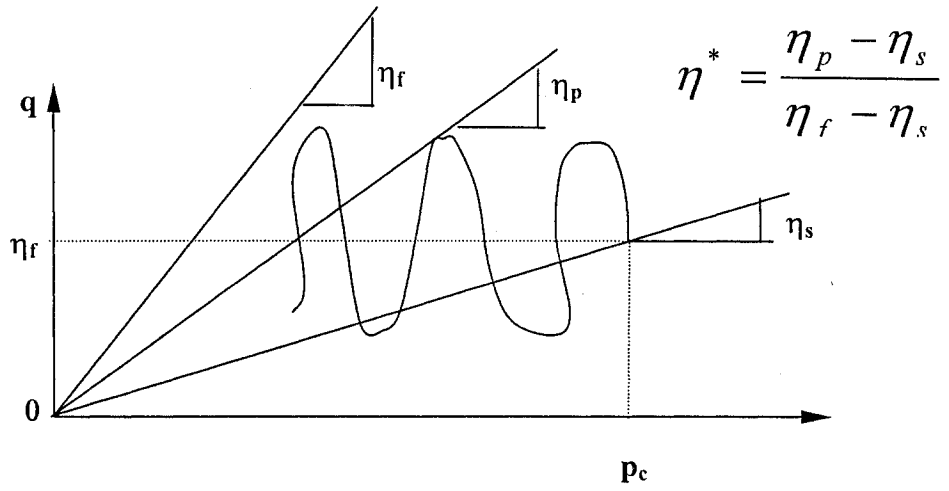

Figure 2.16: Schematic Diagram for Relative Effective Stress Ratio (Hyodo and Sugiyama , 1993)

These parameters were originally introduced for sand by Hyodo et al (1991). By correlating the values of both parameters, the model establishes a simple but useful relationship between the accumulated peak axial strain and the effective stress ratio. The best fit curve for each relation is given by a unique curve formulated as the following equation in spite of the difference of initial static and subsequent cyclic deviator stresses:

$$\eta^* = R/R_f/\{a - (a-1)R/R_f\} \qquad 2.21.$$

where the value of "a" is given as 6.5 by the experiments of Hyodo and Suiyama (1993).

McManus and Kulhway (1993) studied the behavior of cyclic loading of drilled shafts in laboratory-made cohesive soil (Cornell Clay). The applied loading was designed to simulate realistic windstorm events (both one-way and two-way loading), which is an important source of cyclic loading for foundations. Results show that for one-way uplift loading, the upward

displacement accumulated by a drilled shaft was not found to be affected by either the size or the geometry of the model-drilled shafts or by the soil deposit stress history. In case of two-way loading, the direction of loading reverses twice every cycle causing minimal response at low load levels but a sudden degradation in displacement response at moderate load levels, with an associated substantial reduction in capacity.

Bardet (1995) extended the novel concept of scaled memory (SM) model to anisotropic behavior and presented a technique to calibrate the material constants from laboratory data. He showed that SM generalizes closed stress-strain loops and, therefore, avoids the artificial rachetting predicted by bounding surface plasticity. The extended SM model generalizes Ramberg-Osgood and Hardin Drenvich models and is simpler than, but as capable as, multiple yield surface plasticity.

Puzrin et al (1995) showed the consistency of normalized simple shear behavior of soft clays with the Masing rules. The study reveals that the degradation of soil properties in undrained simple shear is considered to be the main reason for deviation of cyclic shear behavior of soft clays from the pattern described by the Masing rules. Using the mean effective stress as a single fatigue parameter, it was found possible to describe this degradation in terms of Iwan's series-parallel model which leads to the concept of a non-degrading, normalized backbone curve. The results of the study also prove that the set of slip stresses degrade proportionally to the decrease in the mean effective stress, whereas the small strain shear modulus appears to be invariant to changes in this stress. The study also reveals that by using the mean effective stress as a single fatigue parameter, it would be possible to describe degradation in terms of the parameters of Iwan's series-parallel model, which leads to the concept of a nondegrading, normalized backbone

curve.

Lefebvre and Pfendler (1996) studied the results of the cyclic constant volume direct simple shear (DSS) on intact specimens of sensitive clay obtained at the St. Alban site in the St. Lawrence valley, 80 km west of Quebec City, Canada. The results of their tests are summarized in Table 2.4. In this table, c_u = monotonic undrained shear strength; I_p = plasticity index; N = number of cycles; N_y = number of cycles at failure; S_t = sensitivity to remolding; w = water content; w_L = liquid limit; w_p = plastic limit; γ = maximum single amplitude shear strain; γ_{st} = shear strain due to initial static shear stress; γ_y = maximum single-amplitude shear strain at failure; σ'_p = pre-consolidation stress; σ'_{vc} = vertical consolidation stress; τ_c = cyclic shear stress; τ_{st} = initial static shear stress; and τ_{tot} = total shear stress. The study shows that the shear strength of intact sensitive clay degrades fairly rapidly with the number of cycles when there is no initial static shear stress as shown in Figure 2.17. However, the shape of the τc/Cu versus N curves indicates a lesser degradation of the cyclic strength with the number of cycles when there is an initial static shear stress as shown in Figure 2.18. The study indicates that at a strain rate equivalent to a 0.1-Hz cyclic loading, the sensitive clay tested in this study can mobilize an undrained shear strength, which is about 40% higher than that determined at a standard strain rate, which is equivalent to a 12% increase per log cycle of the strain rate.

Table 2.4: Results of Cyclic Constant Volume Direct Simple Shear Test (Lefebvre and Pfendler, 1996)

w=56%, LL =41%, PL =21%, I_p=20%, Sensitivity (S_t)=300, σ'_p= 83kPa, c_u=20.6kPa										
							N			
S. No.	σ'_{vc}	τ_{st}/c_u	γ_{st}	τ_c/c_u	τ_{tot}/c_u	τ_{tot}/σ'_p	$\gamma = 3\%$	$\gamma = 5\%$	N_y	γ_y
	kPa									(%)
1	36.9	0	0	0.55	0.55	0.1365	770	790	690	1.7
2	36.9	0	0	0.64	0.64	0.15883	255	270	228	2.1
3	37.1	0	0	0.68	0.68	0.1688	245	260	220	2.1
4	35.7	0	0	0.71	0.71	0.17637	59	63	50	2.1
5	33.9	0	0	0.81	0.81	0.20116	39	46.5	35	2.6
6	35.6	0	0	0.85	0.85	0.2110	26.5	32	22.5	2.5
7	35.5	0	0	0.86	0.86	0.21356	29	33.5	24.5	2.3
8	36.9	0	0	0.98	0.98	0.243	16	21	15.5	2.9
9	36.9	0	0	1.03	1.03	0.2556	4.3	11	10	4.5
10	36.6	0	0	1.28	1.28	0.3177	1.4	3.1	2.6	4.3
11	36.9	0	0	1.35	1.35	0.3351	0.8	1.9	1.7	4.1
12	38.3	0.31	0.28	0.92	1.23	0.3053	17.5	30	28.2	3.9
13	38	0.3	0.17	1.03	1.33	0.3301	2.5	7	7.7	5
14	42.4	0.31	0.22	1.06	1.37	0.3400	0.2	0.9	7	5.1
15	37.9	0.32	0.22	1.23	1.55	0.3847	0.2	2	3.9	6.2
16	35.6	0.52	1.14	0.63	1.15	0.285422	2.2	19	34.5	6
17	37.1	0.5	0.36	0.84	1.34	0.332578	4.1	8	9	4.5
18	37	0.51	0.43	1	1.51	0.374771	0.1	0.3	1.6	7.7
19	37.9	0.72	0.79	0.59	1.31	0.325133	2.7	9.6	9.6	5
20	38.1	0.71	0.74	0.69	1.4	0.34747	2.8	6.4	6.4	5
21	37.9	0.79	1.33	0.39	1.18	0.292867	15	81	81	5
22	36.9	0.8	1.5	0.46	1.26	0.312723	0.2	2.1	2.8	5.7
23	42.4	0.82	1.05	0.49	1.31	0.325133	5.7	14	12	4.3
24	37.9	0.79	1.5	0.57	1.36	0.337542	0.1	1.1	2	6.1

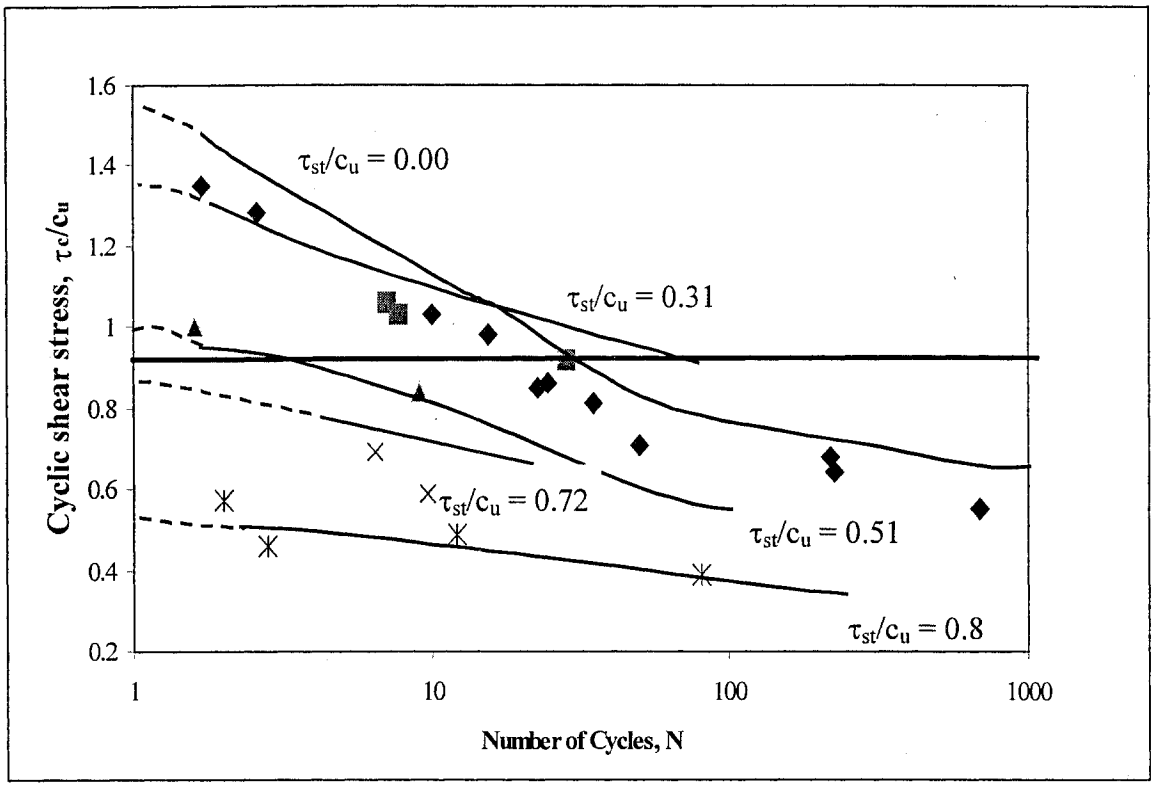

Figure 2.17: Cyclic Shear Stress as Function of Number of Cycles for Initial State Shear Stresses of 0 to 0.8 (Lefebvre and Pfendler, 1996)

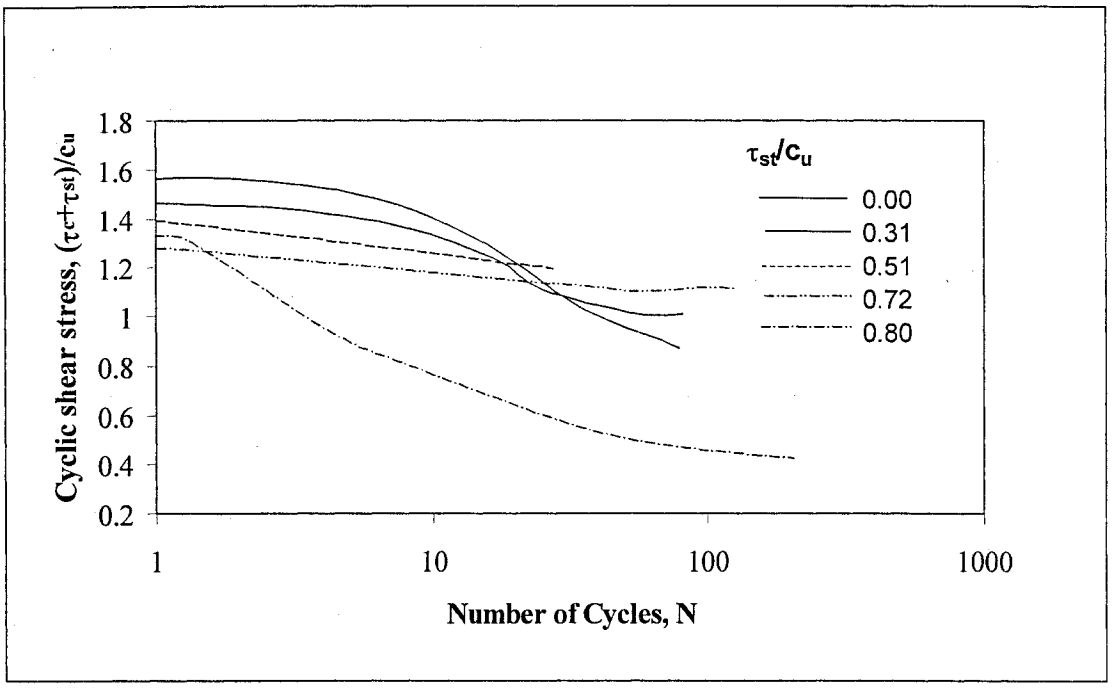

Figure 2.18: Total Undrained Shear Stress as Function of Number of Cycles for InitialStatic Shear Stresses of 0 to 0.8 (Lefebvre and Pfendler, 1996)

The study also proves that, in cyclic tests, the high-strain-rate effect partially compensates for shear strength degradation with the number of cycles in such a way that, at 12 cycles, the cyclic shear strength can be taken as equal to the undrained shear strength determined in monotonic tests at standard rates. Thus, confirming the results of one of the previous studies using triaxial tests tests on another sensitive clay (Lefebvre and LeBoeuf 1987).

Faker et al (1999) studied the behavior of super soft clays, which usually have a water content higher than their liquid limits. The study proposes that a rotary viscometer should be used to measure the yield stress of the super soft clays instead of using a conventional soil mechanics apparatus. By plotting the results of yield stress measurements of soft clays in terms of w/LL, it

could be shown that the true liquid limit is 1.5 – 2 times that which is arbitrarily selected and measured by the established conventional methods. The results of the study also show the variation in shear stress with respect to the liquidity index (Figure 2.19).

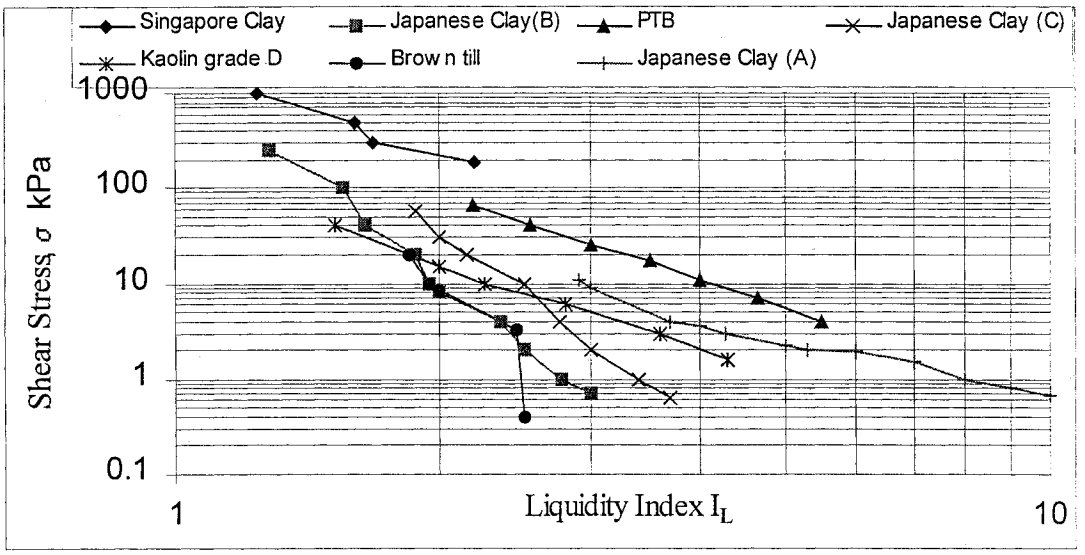

Figure 2.19: Variation in Shear Stress with respect to Liquidity Index (Faker et al, 1999)

Furthermore, it is indicated that the logarithmic of the yield stress of soft clay normalized with respect to the equivalent effective vertical stress (σ^*) on the intrinsic compression line (ICL) is linearly related to the ratio of water content to liquid limit (w/LL) for all clays in the study, and that the lines for each soil are parallel.

Miller et al (2000) studied the behavior of soft compacted clayey soil (used in railroad subgrade) subjected to repeated loading under train traffic. Cyclic triaxial tests were conducted on tube samples at their natural water content (partially drained) and on samples subjected to back-pressure saturation (undrained). The study indicates that, for repeatedly loaded soils, a

critical cyclic stress or normalized cyclic shear strength exists above which the soil will exhibit shear failure. For the highly plastic clay tested, the normalized cyclic shear strength was sensitive to the initial degree of saturation in the relatively narrow range encountered, i.e., a degree of saturation (S) between 90 and 100%. For the samples at natural water content, the normalized cyclic shear strength decreased as the initial degree of saturation increased. An empirical relationship was defined to describe the variation of normalized cyclic strength as a function of the degree of saturation. In the case of tests conducted on back pressure saturated specimens or undrained conditions, the normalized cyclic shear strength fell between 0.50 and 0.79, whereas the normalized undrained shear strength from the static test at the same confining pressure was 0.89. The normalized undrained cyclic shear strength for the specimen with laboratory-induced over consolidation ratio (OCR) of 3 was greater than 0.79 for the same confining stress. The magnitude of the deviator stresses estimated from stress cell measurements under traffic in the Low Track Modulus (LTM) zone suggest that the cyclic shear strengths were frequently exceeded in the nearly saturated sub-grade zones along the test track. Measurement of track settlements and corresponding degrees of saturation appear to corroborate the relationship between cyclic shear strength and degree of saturation.

2.1 Discussion: -

Studies dealing with the sensitive clays are very limited and most of them are not directly linked with the sensitivity (S_t) or with the variation in sensitivity constant (k). Early investigations on sensitive clays were focused on conducting experimental work, the triaxial tests on undisturbed and remolded clay for the purpose of developing relationship between cyclic stress-strain and

pore water pressure (Seed and Chan 1966, Theirs and Seed (1968, 1969), Sangrey 1968, Sangrey et al 1969, France and Sangrey 1977 and Sangrey et al 1978). Their study established the fact that cyclic loading increases the pore water pressure under undrained conditions up to a number of cycle, which defined as a critical level beyond which the failure will occur. Nevertheless the results are limited to the conditions of the experimental work, and accordingly the validity of the empirical formulae is questionable. The introduction of a fatigue parameter as a function of pore water pressure, in a modified Cam Clay Model by Eekelen and Potts (1978), helps in predicting reliable results for shear strength of clays at the end of the given number of cyclic loading. Iwaski et al (1978) defined the quasi-elastic resilient state of soils subjected to regular drained cycling during stress-controlled loading between the two general stress states. Field and lab investigations done by Changnon et al (1979) provides a useful data base for studying the behavior of sensitive clays under varying conditions of index properties. An interesting study reported by Houstan and Hermann (1980) raised a question concerning the relative importance of plasticity and sensitivity and also the need of analysis based on the combination of static and cyclic loading in the case of sensitive clays. Matsui et al (1980) proved experimentally that an over-consolidation clay due to cyclic stress-strain history is similar to strength to one due to the ordinary over-consolidation history. He also established the fact that, in spite of the temporary loss in shear strength and deformation modulus immediately after cyclic loading, the dissipation of pore pressure leads to strength higher than the initial strength. Seed and Idris (1982) established the fact that in case of clay the faster the rate of cycling the more the situation resembles to undrained conditions. The experimental study of Procter and Khaffaf (1984) gives an idea that, if data from load controlled tests are reanalyzed to account for rate effects on shear strength, then a constant value

independent of frequency is obtained. The Lefebyre and LeBoeuf (1987) experimental study on highly sesnitive clays (S_t>100) indicates that the effect of the strain rate on undrained shear strength ratio appears to be the same for both naturally over-consolidated clays and normally consolidated clays. The Ansal and Erken (1989) study confirmed the results of the Sangrey et al (1969) study of critical level of cyclic deviatoric stress. Ansal and Erken (1989) also proposed an empirical model based on their experimental results of kaolinite clay. Wood (1990) modified the value of k = 2, a constant describing the variation in sensitivity with liquidity (given by Bejerrum 1954). He also assigned the values of 2 kPa and 200 kPa for shear strength of clays at their liquid limit and plastic limit respectively. Furthermore, he proposed that it is more desirable to mention maximum shear stress (τ_f) in terms of undrained shear strength (c_u), which is the radius of all the Mohr circles. The model proposed by O' Reilly et al (1991) emphasizes that since both the shear strength and the deformation properties of soils under cyclic loading are anisotropic; therefore, triaxial compression, triaxial extension and direct simple shear (DSS) tests should be included in the laboratory test program for gravity structure of some importance. Liang and Ma (1992) constitutive model's results indicate that it is quite capable of predicting the behavior of saturated clays subjected to undrained cyclic loading, such as degradation of undrained strength and stiffness, accumulation of permanent strain and pore pressure, influence of initial consolidation conditions, and the effect of rotation of principal stress direction. The Wathugala and Desai (1993) modifications for hierarchical single surface (HiSS) model make it capable of capturing the undrained shear behavior of normally consolidated clay, slightly over-consolidated clay, drained behavior during hydrostatic compression tests and stress-strain behavior during cyclic loading. Based on their results on cyclic triaxial tests, Hydo et al (1993) proposed a semi-

empirical model by introducing two parameters: firstly, the ratio of peak cyclic deviator stress to cyclic shear strength in a given number of cycles and secondly, the relative effective stress ratio between initial and final point in p-q (deviator stress-mean effective stress) plane. McManus and Kulhway (1993) indicated that for a drilled shaft in a cohesive soil foundation, a two-way moderate cyclic loading causes a sudden degradation in displacement with an associated substantial reduction in bearing capacity. Bardet (1995) extended the Scaled Memory Model (SM) to accommodate the anisotropic behavior of the clays. The study conducted by Puzrin et al (1995) indicates that by using a mean effective stress as a single fatigue parameter, it would be possible to describe degradation in cohesive soils subjected to cyclic loading. The Lefebvre and Pfendler (1996) study shows that for a sensitive clay (St = 300) the shear strength of clay degrades fairly rapidly with the number of cycles when there is no initial static shear stress as compared to the case when there is an initial static shear stress component. Faker et al (1999) achieved the realistic results by using the rotary viscometer instead of a conventional soil mechanics apparatus to measure the shear strength of super soft clays. This approach can be used for quick clays as well. Results of the Miller et al (2000) study confirms the studies of Sangrey et al (1969), Matsui et al (1980) and Ansal and Erken (1989) for the critical cyclic stress level and established an empirical relationship between cyclic shear strength ratio and the degree of saturation.

Studies conducted so far have covered almost all the aspects of static and cyclic behavior of cohesive soils. Experimental investigations have established very important relationships among shear stress, number of cycles, consolidation history, pore water pressure development and strain accumulations and so forth. Numerical and analytical models further enhanced the concepts of

strain hardening, normal and over-consolidation behavior, total and effective stress paths both for static loadings and cyclic loadings and create the need of a sensitive experimental investigation to evaluate these parameters. A few studies or experimental investigations have been done which established a line of demarcation between sensitive and non-sensitive cohesive clayey soils. It is therefore imperative to conduct such studies which, take into account the sensitivity of clayey soils as a deciding element to establish a reasonable factor of safety for designing foundations subjected to cyclic loading or combination of static and cyclic loading. The study conducted by Houstan and Hermann (1980) has shown that the cyclic strength increase with an increase in plasticity index. On the other hand the literature review of some sensitive clays reveal that highly sensitive clays have a very high bond strength (bonding between clay particles) which at the same time exhibit relatively low plasticity. Hence, the relative importance of sensitivity supercedes that of plasticity. The present investigation helps to emphasize the need of such studies in detail and gives an approach to establish realistic values of shear strength for clays of medium to high sensitivity. The study also indicates how to use a part of Modified Cam Clay Model to cross check the reduction in strength before and after the application of cyclic loading. A relationship is proposed for the number of cycles, factor of safety, cyclic strength ratio with respect to sensitivity of clays. Based on this discussion, the objectives of the present study can be defined as follows:

2.1 Objectives

1. To review the pertinent information available on the subject of sensitive clay, and to prepare the state of the art report which is the subject of this chapter.
2. To analyze the experimental data available at Concordia University as well as laboratory and

field data available in literature.

3. To critically examine the theoretical models and empirical formulae dealing with prediction of shear strength of the sensitive clay.
4. To conduct a parametric study on the parameters believed to govern the behavior of sensitive clay.
5. To develop a design procedure to assist practitioners in designing foundations on sensitive clay.

CHAPTER 3

EXPERIMENTAL INVESTIGATION

3.1 General

In order to achieve the objectives of the present study the experimental investigation conducted by Hanna, (1979) at Concordia University is presented in this chapter. Furthermore, the experimental data available in literature is also summarized in this chapter for convenience and for generating comparison and analysis of data. The tests conducted at Concordia University were on Champlain Clay samples collected from Riquad, Quebec, an area known for its sensitive clay deposits. The site represents the heart of the Champlain clay deposits in Eastern Canada. The soil was post-glacial Champlain marine clay with varying properties including inter-beds or lenses of silt or sands. The clay was described as brittle and sensitive, massive and blocky, with horizontal layers ranging in thickness from millimeters to a few centimeters. The sample was obtained as blocks of 30 x 30 x 30 centimeters from a depth of 4 meters.

The soil was initially tested for physical and index properties followed by a standard consolidation test, static triaxial undrained compression tests, and undrained and drained cyclic triaxial compression tests. The cyclic triaxial compression tests in particular were carried out for cycles of 15 minutes, a frequency proven to be very close from the actual frequencies that wind or wave action imposes on different tall structures (towers, off-shore structures).

3.2 Physical and Index Property Test Results

Table 3.1 gives the data for the index properties of the sensitive clays under present study.

Table 3.1 Summary of Test Data

Location	Depth m	Water content (w.c) %	Liquid limit (L.L) %	Plastic limit (P.L) %	Remold-ed shear strength (c_{ur}) kPa	Sensi-tivity (S_t)	Source
Rigaud	4	70	67	42.5	1.5	8.5	Hanna, 1979
Rigaud	4	72	70	44.75	1.7	6.82	
Rigaud	4	72.5	71	45	2.3	5.67	
St-Ambroise	16.7	56	27	20	0.1	280	Chagnon et al 1979
St-Ambroise	18.2	52	26	20	0.1	279	
St-Ambroise	27.4	50	28	23	0.1	308	
St-Ambroise	38	43	26	18	0.3	270	
Shawinigan	21.3	45	33	18	0.2	157	
Shawinigan	24.3	53	22	18	0.3	156	
Shawinigan	27.4	35	27	18	0.1	500	
Shawinigan	24.3	30	25	18	0.3	200	
Shawinigan	27.4	30	36	18	0.2	294	
Shawinigan	30.4	34	23	18	0.5	134	
St-Barnabe	10	54	33	18	0.2	266	
St-Barnabe	11	45	25	18	0.1	438	
Yamaska	21.3	49	25	18	0.1	477	
Ile-Perrot	18.2	57	36	18	0.1	560	
Shawinigan	15.2	67	56	18	0.3	215	
Shawinigan	18.2	56	52	18	0.3	208	
Shawinigan	21.3	42	44	18	0.2	222	
Yamaska	18.2	51	25	18	0.1	533	
Shawinigan	18.2	35	31	18	0.3	107	
Shawinigan	18.2	49	39	18	0.4	102	Chagnon et al 1979
Shawinigan	30.4	38	25	18	1.4	45	
Shawinigan	15.2	49	37	18	0.6	69	
St-Amable	9.1	67	42	18	0.5	43	
St-Barnabe	8	43	27	18	1.8	18	

St-Barnabe	9	41	24	18	0.8	47	
St-Amable	15.2	63	48	18	0.7	46	
Yamaska	15.2	51	39	18	0.5	111	
Yamaska	9.1	66	50	18	0.5	48	
Yamaska	12.2	69	42	18	0.3	103	
Yamaska	15.2	66	46	18	0.5	82	
Yamaska	18.2	58	41	18	0.7	67	
Yamaska	12.1	61	43	18	0.8	26	
Shawinigan	9.1	66	67	18	1.4	40	
Shawinigan	12.1	56	54	18	1.2	52	
Shawinigan	15.2	46	35	18	2.3	27	
Shawinigan	9.1	69	41	18	0.4	80	
Shawinigan	12.1	68	62	18	0.5	62	
Shawinigan	15.2	57	30	18	0.3	93	
Shawinigan	18.2	54	37	18	2	25	
Shawinigan	21.3	50	44	18	0.8	60	
Yamaska	15.2	60	47	18	0.8	44	
Yamaska	9.1	72	44	18	0.7	23	
Yamaska	12.1	60	59	18	5.1	14	
Yamaska	8	22	21	18	13	3	
Yamaska	9.1	69	67	18	3.2	11	
Yamaska	12.1	66	68	18	2.7	18	
Shawinigan	9.1	33	40	18	8.9	9	
Shawinigan	12.1	39	38	18	2.7	7	
Yamaska	21.3	67	62	18	2.9	17	Chagnon et al 1979
Ile-Perrot	7.6	63	62	18	2.9	8	
Ile-Perrot	9.1	67	63	18	2.3	12	
Ile-Perrot	10.6	65	63	18	2.9	9	
Ile-Perrot	12.1	63	61	18	2.8	11	
Ile-Perrot	13.7	61	59	18	1.4	20	
St-Amable	24.3	64	34	18	1.4	13	
Shawinigan	12.1	42	40	18	4.3	11	
Yamaska	7.6	71	54	18	1.9	15	
Yamaska	10.6	68	59	18	2.4	12	
St-Roch	21.3	54	43	18	10	3	Chagnon et al 1979
St-Leon	9.1	42	32	18	0.8	28	
St-Roch	18.2	37	24	18	5.3	9	
Yamaska	13	67	67	18	2.9	12	
Yamaska	8	70	75	18	2	20	
Yamaska	14	66	66	18	2.5	18	

Yamaska	9	69	58	18	2.8	15
St-Roch	27.4	49	47	18	9.7	6
Vercheres	18.2	64	63	18	6.6	16
Terrebonne	7.6	63	34	18	3.6	11
Terrebonne	10.6	60	31	18	3.7	17
Terrebonne	13.7	60	32	18	5.1	7
Terrebonne	21.3	41	24	18	4.8	13
Rimouski	22.8	32	39	18	11	3
Rimouski	27.4	38	41	18	11	2
St-Roch	42.6	55	42	18	15	10
St-Leon	10.6	71	73	18	5.7	5
Vercheres	22.8	59	50	18	3.3	11
Yamaska	10	71	59	18	2.2	19
St-Leon	12.1	69	71	18	6.6	4
St-Leon	13.7	63	62	18	4.8	5
St-Leon	15.2	54	60	18	6	5
St-Leon	16.7	52	50	18	6	6
St-Leon	18.2	52	63	18	2.6	15
St-Leon	19.8	54	58	18	5.1	7
Yamaska	11	69	67	18	2.5	16
St-Roch	24.3	50	52	18	12	5
Yamaska	7	68	61	18	2.2	13
St-Leon	21.3	50	54	18	4.8	10
Vercheres	16.7	50	61	18	7.2	8

3.3 Conventional Consolidation Test

For this conventional test, a standard load increment duration of 24 hours was taken and at least two load increments, including one increment after the pre-consolidation pressure, a change in height of the sample was recorded with time intervals of approximately 0.1, 0.25, 0.5, 1, 2, 4, 8, 15 and 30 minutes; and 1, 2, 4, 8, and 24 hours. The coefficient of consolidation for each load increment is then computed by using the following equation:

$$c_v = \frac{TH^2}{t} \qquad 3.1$$

where T = the dimensionless time factor ($T=T_{50}=0.197$), t = time corresponding to the particular degree of consolidation ($t = t_{50}$) and, H= length of drainage path at 50% consolidation. For double drainage H_{D50} is half the specimen height at the appropriate increment.

The results of these tests (in general accordance with ASTM standards) are summarized in Table 3.2 and Figure 3.1 shows the graph between time and deformation in mm. The compression index (0.00498) indicates a fairly compressible soil typical of brittle-sensitive clay (Holtz and Kovacs, 1981). Pre-consolidation stress is determined by using the Log-Time Method (due to Casagrande).

Table 3.2 Summary of Consolidation Test

S.No.	Load increment p	Dial gauge reading at the end of load	Change in height ΔH	Change in void ratio Δe	Initial void ratio e	length of drainage H	Co-efficient of consolidation c_v	log p
	kPa	mm	mm			mm	mm^2 / sec	
1	0.00	0.000	0.000	0.000	1.976	-	-	-
2	34.67	0.016	0.016	0.061	1.974	19.35	0.878	1.540
3	69.33	0.034	0.018	0.068	1.974	19.33	0.409	1.841
4	138.66	0.082	0.048	0.186	1.969	19.30	0.532	2.142
5	277.32	0.164	0.082	0.316	1.964	19.23	0.101	2.443
6	138.66	0.126	0.038	0.147	1.971	19.17	1.509	2.142
7	0.00	0.039	0.086	0.332	1.963	19.19	0.636	-

The value for compression index calculated 0.00498

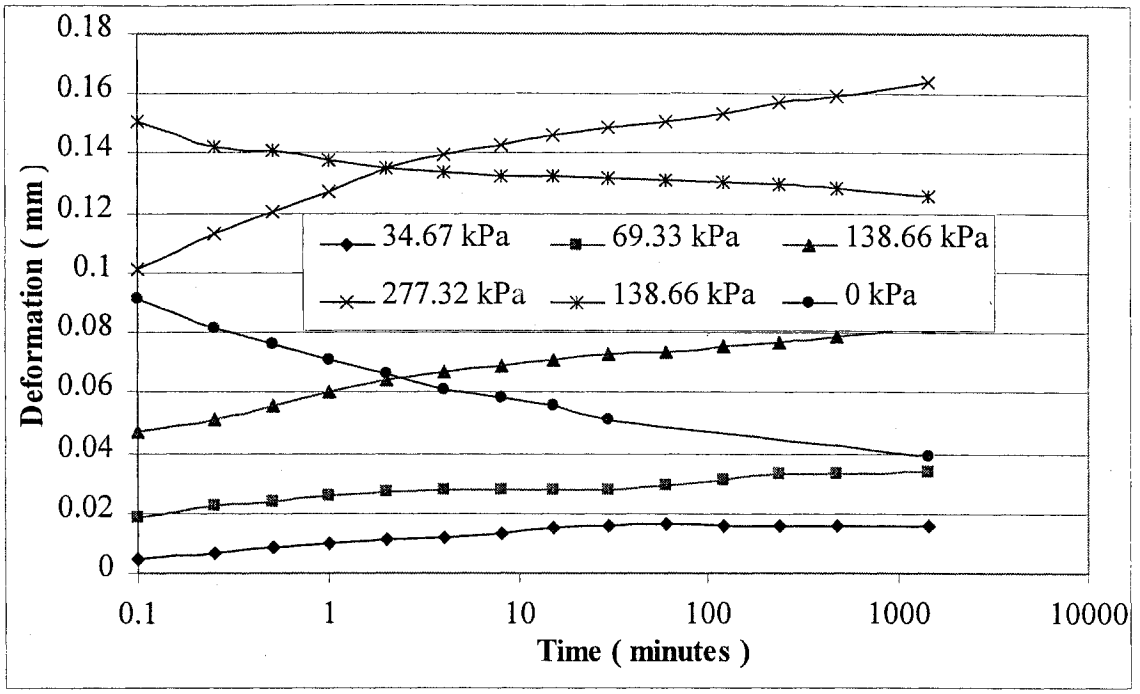

Figure 3.1: Consolidation and Swelling Behavior (Gauge readings Vs Time)

3.4 Static Triaxial Compression Test (Undrained)

A series of three static triaxial compression tests under the undrained conditions were performed to estimate the strength for static loading. A confining stress, σ_3 =207 kPa and an initial pore water pressure of 344.75 kPa was maintained for these tests. Test results are summarized in table 3.3; where PWP = pore water pressure, $\sigma_1-\sigma_3$ = static deviator stress and σ_3 = confining stress. Figure 3.2 exhibits the typical stress-curve for TEST-1, which has the lowest value of deviator stress (σ_1-σ_3 = 44kPa) selected for the present study.

Table 3.3 : Static Triaxial Compression Test Results (Undrained conditions)

S. No.	Axial strain	X-Area	Conf. stress σ_3	TEST-1			TEST-2			TEST-3		
				load	PWP (u)	$\sigma_1-\sigma_3$	load	PWP (u)	$\sigma_1-\sigma_3$	load	PWP (u)	$\sigma_1-\sigma_3$
	$\varepsilon \times 10^{-2}$	m^2	kPa	N	KPa	kPa	N	kPa	kPa	N	kPa	kPa
1	0.00	0.0009	207	0.00	159.96	0.00	0.00	55.16	0.00	0.00	109.06	0.00
2	10	0.0009	207	8.90	176.51	9.88	28.91	91.01	32.12	18.90	135.26	21.00
3	20	0.0009	207	33.36	179.27	37.07	37.81	99.98	42.01	35.58	141.12	39.54
4	30	0.0009	207	55.60	199.96	61.78	50.35	100.67	55.95	52.98	151.81	58.86
5	40	0.0009	207	68.94	213.75	76.60	57.69	107.56	64.10	63.32	162.15	70.35
6	50	0.0009	207	74.28	227.54	82.54	65.74	117.22	73.05	70.01	173.88	77.79
7	60	0.0009	207	75.62	251.67	84.02	75.08	122.73	83.42	75.35	188.70	83.72
8	70	0.0009	207	79.17	262.70	87.97	87.80	126.18	97.56	83.49	195.94	92.77
9	80	0.0009	207	79.17	282.70	87.97	87.80	131.01	97.56	83.49	208.35	92.77
10	90	0.0009	207	76.51	286.14	85.01	85.85	139.28	95.38	81.18	214.21	90.20
11	100	0.0009	207	74.73	299.93	83.03	83.58	144.11	92.86	79.15	223.52	89.45

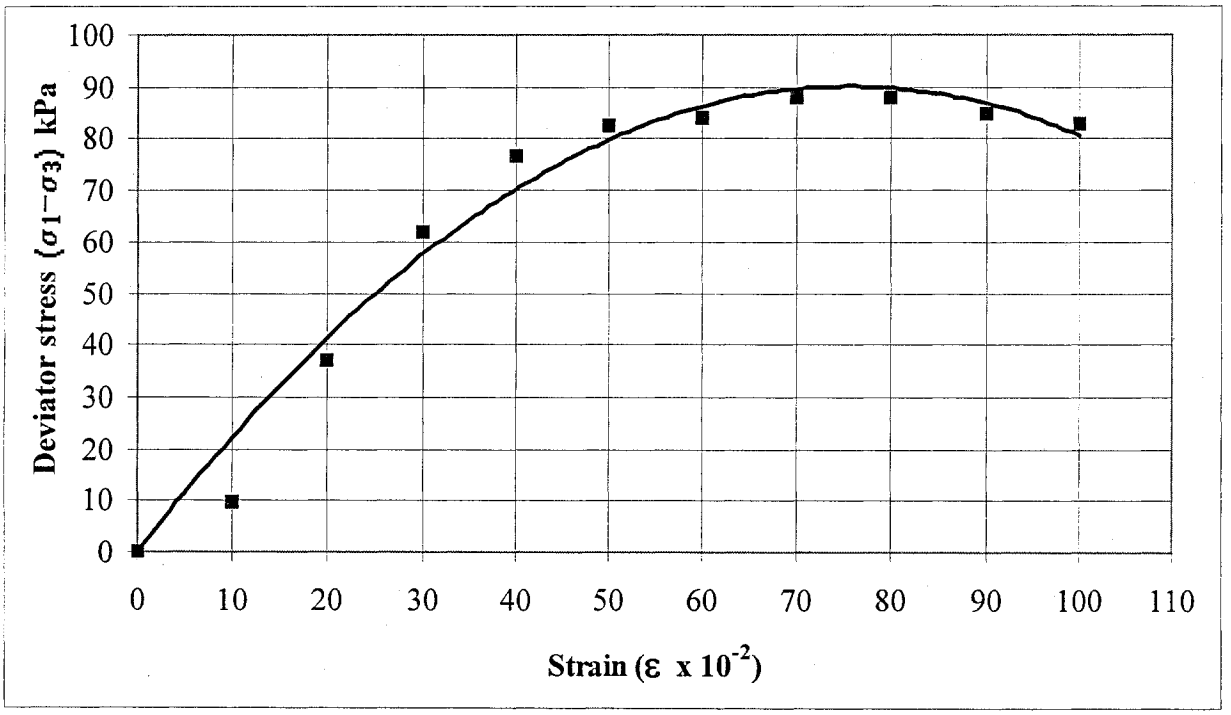

Figure 3.2: Deviator Stress-Strain Curve

Similarly Figure 3.3 shows the increase in pore water pressure with the increase in the accumulation of strain.

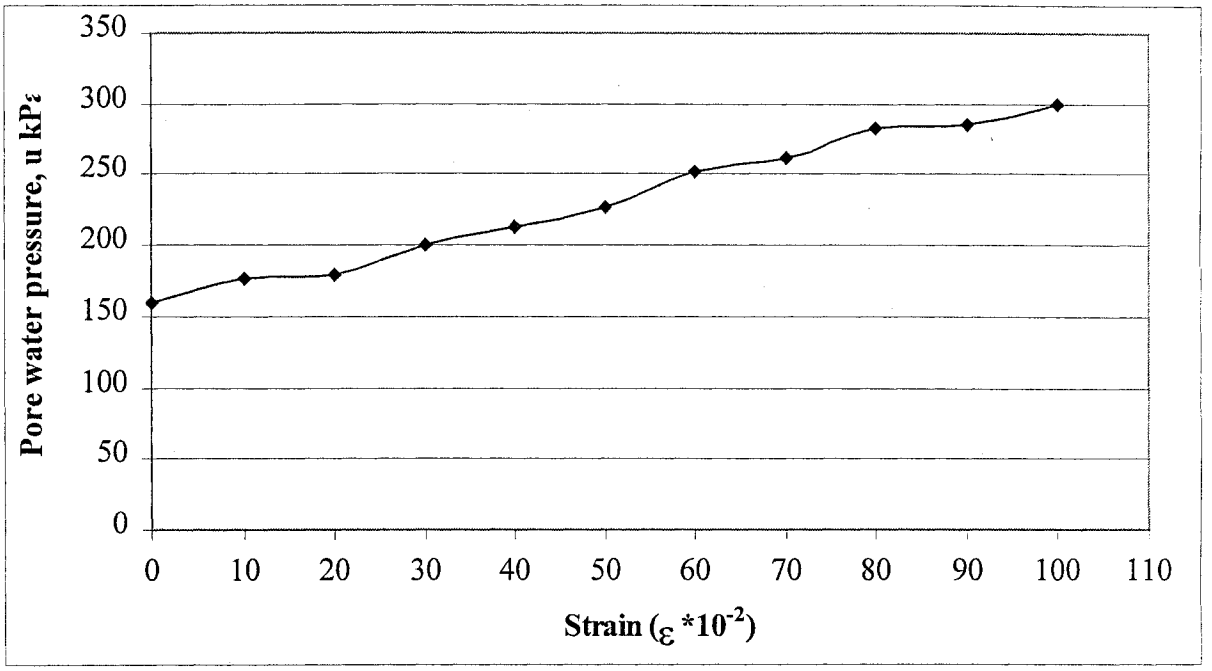

Figure 3.3: Pore Water Pressure (u) versus Strain (ε)

3.5 Cyclic Traxial Compression Test

A series of five cyclic triaxial tests was conducted at the Concordia laboratory out of which three were for undrained conditions and two were for drained conditions. An effective isotropic confining pressure was employed for the initial consolidation stage, for all cyclic loading tests. By opening the drainage valve, the specimen was consolidated isotropically in order to allow complete dissipation of excessive pore-water pressures before starting testing. For undrained tests, the valves were closed after the test started and vice versa for drained tests. The cyclic testing program was devised to expose the sample to constant values of the deviator stress for cycles of 15 minutes. Values were chosen as $1/3^{rd}$ and $2/3^{rd}$ of the ultimate value determined in the static triaxial

compression test. At certain load increments the measurements of pore pressures and volume changes were taken in order to see when and if equilibrium was reached after a certain number of cycles. In all the tests, the deviator stress was reduced to zero and then reloaded to a required $1/3^{rd}$ or $2/3^{rd}$ of the static triaxial strength.

A summary of these cyclic traxial test results is presented in Table 3.4. All the tests were performed under a constant confining pressure (σ_3) of 207 kPa.

Table 3.4 Summary of Cyclic Triaxial Compression Test Results

Test	Initial Degree Of Saturation S %	Initial Void Ratio e_o	Water Content w.c %	Initial Confining Pressure σ_3 kPa	Deviator Stress $(\sigma_1-\sigma_3)_{cyc}$ kPa	Drainage option	Total no. cycles	Failed yes / No
UT-01	90.13%	1.98	0.65	207	64.813	undrained	67	Yes
UT-02	89.13%	1.976	0.64	207	32.407	undrained	121	Yes
UT-03	61.01%	1.976	0.44	207	29.24	undrained	101	No
DT-04	87.36%	1.98	0.63	207	74.12	drained	454	Yes
DT-05	97.06%	1.98	0.70	207	32.407	drained	179	No

3.6 Test for Sensitivity

Sensitivity as defined earlier is the ratio of undisturbed to remolded undrained strength of a clay soil. In order to determine the sensitivity of the clay in the laboratory an unconfined triaxial test was conducted on both undisturbed and remolded samples of Champlain clay. Table 3.5, 3.6 and 3.7 show test results conducted for determining the experimental values of the sensitivity of the clay. Figure 3.4 shows the graphical presentation of the unconfined triaxail test data. The sensitivity (S_t) was found to be in the range of 8.5 to 6, hence, a clay in a category of medium to high sensitivity.

Table 3.5 : Unconfined Triaxail Test-1

Vertical Dial	Strain ε	Area	Proving	Axial load	Shear stress
			ring reading		
10divs=0.0254m	%	m^2	1 Div =1.535 N	P in N	P/2A (kPa)
0	0.000	0.001143	0	0	0
10	0.333	0.001143	1	1.535	0.671
24	0.800	0.001152	2	3.07	1.332
31	1.033	0.001152	3	4.605	1.999
39	1.300	0.001161	4	6.14	2.644
47	1.567	0.001161	5	7.675	3.305
58	1.933	0.001161	6	9.21	3.966
70	2.333	0.001171	7	10.745	4.588
89	2.967	0.00118	8	12.28	5.203
110	3.667	0.00119	8.5	13.0475	5.482
Remoulded.....Remoulded.....Remoulded.....Remoulded.....Remoulded.....					
200	6.667	0.001226	0.8	1.228	0.501
400	13.333	0.00132	1	1.535	0.581
			S_t =	8.5	

Table 3.6 : Unconfined Triaxail Test-2

Vertical Dial	Strain ε	Area	Proving	Axial load	Shear stress
			ring reading		
10divs=0.0254m	**%**	**m^2**	**1 Div =1.535 N**	**P in N**	**P/2A (kPa)**
0	0.000	0.001143	0	0	0
5	0.167	0.001143	1	1.535	0.671
10	0.333	0.001143	2	3.07	1.343
19	0.633	0.001152	3	4.605	1.999
24	0.800	0.001152	4	6.14	2.665
32	1.067	0.001152	5	7.675	3.331
40	1.333	0.001161	6	9.21	3.966
54	1.800	0.001161	7	10.745	4.627
60	2.000	0.001166	7.5	11.5125	4.937
Remoulded.....Remoulded.....Remoulded.....Remoulded.....Remoulded.....					
20	0.667	0.001152	0.5	0.7675	0.333
90	3.000	0.0011799	0.6	0.921	0.390
180	6.000	0.001217	1	1.535	0.631
220	7.333	0.00124	1.1	1.6885	0.681
			S_t =	6.82	

Table 3.7: Unconfined Triaxail Test-3

Vertical Dial	Strain ε	Area	ring-Dial	Axial load	Shear stress
10divs=0.0254m	%	m^2	1 Div =1.535 N	P in N	P/2A (kPa)
0	0.000	0.001143	0	0	0
9	0.300	0.001143	1	1.535	0.671
15	0.500	0.001152	2	3.07	1.332
22	0.733	0.001152	3	4.605	1.999
29	0.967	0.001152	4	6.14	2.665
37	1.233	0.001157	5	7.675	3.317
43	1.433	0.0011613	6	9.21	3.965
50	1.667	0.0011613	7	10.745	4.626
57	1.900	0.0011613	8	12.28	5.287
77	2.567	0.001171	8.5	13.0475	5.571
Remoulded.....Remoulded.....Remoulded.....Remoulded.....Remoulded.....					
0	0.000	0.001152	0	0	0.000
32	1.067	0.001152	0.5	0.7675	0.333
95	3.167	0.0011799	0.7	1.0745	0.455
227	7.567	0.00124	1	1.535	0.619
258	8.600	0.001254	1.2	1.842	0.734
430	14.333	0.00134	1.4	2.149	0.802
470	15.667	0.001356	1.5	2.3025	0.849
			S_t =	5.67	

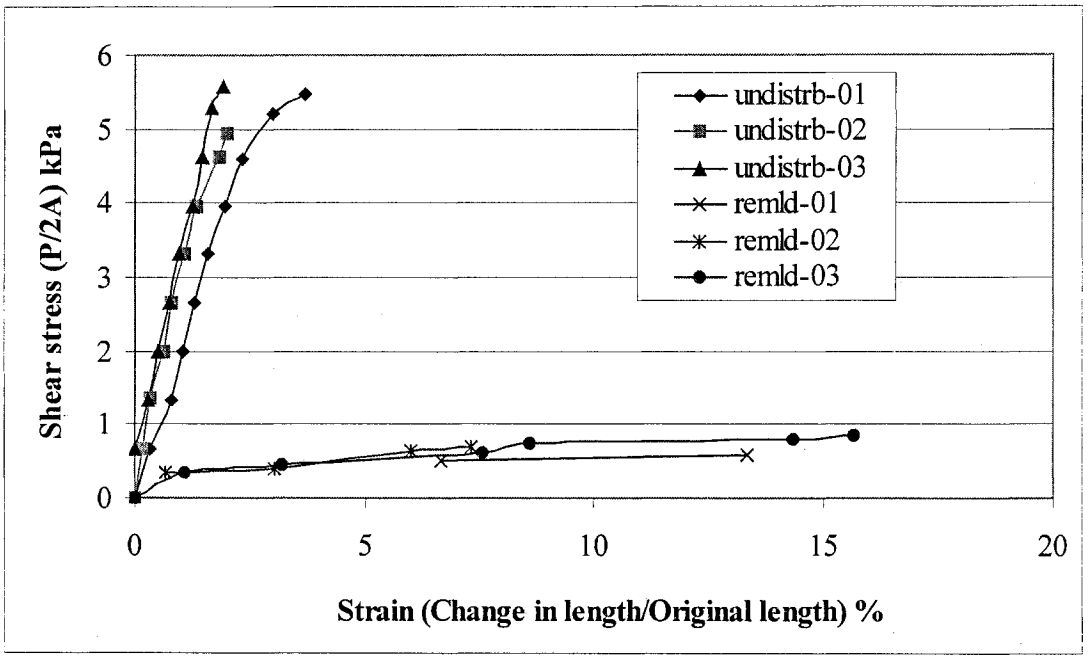

Figure 3.4: Shear Stress versus Strain for Undisturbed and Remolded Samples

3.7 Discussion

Physical and index property test results for the sensitive clays show that the sensitivity varies with the change in the natural water content and the depth from where these samples were taken. In other words, sensitivity varies with the liquidity index and pre-consolidation pressure in these sensitive clays. The results of the standard consolidation test for Champlain clay samples indicate that it was a normally consolidated clay (NCC). The co-efficient of consolidation (c_v) obtained range from maximum of 1.509 mm^2/sec at 138.66 kPa (unloading) to a minimum of 0.101 mm^2/sec at 277.32 kPa (loading). Results of the static triaxial compression tests show the static deviator stress ($q_s = \sigma_1 - \sigma_3$) varied from 87.97 kPa to 97.56 kPa. A lower value of 87.97 kPa has been selected for the present study. For saturated samples subjected to undrained loading, the cyclic shearing behavior depends upon two main factors: the build up of pore water pressures and the reduction in effective stress. The three undrained cyclic triaxial tests (UT-01, UT-02 & UT-03) were conducted on samples consolidated to an initial stress σ_3 of 207 kPa. Results of cyclic triaxial compression tests indicate that, for a value of 30 kPa of cyclic deviator stress, this clay can reach a quasi elastic equilibrium state without failure. A maximum accumulated strain of 0.48% under a constant deviator stress of 74.12 kPa on unloading at the end of 454^{th} cycle in the case of DT-04 (drained) and a minimum of 0.08% at the end of 101^{th} cycle in the case of UT-03 (undrained) under a constant deviator stress of 29.24 kPa were achieved. The clay showed a sensitivity range of 6 to 8.5 when measured in the conventional manner which involved the thorough remolding of the clay and the use of standard odeometer test. The results for drained and undrained triaxial tests clearly

indicate the importance of keeping track of the pore water pressure during the test and also in the case of design computations. In the case of sands, drainage is likely to occur during the design storm; so it is necessary to analyze pore pressure behavior more critically in order to have feasible values for cyclic shear strength. The literature reviews for cyclic triaxial tests indicate that the laboratory pore pressure measurements are more difficult to perform with good accuracy in clays than in sands (Reilly and Brown, 1991). Since proper drainage does not take place in clays, it is therefore, preferable to use the shear strain to determine the cyclic shear strength for clays. Specifically for situations where the cyclic shear strength and the cyclic shear moduli under undrained conditions are of primary interest, the shear strain plays a role of more direct parameter than the pore water pressure.

CHAPTER 4

ANALYSIS

4.1 General

In this chapter field and laboratory test results given in Chapter 3 will be analysed. The objective of this analysis is to identify the parameters, which appear to govern the behavior of sensitive clays under cyclic loading. A design procedure is proposed which takes into account the sensitivity (S_t) parameter as a deciding factor in predicting the shear strength for sensitive clay under these given loading conditions.

4.2 Analysis of Undrained and Drained Test Results

Undrained shear strength behavior of sensitive clay differs significantly if test at in-situ stresses, or if test at stresses higher than the preconsolidation pressure (σ_p). Figure 4.1 is based on the conventional consolidation test results. The plot between void ratio (e) and the effective stress (p) is linear, which indicates the normally consolidated clay. The line of the plot is termed as virgin compression line (Craig, 1978). Although a significant part of the curve is under normally consolidated region, but on the other hand, the importance of over consolidated region cannot be overlooked, which usually causes a negative pore water pressure. The effective stress which govern the undrained shear strength in a sensitive clay foundation is a vertical effective stress in the soil at the time of construction, and the highest vertical stress previously experienced by the soil. The lowest undrained shear strength occurs when the current vertical effective stress equals the previous maximum value, which is a state of normally consolidated clay. Hence, the normally consolidated clay samples give more realistic critical values for shear strength during the undarined period. Test results for cyclic triaxial stress-strain data for undrained

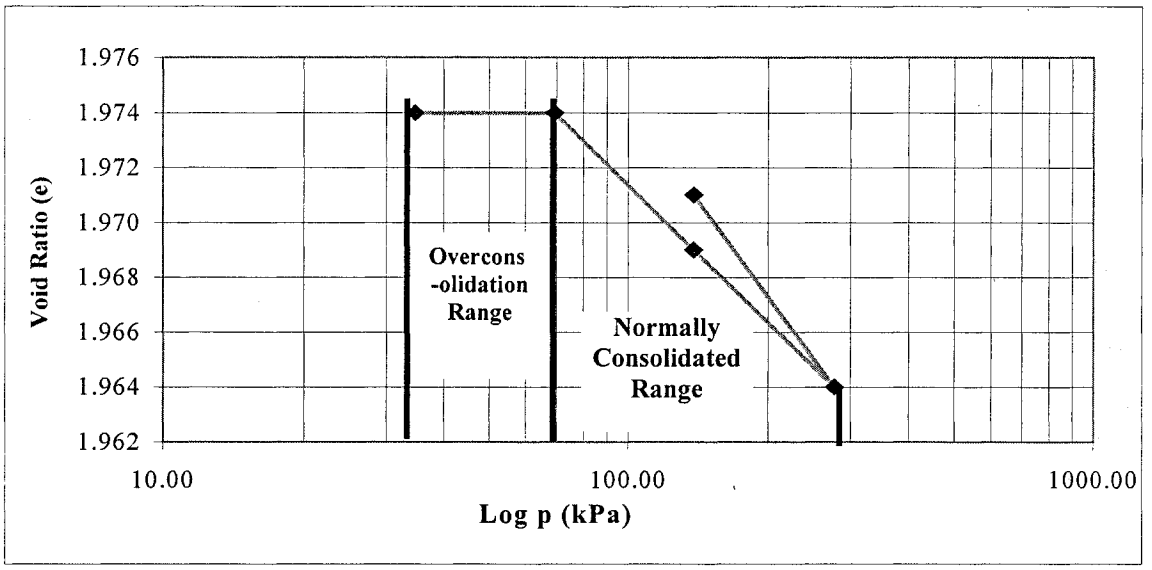

Figure 4.1: Void Ratio Versus Effective Stress

tests UT-01, UT-02, UT-03 and drained tests DT-04 and DT-05 are presented in Figures 4.2 (a), 4.2 (b), 4.3, 4.4 & 4.5 in terms of cyclic deviator stress (q_{cyc}) versus the axaial strain (ε). The results depict consistent hysterisis loops with incremental permanent strain decreasing with each cycle of loading. Tests UT-01 and DT-04 were performed at the cyclic deviator stress equal to $2/3^{rd}$ of the static deviator stress. DT-04 exhibited a shear failure with an accumulated strain of 0.48% at 454^{th} cycle, on the other hand, undrained test UT-01 showed failure with an accumulated strain of 0.30% at 67^{th} cycle. A similar comparison can be found among the undrained tests UT-02, UT-03 and drained test DT-05. The comparison of accumulated stress-strain for the drained test DT-04 and undrained test UT-01 clearly indicates that the sample under undrained condition failed much earlier and at a relatively lower cyclic deviator stress (q_{cyc}) than drained test DT-04.

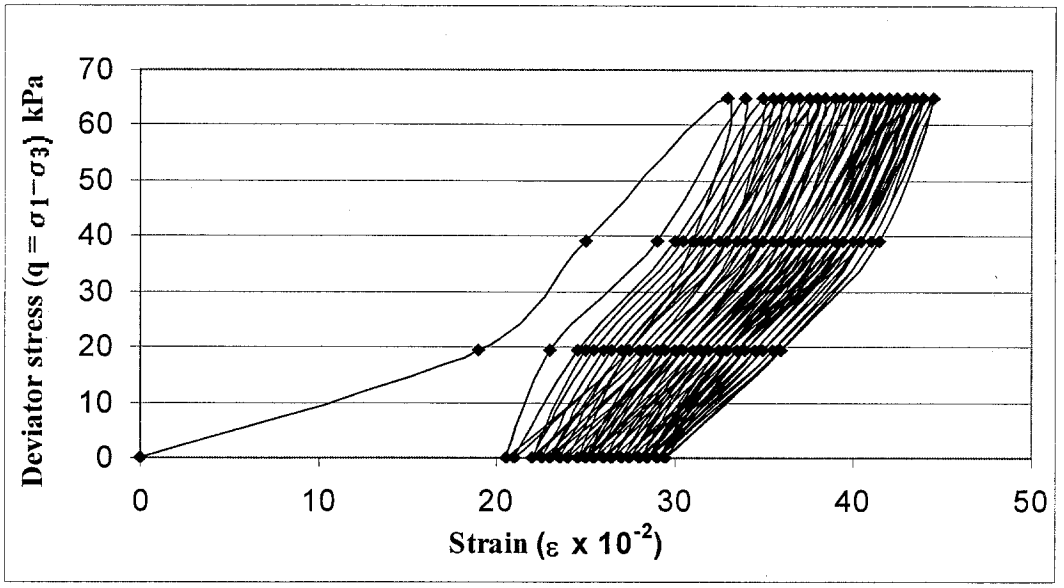

Figure 4.2 (a): Deviator Stress versus Axial Strain (UT-01)

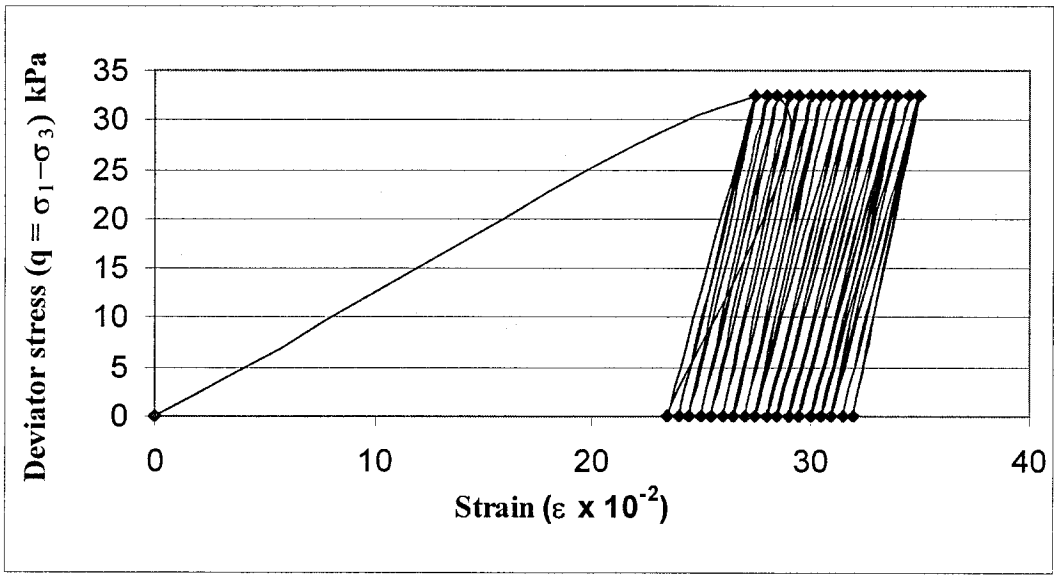

Figure 4.2(b): Deviator Stress versus Axial Strain (UT-02)

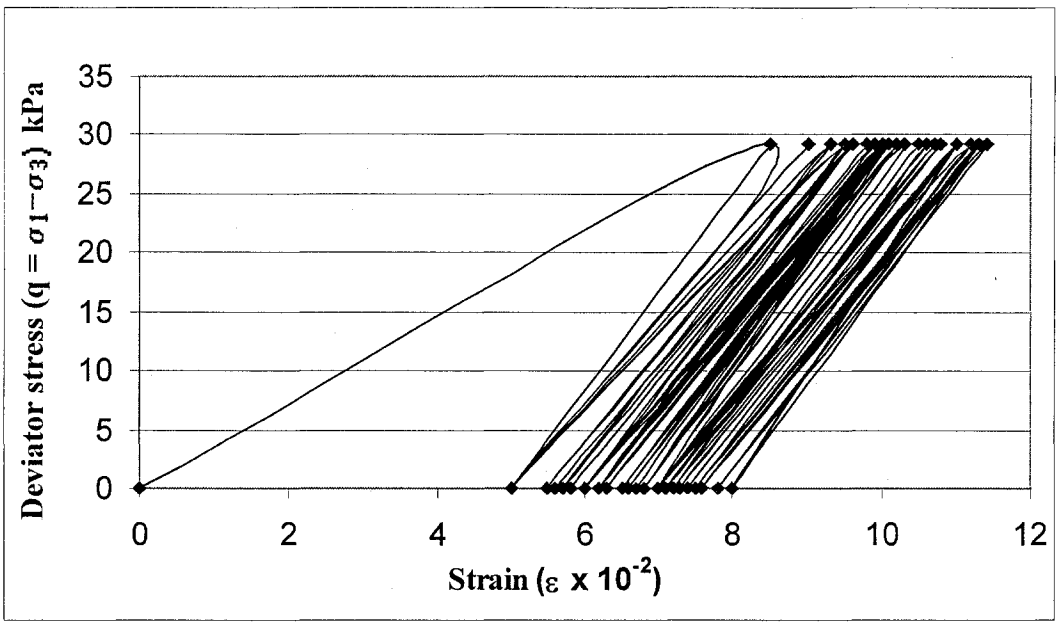

Figure 4.3: Deviator Stress versus Axial Strain (UT-03)

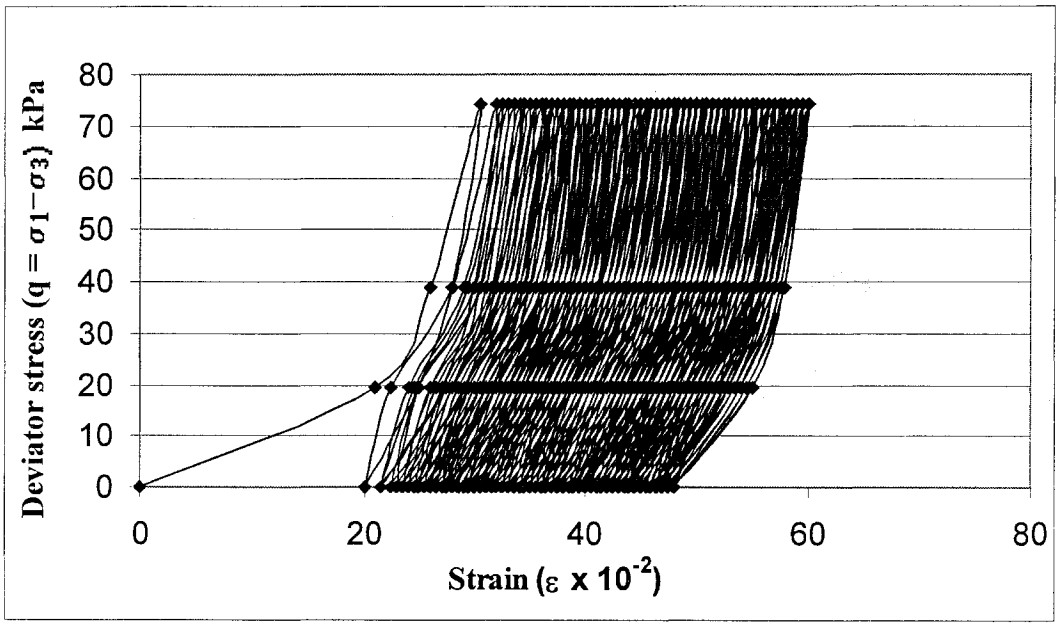

Figure 4.4: Deviator Stress versus Axial Strain (DT-04)

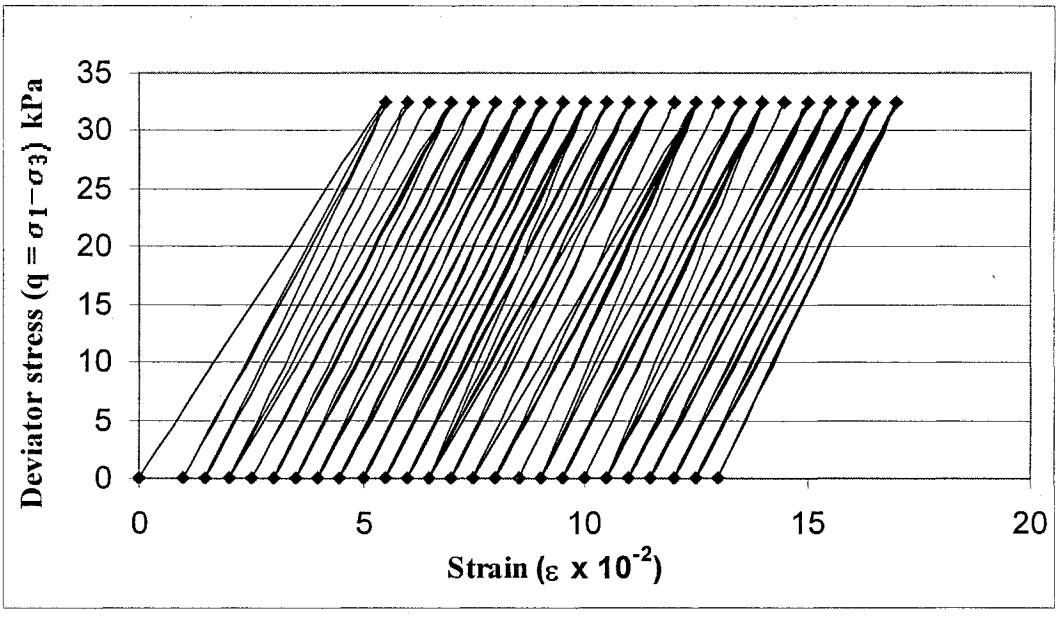

Figure 4.5 : Deviator Stress versus Axial Strain (DT-05)

The evidence that the undrained condition is more sensitive to failure is further supported by plotting the data of pore water pressure with respect to strain for both undrained and drained cyclic triaxial tests. Figures 4.6, 4.7, 4.8, 4.9 and 4.10 show the graphical presentation of pore water pressure versus strain for the tests UT-01, UT-02, UT-03, DT-04 and DT-05, respectively.

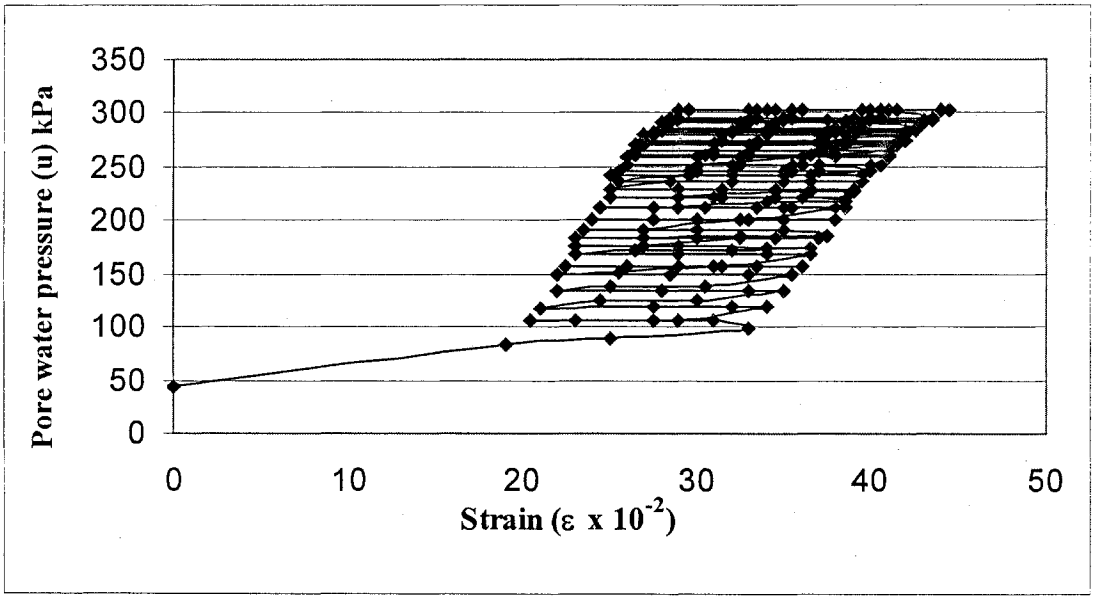

Figure 4.6 : Pore Water Pressure versus Axial Strain (UT-01)

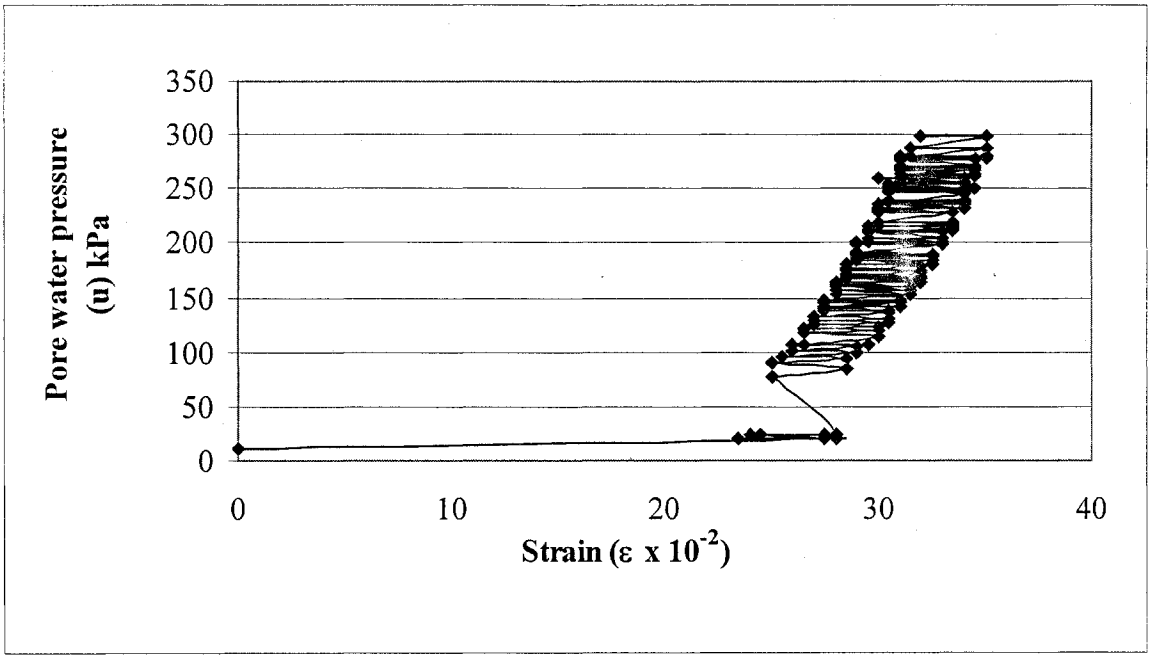

Figure 4.7: Pore Water Pressure versus Axial Strain (UT-02)

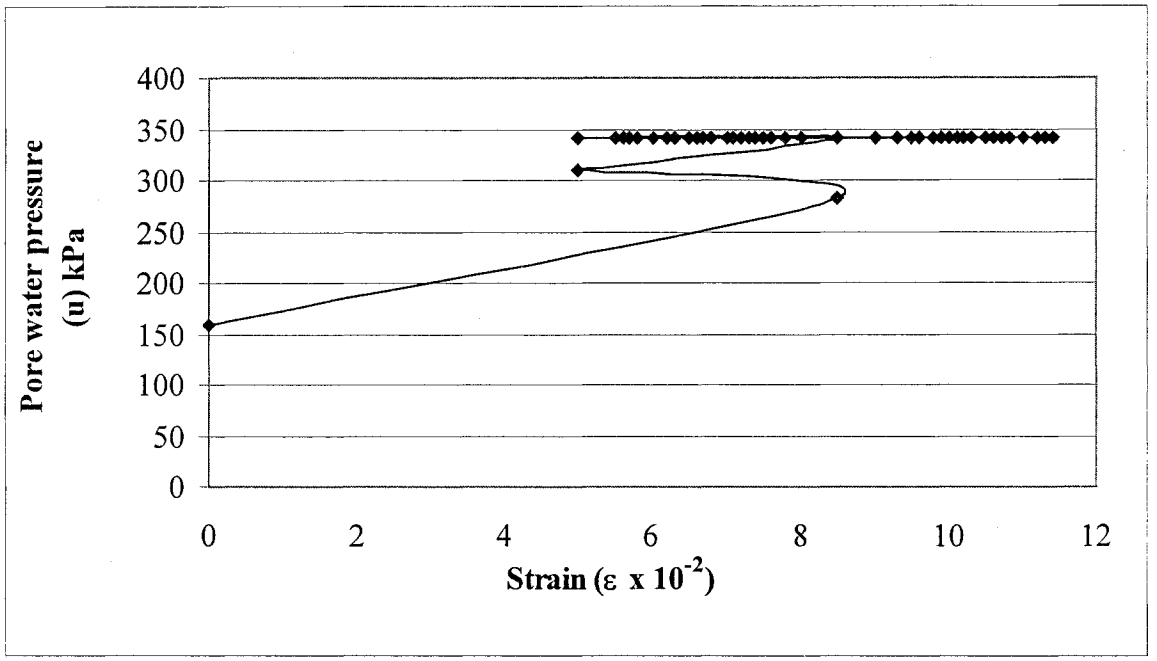

Figure 4.8: Pore Water Pressure versus Axial Strain (UT-03)

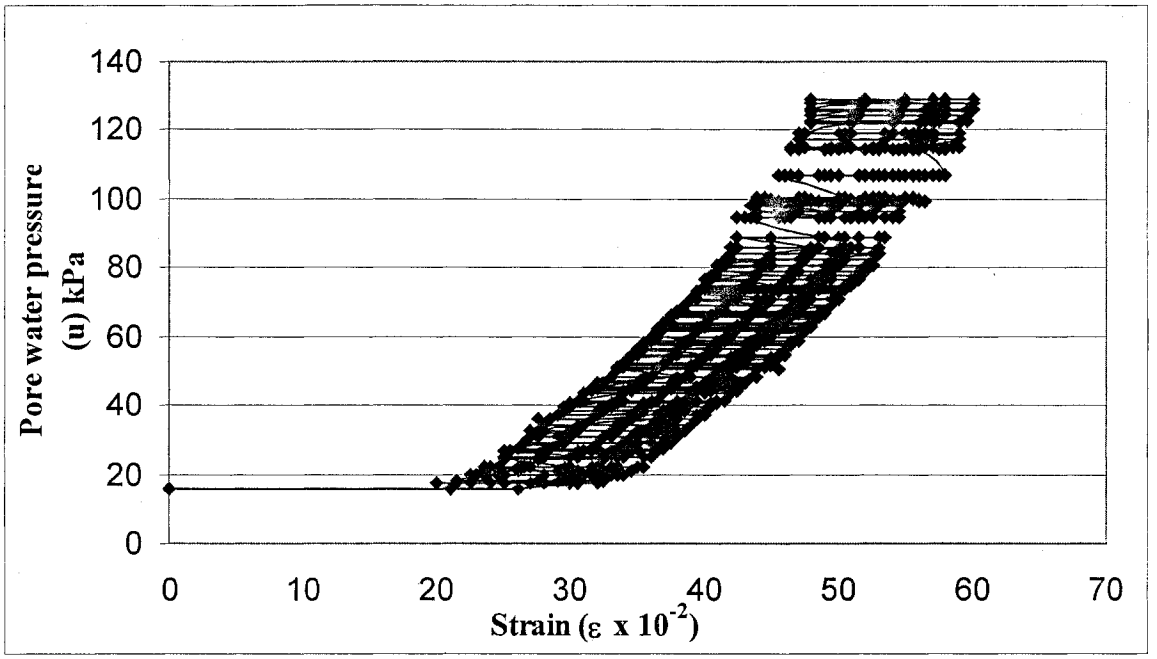

Figure 4.9: Pore Water Pressure versus Axial Strain (DT-04)

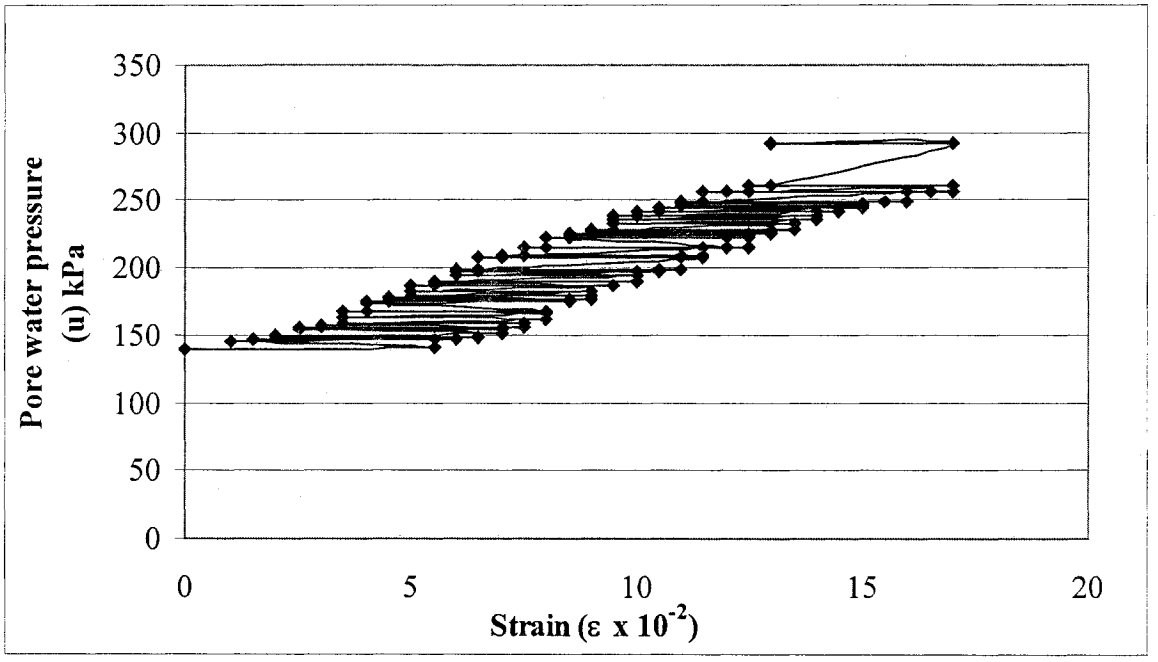

Figure 4.10: Pore Water Pressure versus Axial Strain (DT-05)

The increase in pore pressure is associated with the strength reduction in cyclic loading and can be interpreted as showing that the structure of clay is changed significantly by

the action of the applied cyclic loading. In other words reduction in shear stress is directly proportional to an increase in pore water pressure during cyclic loading which in turn is directly proportional to the number of cyclic loadings. Hence, the undrained cyclic loading of sensitive clay is more likely to cause effective stress failures due to a continued increase in excessive pore water pressure as compared to drained conditions.

Based on the analysis given above, it can be reported that the undrained condition is more critical in terms of reductions in shear stress which as a result directly proportional to the number of cyclic loading (N) which is the major factor in increasing the pore water pressure. Consequently the present investigation is limited to undrained conditions.

4.3 Parametric Study for Undrained Shear Strength of Sensitive Clay

The parameters governing the behavior of sensitive clay subjected to cyclic loading can be divided into, two categories, A and B. A includes parameters like; cyclic deviator stress (q_{cyc}), pore water pressure (u), axial strain (ε), preconsolidation (σ_p) and confining pressure (σ_3 or σ_c), over consolidation ratio (OCR) and number of cycles (N). B includes parameters like; natural water content (w), liquid limit (LL), plastic limit (PL), plasticity index (I_P), liquidity index (I_L), sensitivity (S_t), constant of variation in sensitivity (k) and initial degree of saturation (S). Category A can be expressed in terms of number of cyclic loading, whereas, Category B cannot be directly linked with the number of cyclic loading. For linking the two categories the test data from Concordia University and Miller et al, (2000) is used. The analysis of the data show that initial degree of saturation can be used as a gateway for expressing both categories in terms of number of cycle.

4.3.1 Effect of Pore Water Pressure

Figure 4.11 shows the relationship between normalized pore water pressure ($\Delta u/\sigma_c$) and the number of cycles (N) for undrained consolidated triaxial compression tests; UT-01, UT-02 and UT-03, where Δu is the difference between the current and the initial pore water pressure and σ_c is the confining stress.

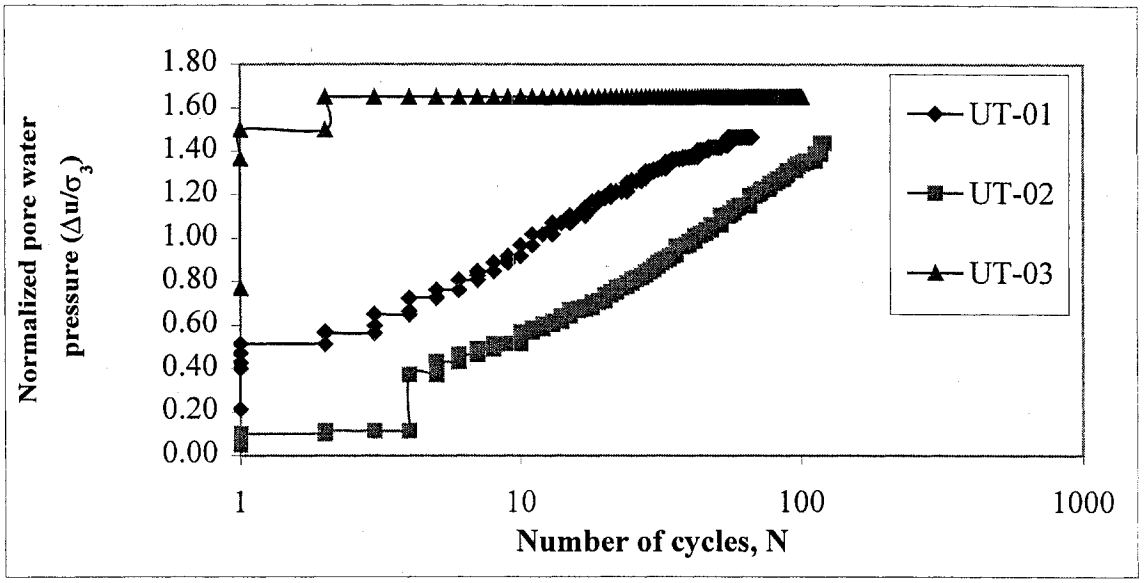

Figure 4.11: Normalized Pore Water Pressure versus Number of Cycles

Results of test UT-01, which was done at a cyclic deviator stress (q_{cyc}) $2/3^{rd}$ of the static deviator (q_s) indicate that the pore water pressure (Δu) is cycled over a nearly constant range for approximately first five cycles after a rapid initial buildup at the very first cycle. The test sample failed before reaching equilibrium state or quasi-elastic resilient state. Test UT-02 was done at a cyclic deviator stress, which was slightly higher than $1/3^{rd}$ of the static deviator stress. A linear increase in pore water pressure was observed till failure. Test UT-03 was done at a cyclic deviator stress exactly equals to $1/3^{rd}$ of the static deviator stress. The test shows a constant pore water pressure uptil 20^{th} cycle after a

rapid initial buildup at the very first cycle. The test sample reached quasi-elastic resilient state without failure. It is interesting to note that UT-03 shows a maximum normalized pore water pressure as compared to the other two tests UT-01 and UT-02, which resulted in shear failure before reaching equilibrium stage. A possible explanation can be that samples UT-01 and UT-02 showed a tendency for dilation due to shear failure, otherwise higher shear induced pore water pressures would be expected for failing samples.

4.3.2 Effect of Axial Strain

Stress strain data for the first 10 cycles 4.12a for test UT-01 and UT-03. The reason for selecting these two tests is due to a clear difference in cyclic deviator stress. In general the results exhibits consistent hysteresis loops with incremental strain decreasing each cycle of loading. Stress strain data from test UT-03 indicate that the magnitude of permanent strain per cycle was small. On the other hand, data from test UT-01, during which shear failure occurred, show significant permanent strain accumulating out to 67 cycles. Furthermore, Figure 4.12b the graph for the axial strain plotted against the number of load cycles supports the above evidence. Data for test UT-03 indicate that the accumulated axial strain was relatively small at about 0.09% after 10 cycles of loading, and the rate of permanent strain accumulation became very slow after 15 cycles and finally reached at a constant value of 0.1% after 25 cycles. On the other hand data for test UT-01 indicate that a large permanent strain of nearly 0.38% was achieved after 10 cycles and that the rate of permanent strain accumulation at the end of the test was quite substantial and finally reached 0.45%

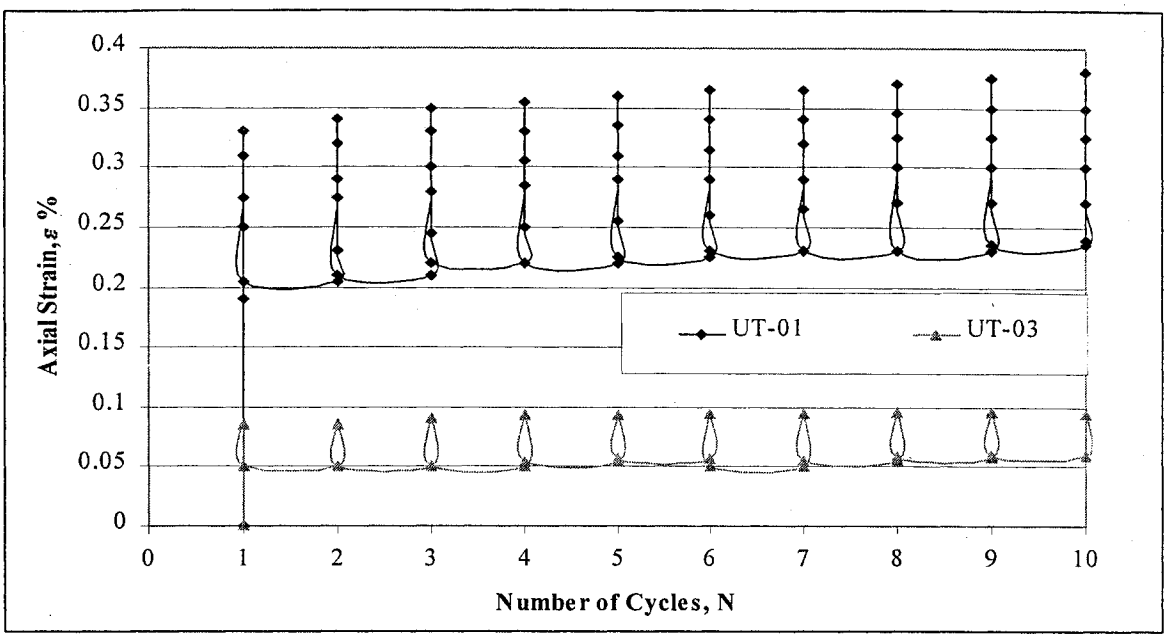

Figure 4.12(a): Comparison of Axial Strain for the First Ten Cycles between UT-01 and UT-03

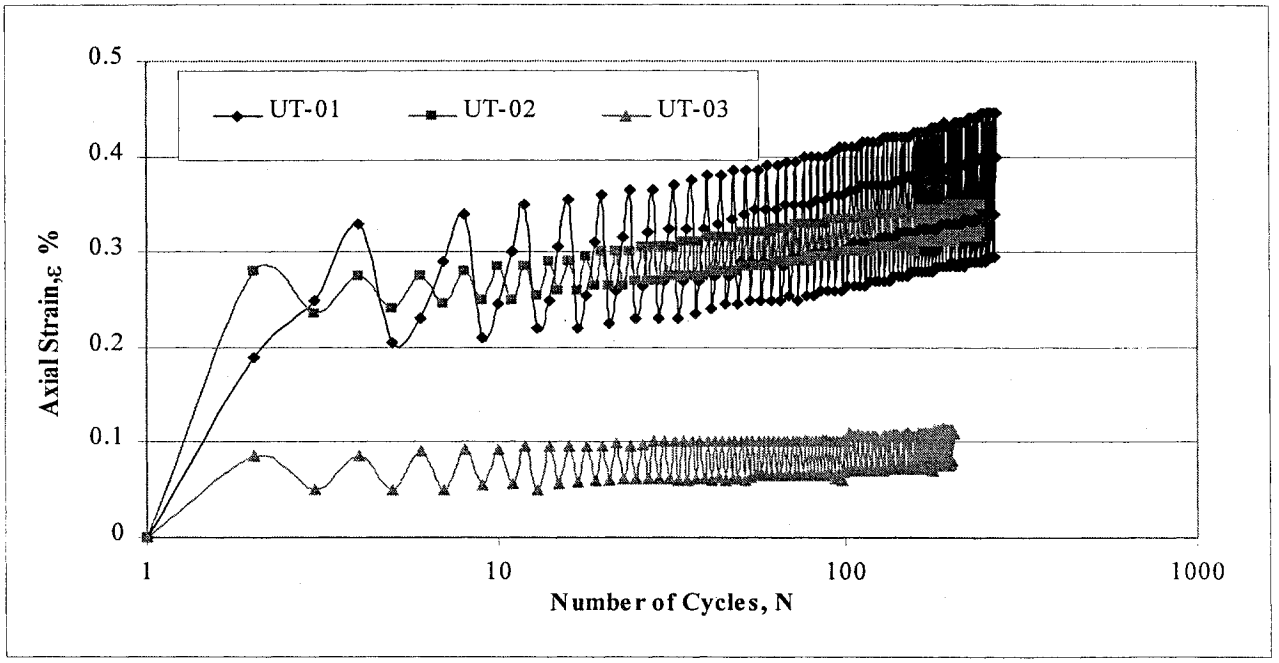

Figure 4.12(b): Strain Versus Number of Cycles

4.3.3 Effect of Cyclic Deviator Stress

The effect of cyclic loading is like a remolding agent in case of sensitive clay. The cyclic loading disturbs the structure of sensitive clay plus helps the available water to dissolve down the salts results in further reducing the strength of the clay. The undisturbed clay sample gets remolded and reach its remolded shear strength or some time below then that depending upon available natural water content. Figures 4.13, 4.14 and 4.15 show the cyclic mobility or movement of effective stress path controlled by cyclic deviator stress and number of cycles, N. The effect of an increase in load cycles causes an increase in the pore water pressure, which in turn moves the effective stress path towards the failure plane.

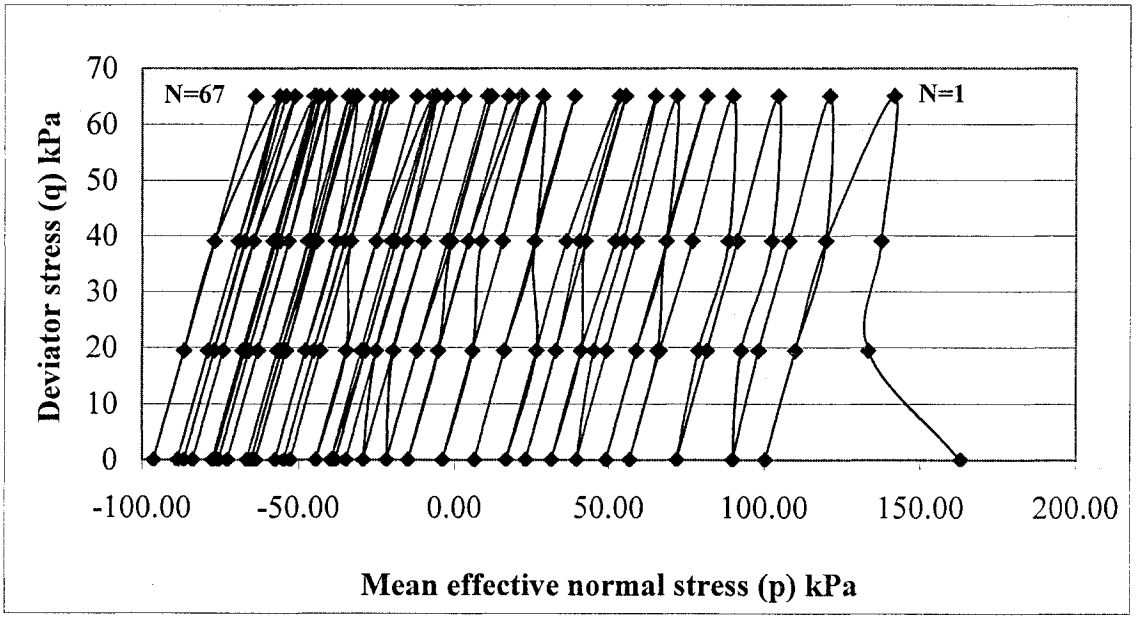

Figure 4.13: Deviator Stress Versus Effective Stress (UT-01)

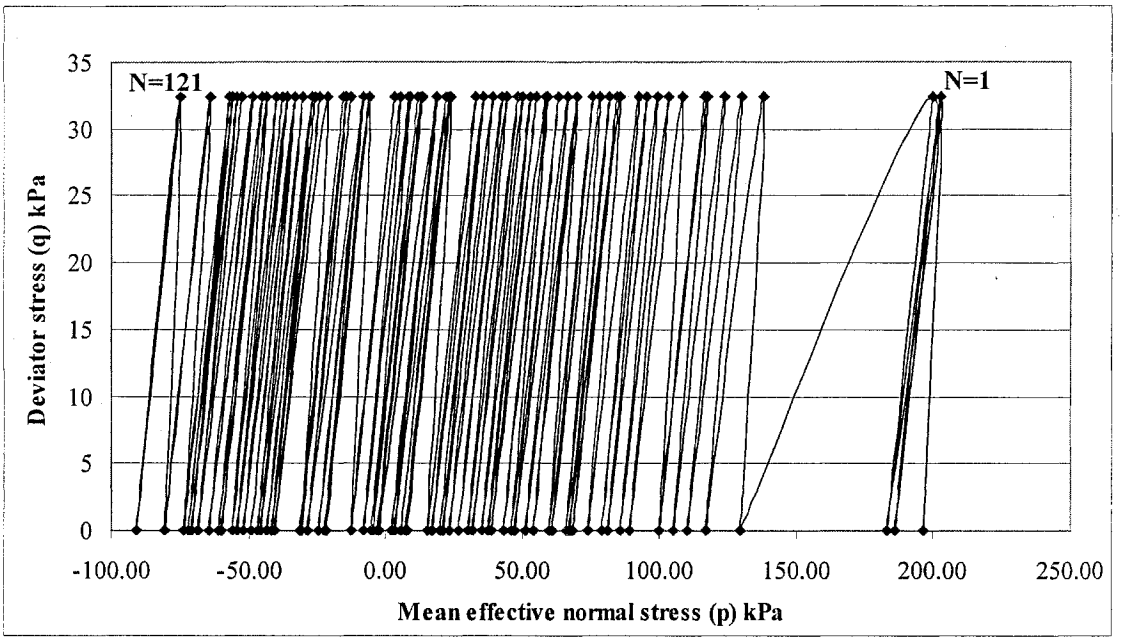

Figure 4.14: Deviator Stress Versus Effective Stress (UT-02)

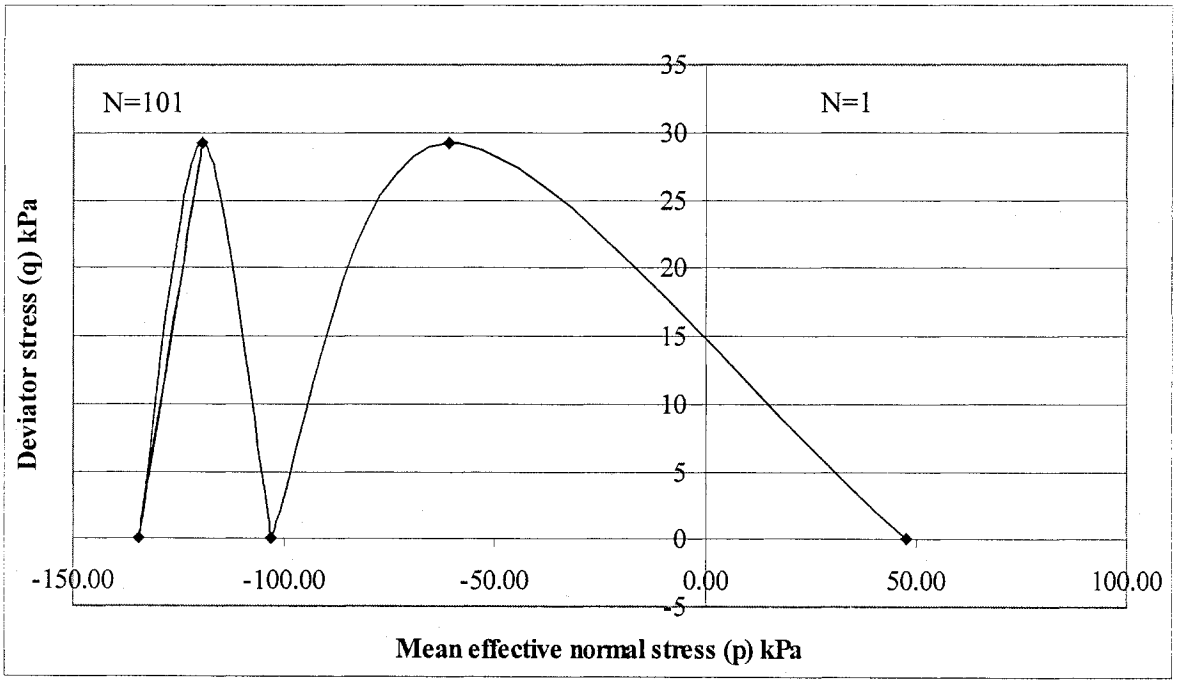

Figure 4.15: Deviator Stress Versus Effective Stress (UT-03)

4.3.4 Effect of Initial Degree of Saturation

Table 4.1 shows that the cyclic shear strength also depends upon the initial degree of saturation (S), which in turn is a function of the water content or liquidity index. The table shows that samples having higher initial degree of saturation failed as compared to those with lesser value of S, although they were tested under the same stress conditions. One possible explanation is that the relationship between strength and degree of saturation is because the pore water pressure is a function of degree of saturation. Since metric suction is inversely related to the degree of saturation and directly related to shear strength, samples with lower S are expected to be stronger (Bishop et al. 1969). This theory opens the gateway for connecting the parameters of category B with respect to the number of cyclic loading (N).

Table 4.1 Effect of Initial Degree of Saturation

Test	Initial Degree Of Saturation S %	Initial Void Ratio e_o	Natural Water Content w.c %	Initial Confining Pressure σ_3 kPa	Deviator Stress $(\sigma_1-\sigma_3)_{cyc}$ kPa	Total No. Cycles	Failed yes / No	Data Source
UT-01	90%	1.98	65	207	64.813	67	Yes	Hanna, 1979
UT-02	89%	1.976	64	207	32.407	121	Yes	Hanna, 1979
UT-03	61%	1.976	44	207	29.24	101	No	Hanna, 1979
	92 %	0.99	31.6	35	35	18,254	No	Miller, et al 2000
	90.4%	1.08	34	14	55	72900	No	Miller, et al 2000
	100%	1.03	36.8	14	55	3250	Yes	Miller, et al 2000
	100%	1.10	39	35	55	18500	No	Miller, et al 2000
	100%	1.05	37.5	35	55	325	Yes	Miller, et al 2000

	100%	0.96	34.3	35	35	10100	No	Miller, et al 2000
	92.3%	1.01	33.3	22	76	177	Yes	Miller, et al 2000
	96.8%	1.08	37.3	22	55	64	Yes	Miller, et al 2000
	97.5%	1.03	35.9	35	55	7454	Yes	Miller, et al 2000
	93.4%	1.04	34.7	35	35	10200	Yes	Miller, et al 2000
	93.6%	1.04	34.77	14	35	21513	No	Miller, et al 2000
	98.8%	1.10	38.88	14	35	4200	Yes	Miller, et al 2000

4.3.5 Effect of Liquidity index

Since the liquidity index reflects the combined effect of water content (w), liquid limit (LL), plastic limit (PL), plasticity index (I_p), sensitivity (S_t), constant of variation in sensitivity (k) and initial degree of saturation (S). Therefore data from Hanna, (1979), Chagnon et al (1979), Bejerrum, (1967), Bejerrum & Simon, (1960), Bejerrum, (1954) and Skempton and Northey, (1953) are analyzed to establish the importance of liquidity index in deciding the undrained shear strength of sensitive clays. Table 4.2 shows the analysis of the data given in Chapter 2 and Chapter 3 index properties related to shearing strength of sensitive clays. The values for liquidity index (I_L), the plasticity index (I_p), the undrained shear strength (c_u), the pre-consolidation stress (σ_p), the sensitivity variation constant (k), the clay density (γ) and the void ratio (e) in table 4.2, are calculated by using pre-established relationships.

For preconsolidation stress (σ_p) a relationship given by Skempton (1954, 1957) is used. Skempton showed data of cu/σ_p for a number of soils that were supposedly normally compressed, obeying the following relationship:

$$\frac{c_u}{\sigma_p} = 0.11 + 0.37 I_p \quad \text{.....4.1}$$

For the constant describing the variation in sensitivity (k) equation number 2.2 is used.

For determining the density, γ the following relationship is used:

$$\gamma = \frac{G_s(1 + w.c)\gamma_w}{1 + G_s w.c} \quad \text{.....4.2}$$

For void ratio, e following relationship is used:

$$e = \frac{G_s(1 + w.c)}{\gamma}\gamma_w - 1 \quad \text{.....4.3}$$

Table 4.2 Analysis of Test Results

I_P	I_L	c_u	σ_P	k	γ	e	Data Source
		kPa	KPa		kN / m^3		
26	1.06	13	63.31	2	15.75	1.96	Hanna, 1979
25	1.08	12	56.61	2	15.77	1.94	Hanna, 1979
25	1.12	13	65.03	2	15.88	1.89	Hanna, 1979
6	3.67	32	245.08	1	17.87	1.16	Changnon, et al 1979
16	2.06	50	295.51	2	16.92	1.46	Changnon, et al 1979
21	1.86	22	114.97	2	16.42	1.65	Changnon, et al 1979
10	2.10	62	422.45	2	17.58	1.24	Changnon, et al 1979
42	0.98	56	211.00	4	16.11	1.78	Changnon, et al 1979
16	2.56	20	116.90	1	16.05	1.81	Changnon, et al 1979
23	1.57	37	187.19	2	16.49	1.62	Changnon, et al 1979
5	3.60	63	490.27	1	18.39	1.03	Changnon, et al 1979
21	1.71	33	174.00	2	16.29	1.70	Changnon, et al 1979
5	4.40	37	285.29	1	18.07	1.11	Changnon, et al 1979
23	1.70	23	115.63	2	16.11	1.78	Changnon, et al 1979
31	1.06	62	277.70	4	16.77	1.51	Changnon, et al 1979
23	1.26	50	255.25	3	17.23	1.35	Changnon, et al 1979
28	1.21	33	153.84	3	15.99	1.84	Changnon, et al 1979
18	1.94	44	246.60	2	16.63	1.57	Changnon, et al 1979
13	1.92	43	274.95	2	17.32	1.32	Changnon, et al 1979
18	2.56	33	185.73	2	15.94	1.86	Changnon, et al 1979
23	1.87	37	189.13	2	16.11	1.78	Changnon, et al 1979
12	3.25	28	180.70	1	16.70	1.54	Changnon, et al 1979

14	1.71	37	226.95	3	17.32	1.32	Changnon, et al 1979
17	2.59	32	184.67	2	15.94	1.86	Changnon, et al 1979
16	1.75	50	295.21	3	17.15	1.38	Changnon, et al 1979
6	1.17	39	297.28	1	20.66	0.59	Changnon, et al 1979
16	1.06	19	111.70	2	18.28	1.05	Changnon, et al 1979
31	1.03	23	103.25	2	16.29	1.70	Changnon, et al 1979
33	1.06	26	112.45	2	16.17	1.76	Changnon, et al 1979
16	0.56	80	473.40	4	18.99	0.89	Changnon, et al 1979
32	1.06	31	134.85	2	16.29	1.70	Changnon, et al 1979
41	1.05	35	134.51	2	15.94	1.86	Changnon, et al 1979
15	1.13	47	285.80	2	17.97	1.13	Changnon, et al 1979
34	1.12	28	117.05	2	16.05	1.81	Changnon, et al 1979
32	1.28	29	126.09	2	15.99	1.84	Changnon, et al 1979
15	3.00	18	109.97	1	16.23	1.73	Changnon, et al 1979
35	1.03	71	298.12	3	16.49	1.62	Changnon, et al 1979
31	1.55	29	126.84	2	15.83	1.92	Changnon, et al 1979
35	1.14	49	205.85	2	16.05	1.81	Changnon, et al 1979
40	0.95	49	188.37	3	16.11	1.78	Changnon, et al 1979
29	1.07	28	128.85	3	16.42	1.65	Changnon, et al 1979
20	2.40	15	81.25	1	15.77	1.94	Changnon, et al 1979
18	0.83	23	127.97	1	18.39	1.03	Changnon, et al 1979
16	1.69	31	180.85	1	16.92	1.46	Changnon, et al 1979
15	0.53	34	204.83	2	19.12	0.86	Changnon, et al 1979
39	0.95	26	103.81	1	15.94	1.86	Changnon, et al 1979
32	1.03	24	105.08	2	16.29	1.70	Changnon, et al 1979
41	0.95	29	108.90	2	15.83	1.92	Changnon, et al 1979
28	0.79	30	140.45	2	16.92	1.46	Changnon, et al 1979
26	0.92	58	278.86	2	17.23	1.35	Changnon, et al 1979
24	1.08	36	181.09	2	17.07	1.40	Changnon, et al 1979
19	1.11	58	322.80	2	17.32	1.32	Changnon, et al 1979
30	0.87	36	161.54	2	16.92	1.46	Changnon, et al 1979
4	8.00	36	286.06	0	16.49	1.62	Changnon, et al 1979
33	0.67	58	248.17	3	17.23	1.35	Changnon, et al 1979
5	3.60	48	371.21	1	18.50	1.00	Changnon, et al 1979
28	0.86	48	224.72	3	17.23	1.35	Changnon, et al 1979
19	1.68	151	837.49	1	16.84	1.49	Changnon, et al 1979
22	1.41	36	189.66	2	16.56	1.59	Changnon, et al 1979
5	6.80	40	308.17	0	16.29	1.70	Changnon, et al 1979
38	1.00	35	138.87	2	16.05	1.81	Changnon, et al 1979
35	1.20	29	119.42	2	15.99	1.84	Changnon, et al 1979
7	3.43	62	459.16	1	18.07	1.11	Changnon, et al 1979
34	0.68	39	165.39	4	17.07	1.40	Changnon, et al 1979
31	1.35	42	186.92	2	15.94	1.86	Changnon, et al 1979
37	1.05	40	162.01	3	15.94	1.86	Changnon, et al 1979

33	1.03	106	454.98	3	16.23	1.73	Changnon, et al 1979
2	15.50	63	535.78	0	16.49	1.62	Changnon, et al 1979
37	1.00	45	182.26	3	16.11	1.78	Changnon, et al 1979
32	1.38	42	183.01	2	15.83	1.92	Changnon, et al 1979
44	0.89	40	146.63	3	15.88	1.89	Changnon, et al 1979
13	1.77	22	141.68	2	17.97	1.13	Changnon, et al 1979
11	1.36	30	198.81	3	18.74	0.95	Changnon, et al 1979
4	3.75	63	504.65	1	18.86	0.92	Changnon, et al 1979
3	11.33	50	412.22	0	16.99	1.43	Changnon, et al 1979
9	2.33	33	230.08	2	17.67	1.22	Changnon, et al 1979
6	1.83	60	453.86	3	19.39	0.81	Changnon, et al 1979
26	1.15	52	252.18	5	16.77	1.51	Changnon, et al 1979
31	1.35	56	248.78	4	16.05	1.81	Changnon, et al 1979
23	0.91	40	204.82	6	17.97	1.13	Changnon, et al 1979
9	3.33	40	278.44	2	16.92	1.46	Changnon, et al 1979
8	3.13	73	522.21	2	17.87	1.16	Changnon, et al 1979
6	5.33	25	189.94	1	17.07	1.40	Changnon, et al 1979
7	5.14	28	206.03	1	16.77	1.51	Changnon, et al 1979
14	0.57	50	308.90	10	19.39	0.81	Changnon, et al 1979
5	5.40	37	287.63	1	17.23	1.35	Changnon, et al 1979
3	7.67	57	470.19	1	17.67	1.22	Changnon, et al 1979
6	5.00	43	324.74	1	17.32	1.32	Changnon, et al 1979
7	2.14	35	257.54	3	18.74	0.95	Changnon, et al 1979
6	5.33	37	282.22	1	17.15	1.38	Changnon, et al 1979
8	3.63	39	280.80	2	16.70	1.54	Changnon, et al 1979
	0.5			1			Skempton & Northey, 1953
	0.5			1			Bejerrum & Simon, 1960
	0.6			2			Skempton & Northey, 1953
	0.5			2			Skempton & Northey, 1953
	0.75			1			Bejerrum & Simon, 1960
	0.55			2			Skempton & Northey, 1953
	0.5			3			Bejerrum, 1954
	0.58			2			Bejerrum, 1954
	0.8			2			Bejerrum & Simon, 1960
	0.9			2			Skempton & Northey, 1953
	0.4			4			Bejerrum & Simon, 1960
	0.45			4			Bejerrum & Simon, 1960
	0.5			3			Bejerrum & Simon, 1960
	0.7			2			Bejerrum, 1954
	0.8			2			Skempton & Northey, 1953
	1.3			1			Bejerrum & Simon, 1960
	0.85			2			Skempton & Northey, 1953
	0.6			3			Skempton & Northey, 1953
	0.75			3			Bejerrum & Simon, 1960

	1.2			2			Bejerrum, 1967
	0.85			2			Bejerrum, 1954
	0.9			2			Bejerrum, 1954
	0.8			3			Bejerrum & Simon, 1960
	0.87			2			Bejerrum, 1954
	0.9			2			Skempton & Northey, 1953
	0.8			3			Bejerrum & Simon, 1960
	1			2			Bejerrum & Simon, 1960
	1.4			2			Bejerrum & Simon, 1960
	3.6			1			Bejerrum & Simon, 1960
	1.5			2			Bejerrum & Simon, 1960
	1.2			2			Skempton & Northey, 1953
	2.3			1			Bejerrum, 1954
	1.4			3			Bejerrum & Simon, 1960
	1.75			2			Bejerrum, 1954
	1.4			3			Bejerrum & Simon, 1960
	1.45			3			Bejerrum & Simon, 1960
	1.68			2			Bejerrum, 1954
	1.5			3			Bejerrum & Simon, 1960
	1.6			3			Bejerrum & Simon, 1960
	2.4			2			Bejerrum, 1954
	1.55			3			Bejerrum & Simon, 1960
	2.4			2			Bejerrum, 1954
	1.8			3			Skempton & Northey, 1953
	2			3			Bejerrum, 1954
	2.3			2			Bejerrum, 1954
	1.9			3			Bejerrum, 1967
	2.8			2			Bejerrum, 1967
	2.5			2			Bejerrum, 1967
	2.7			2			Bejerrum, 1967
	2.95			2			Bejerrum, 1967
	3.3			2			Bejerrum, 1967

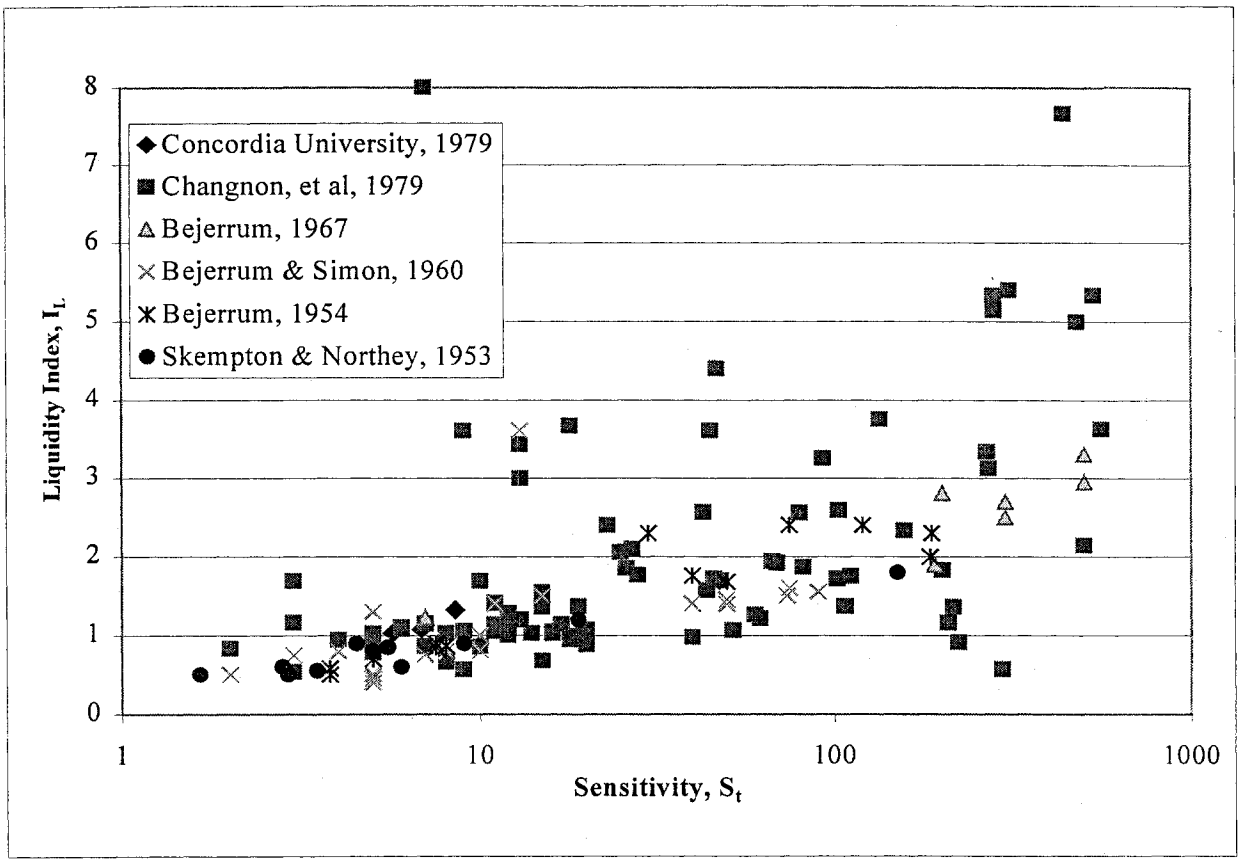

Figure 4.16 Test Data for Establishing the Importance of Liquidity Index for Sensitive Clays

Figure 4.16 shows the data used for establishing the importance of liquidity index in case of sensitive clays. The data shown in Table 4.2 is analysed to single out a primary controlling parameter for deciding the shear strength. As a first attempt constant of variation in sensitivity, k introduced by Bjerrum, (1954) is taken as a primary controlling factor for deciding the shear strength. Based on this, a graph is plotted by sorting the Table 4.2 for k values of 1, 2, 3 and 4. In a few cases the values for k exceeded more than 4 and can be ignored for the sake of simplifying the analysis. Figure 4.17 shows the relationship between sensitivity and the liquidity index. The thin lines on graph indicate the lines joining data points for k=1,2,3 & 4. The thick lines show the best-fit line for

each value of k. The best-fit curves establish a log linear relationship between sensitivity and liquidity index as follows;

$I_L = x\ln(S_t) + y$.....4.4

Where x and y are the constant and can be easily determined by using regression analysis. Although the trend of Figure 4.17 resembles the Wood, (1990) study, but there is a clear difference in the two graphs. Wood, 1990 analysis shown in Figure 2.12 indicates an on going increasing trend of liquidity index with the sensitivity. Whereas Figure 4.17 shows that there is a threshold value for liquidity index after which the liquidity index becomes constant or meaningless with respect to the increase in sensitivity. Furthermore, the analysis done by Wood, (1990) is based on 52 test results whereas the present study analysis shown in Figure 4.17 is based on 142 test results.

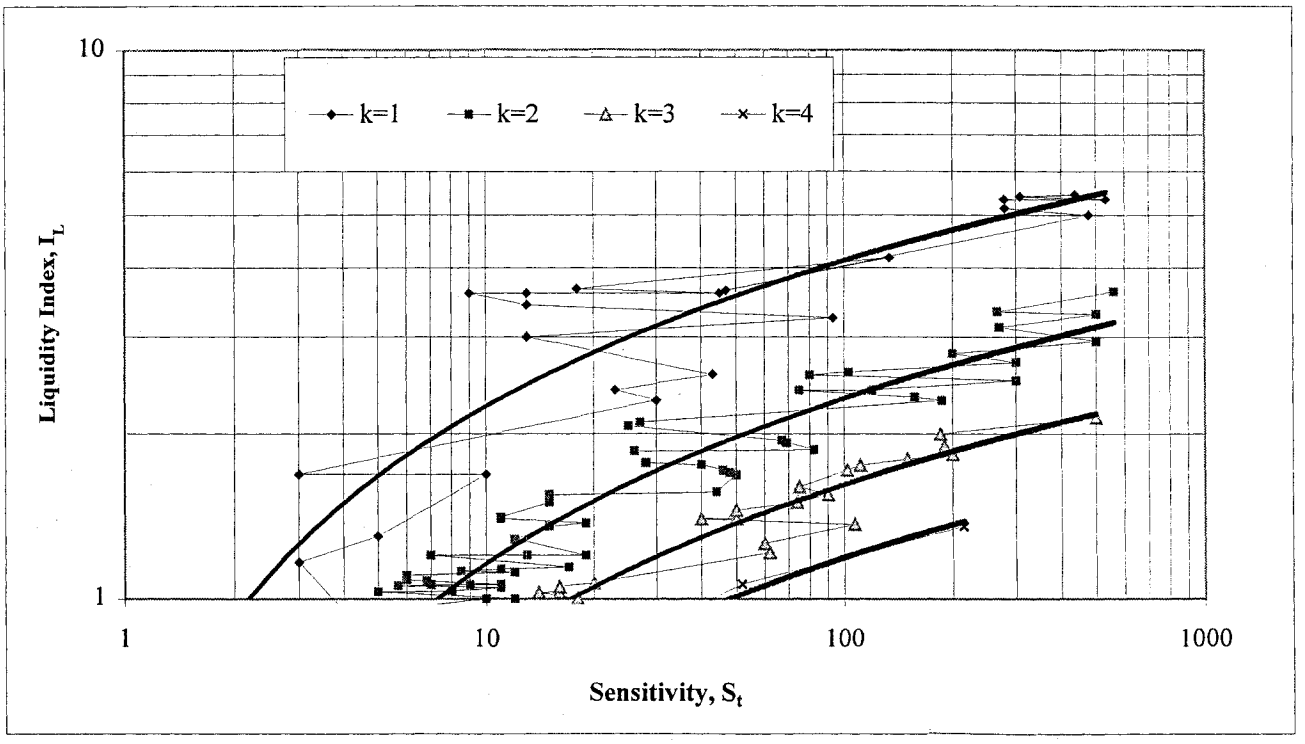

Figure 4.17 Effect of Liquidity Index

After a critical review of figure 4.17 it is clear that the data points for k values equal to 2 or higher, mostly lie on the best fit curve given by equation 4.4. This indicates that equation 4.4 holds good for highly sensitive clays. It is also to be noted that for a sensitive clay there must be secondary controller to control the variation of sensitivity specially when the soil sample are taken from different depths and showing same sensitivity values. This problem can be solved by introducing a preconsolidation (σ_p) pressure as secondary controller. Test data of Table 4.2 is reanalyzed by dividing the whole data into different preconsolidation ranges, keeping in view to have reasonable data points to set the relationship between undrained shear strength and the liquidity index with respect to constant of variation in sensitivity (k). For this the whole data is divided into five preconsolidation ranges; 0-100 kPa, 100-150 kPa, 150-200 kPa, 200-250 kPa and 250-300 kPa. Figure 4.18 and 4.19 gives the results of this analysis. The primary controller 'k' is kept constant and hence showing the decrease in shear strength with increase an increase in liquidity index by varying the secondary controller 'σ_p'. The results of the analysis shown in Figure 4.17 are reanalyzed by narrowing down the range of secondary controller (σ_p) between 250-300 kPa. Figure 4.20 shows the best possible results which are very close to field value plus they indicate a realistic explanation of threshold value of liquidity index after that it does not changes with sensitivity. The results of this analysis further indicate the sensitive importance of preconsolidation pressure in predicting the behavior of sensitive clays. The range of preconsoliadtion 250 to 300 kPa is still very wide, the results would be more realistic if this range could be narrow down further.

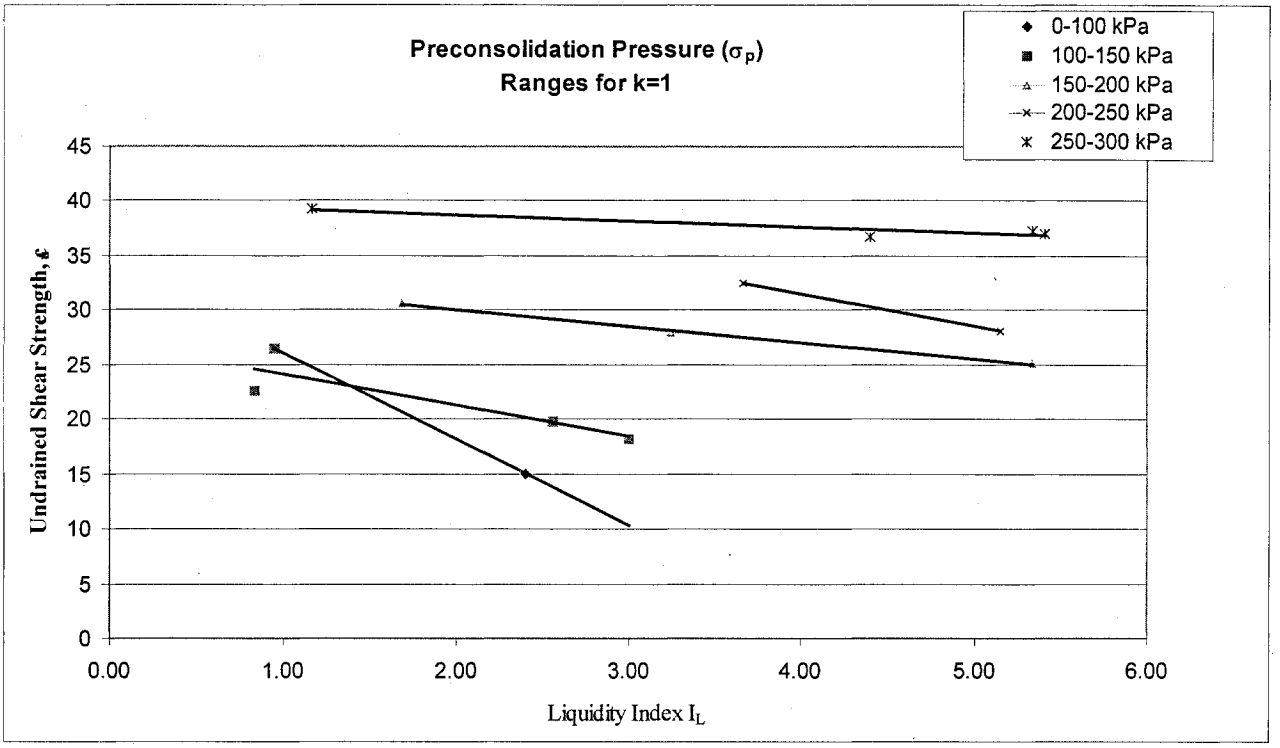

Figure 4.18 k=1 as a Primary Controller to Predict the Shear Strength and σ_p as Secondary Controller

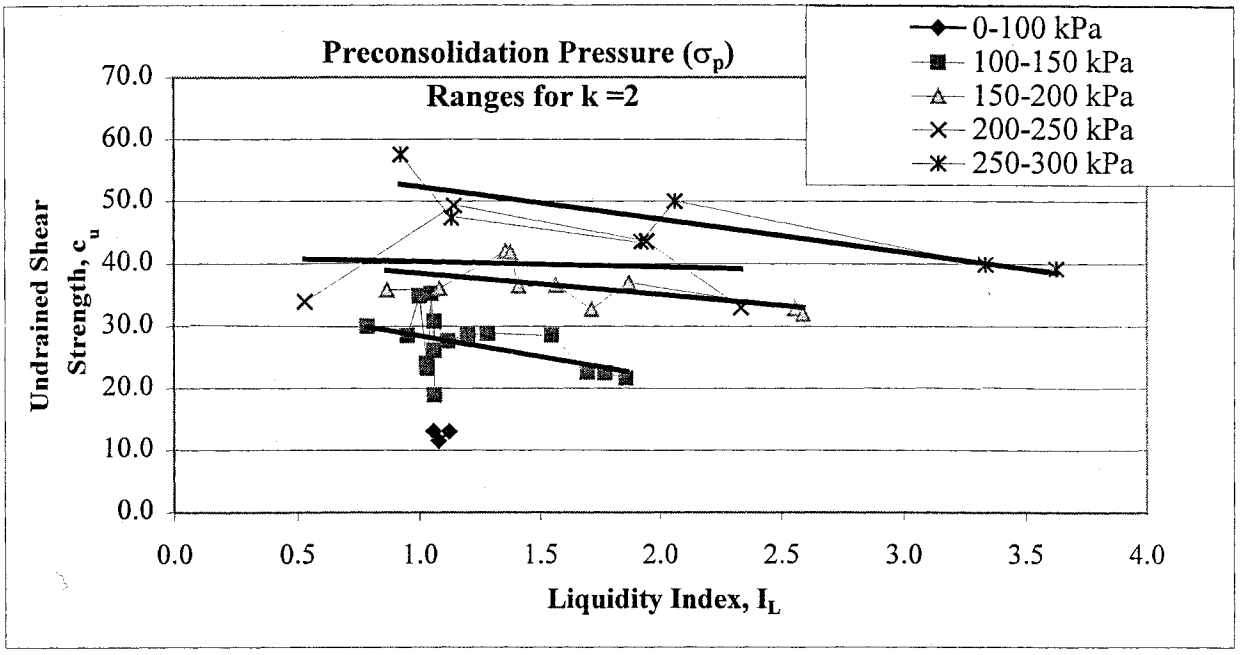

Figure 4.19: k=2 as a Primary Controller to Predict the Shear Strength and σ_p as Secondary Controller

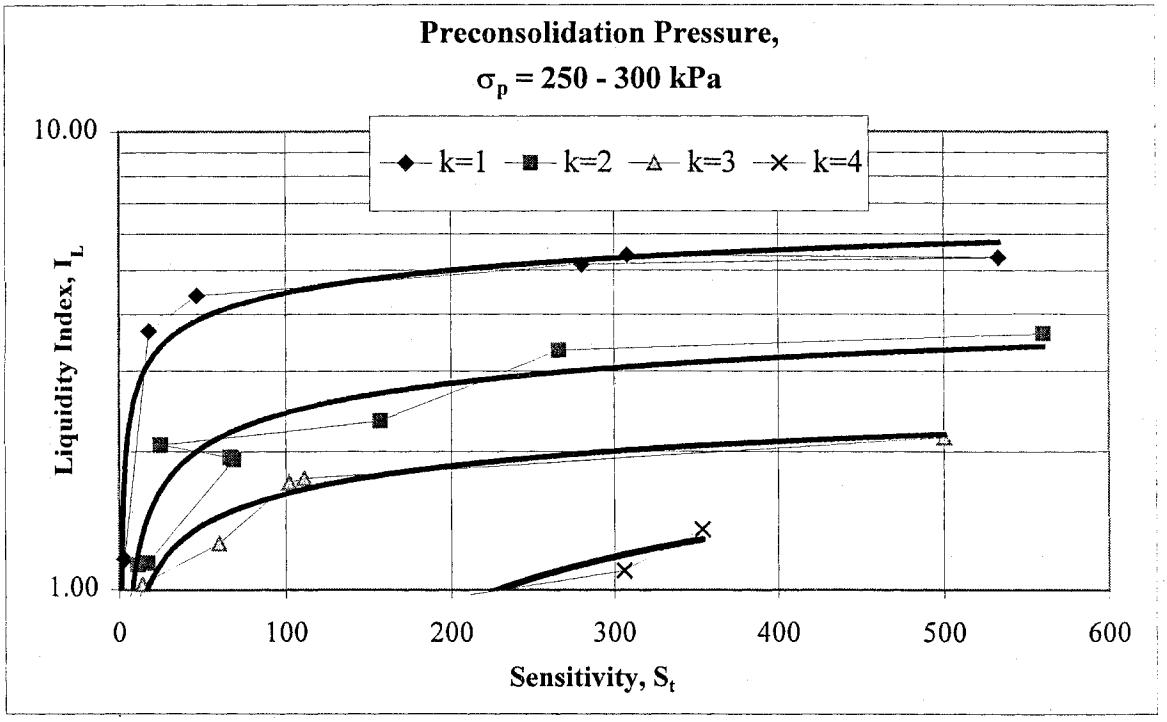

Figure 4.20: Sensitivity versus Liquidity index for σ_p range of 250 – 300 kpa

4.4 Design Procedure for Estimating Cyclic Shear Strength for the Sensitive Clay

Based on the parametric study, a simplified design procedure can be proposed which will help the engineers deal with the shearing strength of sensitive clays (see Figure 4.21). The following steps are involved in this design procedure:

1. Gather all the possible input data, such as index properties, preconsolidation pressure, possible number of cycles and duration of undrain period.
2. Assuming preconsolidation pressure as a secondary controller determine the value of constant of varition for sensitivity, k.
3. Estimate the corresponding values of liquidity index and sensitivity and crosscheck with any available data.
4. Estimate the value of shearing strength (c_u) by using index properties relationships
5. Cross check the values of c_u by using the modified cam clay model
6. Select the lowest value of (c_u) from the above two methods.
7. Take maximum shear stress equal to c_u.
8. Calculate the static deviator stress (q_s) as:

   $q_s = 2\tau_f$

9. Take cyclic deviator stress (q_{cyc}) equal to $1/3^{rd}$ of the static deviator stress (q_s).
10. Estimate the length of undrained period and possible number of cycles and based on that assume the safety factor.
11. Calculate cyclic shear stress and number of cycles by using equation 2.32 of Hyodo et al (1993) and cross check with the estimated values, select a maximum for the number of cycles and a minimum for cyclic deviator stress or cyclic shear stress.

12. Use strain data from the triaxial tests to evaluate the peak effective stress ratio (η_p) as: $\eta_p = 2\varepsilon_p / (1+\varepsilon_p)$ used by Hyodo et al, (1993).
13. Calculate final effective stress ratio by using η_f = static deviator stress (q_s) / mean effective confining stress (p_c).
14. Calculate the initial effective stress ratio (η_s) by taking ratio: initial consolidation pressure to the initial effective stress.
15. Calculate the factor of safety (T_f / T). If it is less than the required factor of safety, do a back calculation and determine the value of the shear strength.
16. Calculate the peak effective stress (η_p) based on this factor of safety and compare it with the one evaluated by using the axial strain.
17. Calculate the new values of the strain based on the revised peak effective stress.

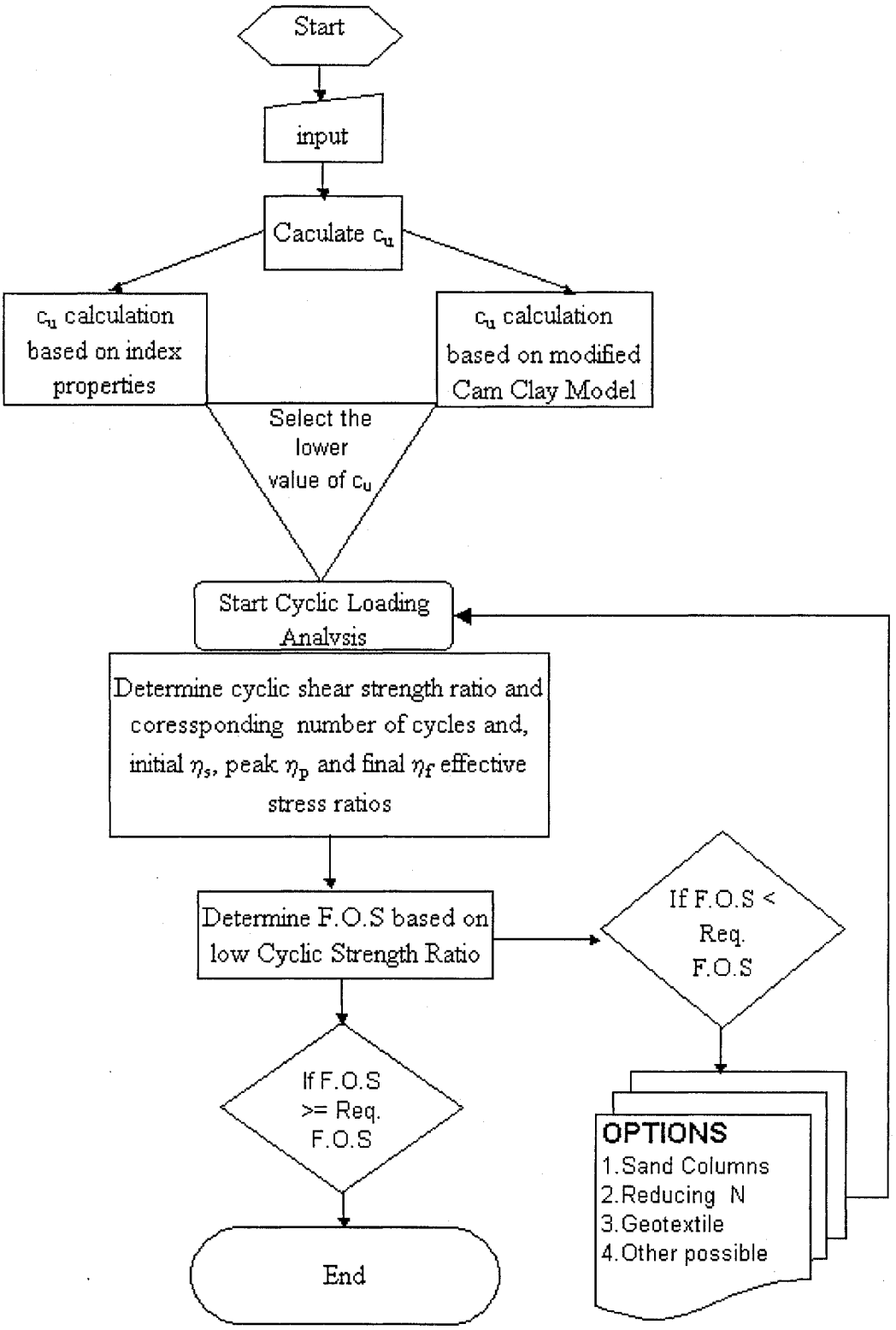

Figure 4.21: Flow Chart Diagram Showing Design Procedure For Estimating The Cyclic Loading Behavior of Sensitive Clay

4.5 Design Procedure's Application

Table 4.3 shows the result of undrained strength of Champlain Clay based on its index properties. The predicted values for undrained shear strength (c_u) seems to be a little higher than the experimental values.

Table 4.3 Experimental and Predicted Values for Undrained shear strength Based on equation 2.30

Experimental			Predicted Values				
c_u	S_t	I_L	c_L	R	S_t	c_u	k
kPa			kPa			kPa	
41.38	8.50	1.12	7.24	27.62	8.88	43.45	1.95
44.14	6.82	1.08	8.28	24.17	7.00	44.83	1.80
46.21	5.67	1.06	8.97	22.31	6.40	46.21	1.75
43.91	7.00	1.09	8.16	24.70	7.43	44.83	1.83

Such a difference is negligible, specially when the predicted values are solely based on the liquidity index. As well, the values of k and c_L are to be noted. The value c_L = 2 kPa corresponding to c_P = 200 kPa proposed by Wood (1990) are not suitable in case of sensitive clays. Anyhow, the values for k can be considered appropriate especially when the experimental values of S_t and c_u are very near to the predicted values. Figure 4.27 shows the comparison between observed and predicted behavior of Champlain clay under static triaxial compression. The value of M is obtained from experimental data (87.66/109.66 = 0.8). The value of attraction factor 'a' is assumed to be zero. A plot between $log\ q$ versus $log\ p_c$ at a fixed p_o =207 kPa gives $\Lambda = 0.9$ from equation 2.9. Using the value of Λ and M and adopting the value of $\lambda = 0.3$, derived from virgin compression curves (Bjerrum, 1967), one obtains the Stable-State Boundary Surface (SSBS) as shown in Figure 4.22. It is seen that the predicted strength is greater than that of the

experimental values. Furthermore, the experimental stress path do not follow the SSBS. The value of maximum shear strength (τ_f) also matches with the experimental values.

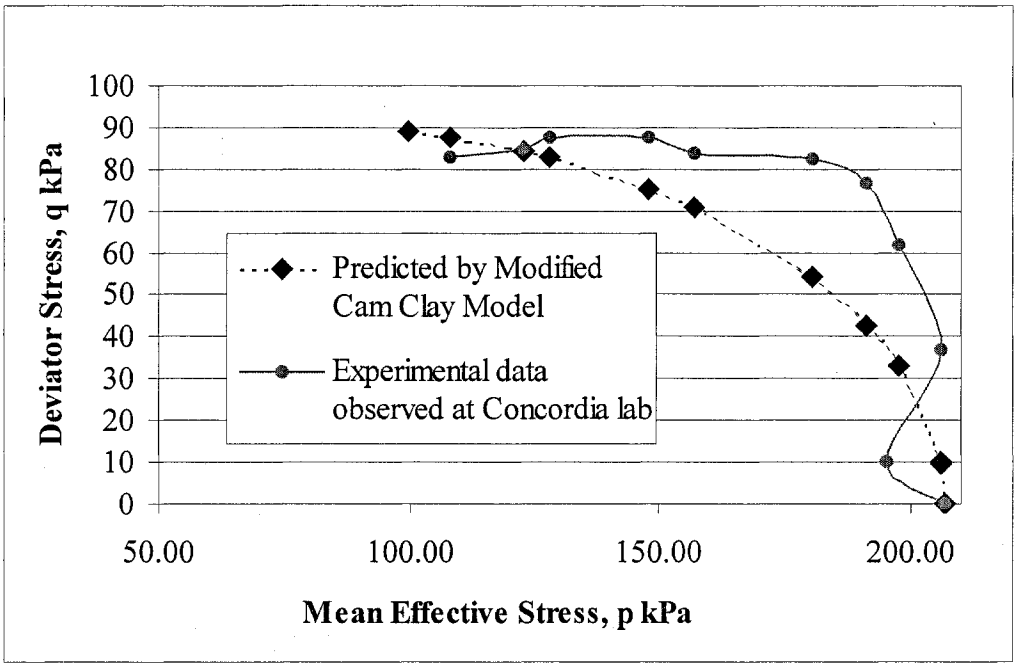

Figure 4.22: Predicted and Observed Behavior under Static Triaxial Compression (Using Modified Cam Clay Model)

The values of maximum static deviator strength are also approximately the same, but a little higher than those predicted. One possible reason may be that the value of attraction factor 'a' is taken as zero, which can be estimated by a trial-error method to bring the predicted values closer to the observed values. Table 4.4 shows the results of the Modified Cam Clay Model. Overall results for the static compression triaxial test on Champlain clay match those predicted by the Modified Cam Clay Model used by Ekelen and Pott (1979) for Drammen Clay. The model gives good results for over consolidation ratio (OCR) value of one, which is the case of the Champlain clay in the present study. By comparing the results of equation 2.30 (Wood, 1990) and the static strength (T_f) given by the Cam Clay Model, the values of the undrained shear strength are found to be lower

than those predicted by the Cam Clay Model. Hence, for the design purpose, it is always recommended to take the minimum predicted strength.

Table 4.4 Results of Modified Cam Clay Model with Attraction Parameter 'a' =0

input	input	input	input	input			input															
M	L	a	l	k	η	OCR	u	ul	po	pc	p	p/pc	pu	d	q	S	α	τ	sinϕ	b	lode	$T_f=q_f$
		kPa							kPa	kPa	kPa		kPa		kPa			kPa			angle	kPa
0.8	0.9	0.0	0.3	0.03	0.0	1.0	2.9	4.3	207.0	207.0	206.9	1.0	207.0	0.5	3.4	0.0	0.005		0.4	0.5	-30.0	
0.8	0.9	0.0	0.3	0.03	0.2	1.0	2.9	4.3	207.0	207.0	195.2	0.9	207.0	0.5	36.0	0.2	0.005		0.4	0.5	-30.0	
0.8	0.9	0.0	0.3	0.03	0.1	1.0	2.9	4.3	207.0	207.0	206.1	1.0	207.0	0.5	10.4	0.1	0.005		0.4	0.5	-30.0	
0.8	0.9	0.0	0.3	0.03	0.2	1.0	2.9	4.3	207.0	207.0	197.7	1.0	207.0	0.5	32.2	0.2	0.005		0.4	0.5	-30.0	
0.8	0.9	0.0	0.3	0.03	0.2	1.0	2.9	4.3	207.0	207.0	191.3	0.9	207.0	0.5	41.2	0.3	0.005		0.4	0.5	-30.0	
0.8	0.9	0.0	0.3	0.03	0.3	1.0	2.9	4.3	207.0	207.0	180.4	0.9	207.0	0.5	52.1	0.4	0.005		0.4	0.5	-30.0	
0.8	0.9	0.0	0.3	0.03	0.4	1.0	2.9	4.3	207.0	207.0	157.0	0.8	207.0	0.5	66.9	0.5	0.005		0.4	0.5	-30.0	
0.8	0.9	0.0	0.3	0.03	0.5	1.0	2.9	4.2	207.0	207.0	148.0	0.7	207.0	0.5	70.8	0.6	0.005		0.4	0.5	-30.0	
0.8	0.9	0.0	0.3	0.03	0.6	1.0	2.9	4.2	207.0	207.0	128.0	0.6	207.0	0.5	76.5	0.7	0.005		0.4	0.5	-30.0	
0.8	0.9	0.0	0.3	0.03	0.6	1.0	2.9	4.2	207.0	207.0	123.1	0.6	207.0	0.5	77.5	0.8	0.005		0.4	0.5	-30.0	
0.8	0.9	0.0	0.3	0.03	0.7	1.0	2.9	4.2	207.0	207.0	108.3	0.5	207.0	0.5	79.2	0.9	0.005		0.4	0.5	-30.0	
0.8	*0.9*	*0.0*	*0.3*	*0.03*	*0.7*	*1.0*	*2.9*	*4.2*	*207.0*	*207.0*	108.3	*0.5*	*207.0*	*0.5*	*79.2*	*0.9*	*0.005*	*49.3*	*0.4*	*0.5*	*-30.0*	*98.6*

Figure 4.23 shows the observed and predicted variations in peak axial strain with respect to the number of the cyclic loading. The loading follows the same initial pattern as in the case of static loading. The results show that the predicted values are fairly close to the observed values. The graph below is shown for the undrained test UT-01. The same pattern is observed for tests UT-02, UT-03, DT-04 and DT-05. Figure 4.24 shows the relationship between the number of cycles (N) and maximum cyclic stress ratio $(T_{fc})_N$. Different values of initial static deviator stress (q_s): 0, 62.07 124.14, 186.21 and 248.28 are assigned to check the model. Results show parallel straight lines for each initial static deviator stress as shown in the Figure 4.24.

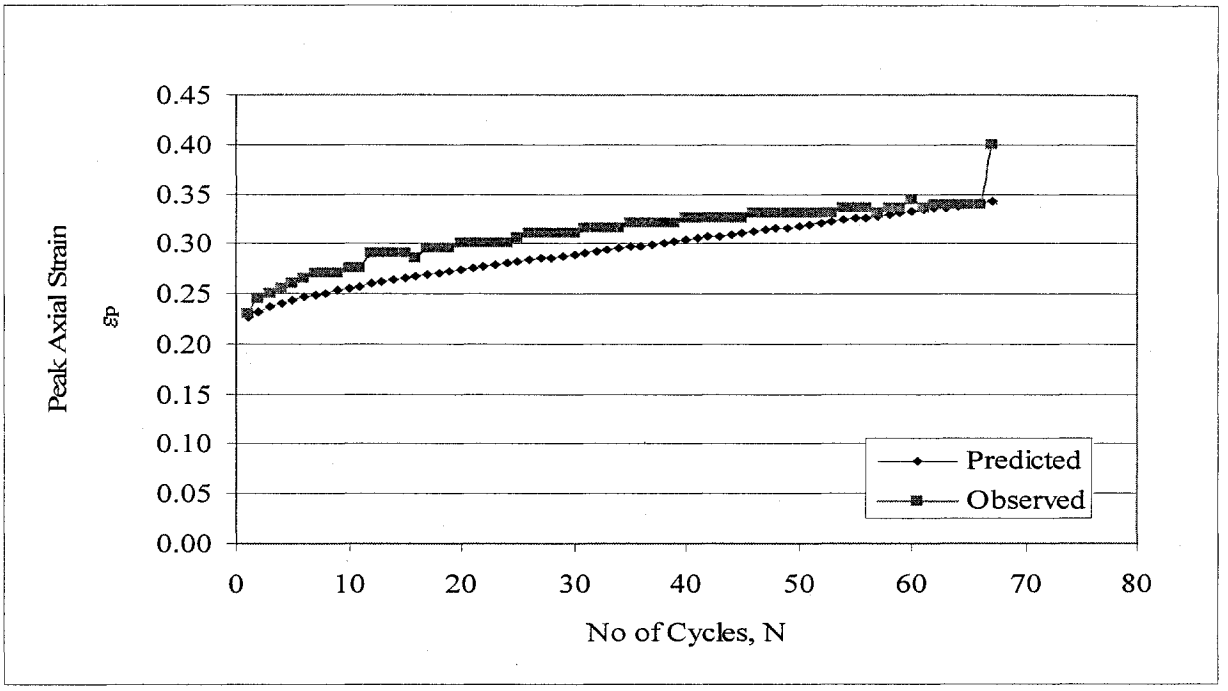

Figure 4.23: Number of Cycles (N) Versus Peak Axial Strain (ε_p) for Undrained Test (UT-01)

It is also clear that the maximum cyclic stress ratio increases with the increase in the value of initial static deviator stress. On the other hand, the number of cycles to failure is reduced. Figure 4.25 shows a relationship between peak effective stress ratio and peak axial strain. The observed value is a little bit higher than the predicted value. The graph for the predicted value is then extended with help of the trend line (a third degree polynomial equation) to predict the behavior of Champlain clay at a low level of effective stresses. The graphical trend agrees with the theoretical explanation of maximum axial strain corresponding to the peak cyclic stress on the compression side in each cyclic loading. Hence, it is clear that there exists a unique relationship between the peak axial strain and the effective stress ratio; the third degree polynomial equation can be written as:

$$\varepsilon_p = 0.3128\,\eta_p^3 + 0.1131\,\eta_p^2 + 0.5406\,\eta_p - 0.0044 \quad \ldots\ldots 4.8$$

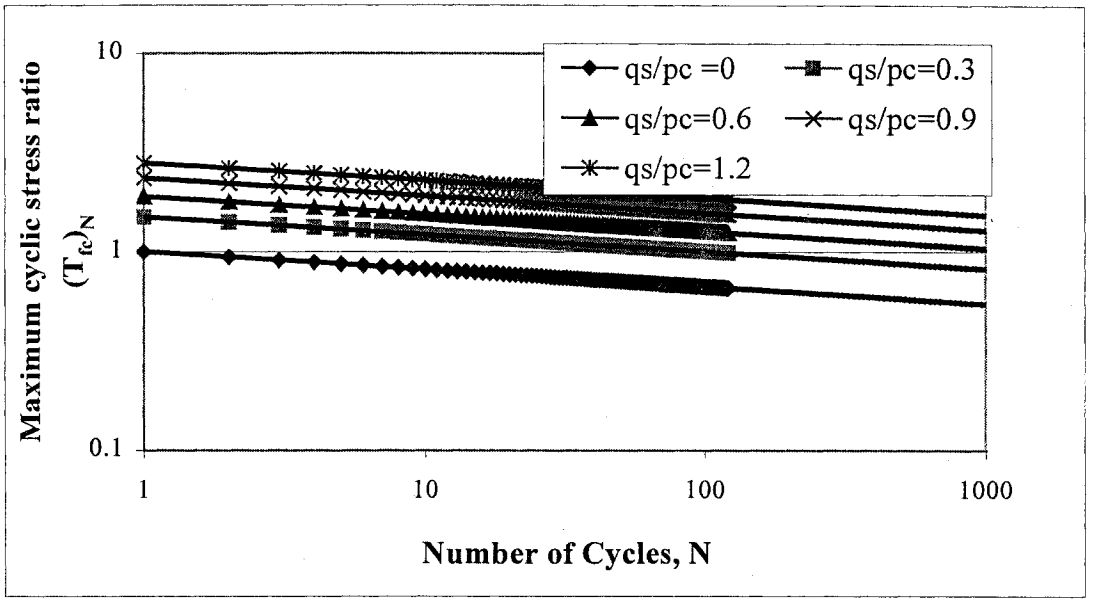

Figure 4.24 Number of Cycles (N) Versus Maximum Cyclic stress Ratio $(T_{fc}/p_c)_N$

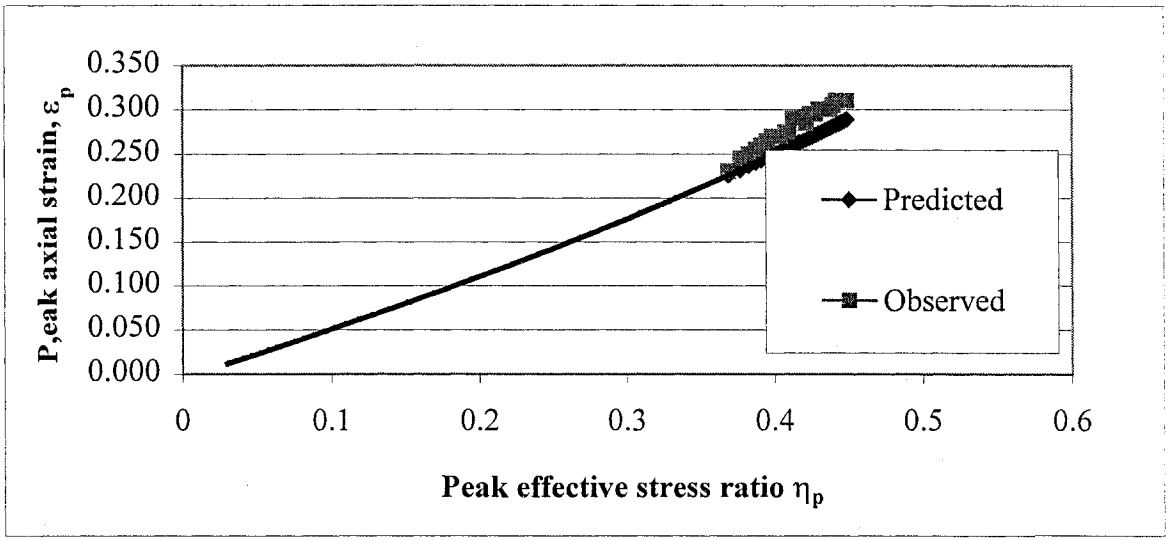

Figure: 4.25 Peak Axial Strain (ε_p) Versus Peak Effective Stress (η_p)

Figure 4.26 gives a relationship between the factor of safety (F) and the cyclic strength ratio (T_{fc}/p_c). Again different values of the initial static deviator stress are assigned to

predict the behavior of Champlain clay. The figure clearly indicates that with the increase of maximum cyclic strength a more reliable F value can be obtained. The graph gives a very useful relationship, which can easily be applied as a thumb rule on construction sites.

Figure 4.27 shows that there is a rapid increase in cyclic strength ratio with the number of cycles; and then at a later stage, the relative effective stress increases rapidly to reach the failure point, which is a typical clay behavior when it is subjected to cyclic loading (see Chapter-2 literature review, and Chapter-3 experimental investigations).

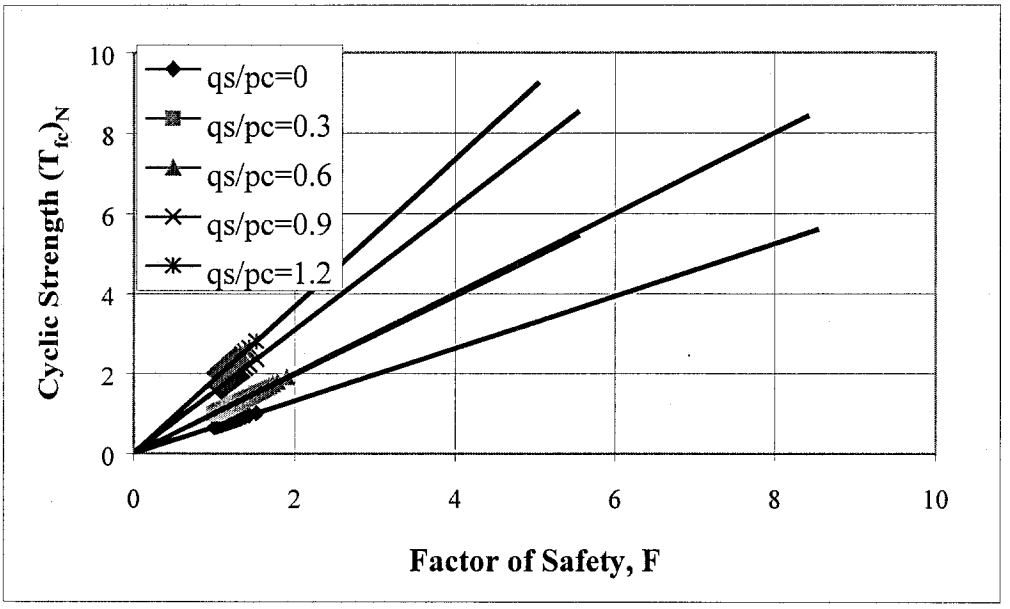

Figure 4.26: Factor of Safety (F) Versus Cyclic Strength Ratio $(T_{fc})_N$

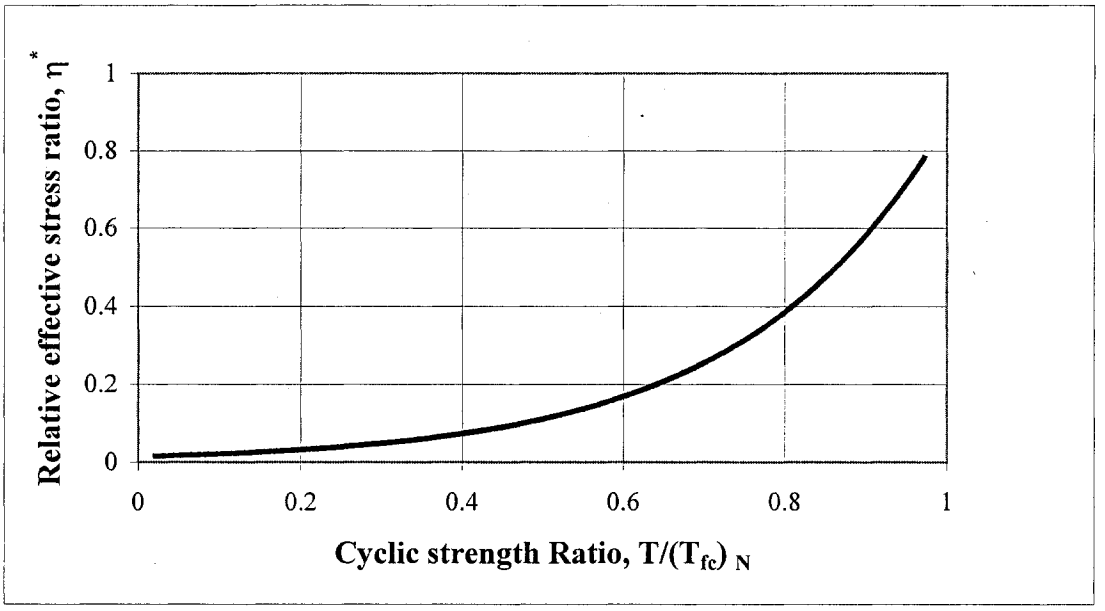

Figure 4.27 : Cyclic Strength Ratio ($T/(T_{fc})_N$) Versus Relative Effective Stress Ratio (η^*)

Figure 4.28 also reveals the behavior of Champlain clay with respect to an increase in number of cyclic loading. It is clear that for any soil the value of F will decrease with an increase in the number of cyclic loading. Figure 4.28 summarizes the overall behavior of clay for both undrained and drained conditions. The model confirms the test results that the behavior of clay is more critical under undrained condition as compared to the drained condition. Drained tests DT-04 and DT-05 show a high factor of safety corresponding to number of cycles for which undrained tests UT-01, UT-02 and UT-03 show a lower factor of safety

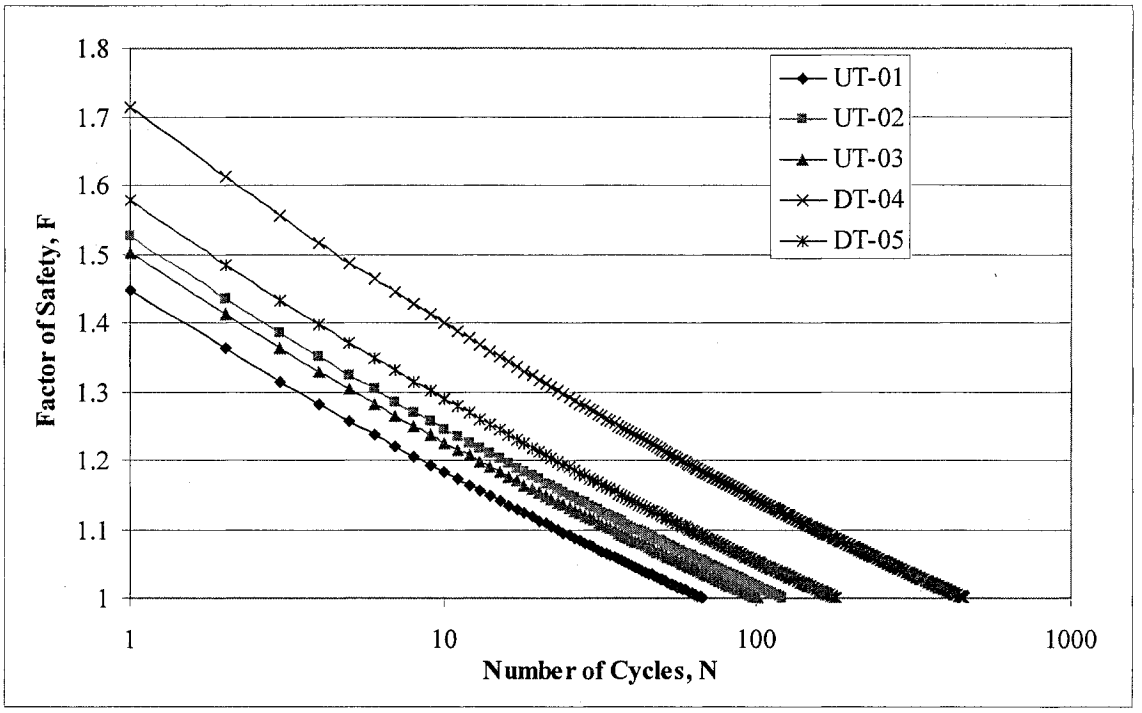

Figure 4.28: Number of Cycles (*N*) Versus Factor of Safety (*F*)

CHAPTER 5

CONCLUSIONS AND RECOMMENDATIONS

Based on the experimental and theoretical investigation performed on the shear strength of sensitive clay, the following can be concluded.

1. The level of sensitivity is defined as the ratio of the undisturbed shear strength (c_u) to the remolded shear strength (c_{ur}). The higher this value the faster the clay looses its shear strength under cyclic of loading.
2. Sensitive clay under cyclic loading is particularly critical for this clay under undrained conditions. This further, may lead to quick clay condition and catastrophic failure.
3. Shear strength of a sensitive clay subjected to cyclic loading is directly related to; number of cycles (N), cyclic deviator stress (σ_1-σ_3), pore water pressure (u), axial strain (ε), preconsolidation (σ_p) and confining pressure (σ_c).
4. Shear strength of a sensitive clay is indirectly related to; natural water content (w), liquid limit (LL), plastic limit (PL), plasticity index (I_P), liquidity index (I_L), sensitivity (S_t), constant of variation in sensitivity (k) and initial degree of saturation (S)

5. Shear strength of sensitive clay decreases due to;

    a) Increase in number of cyclic loading (N).

    b) Increase in cyclic deviator stress (σ_1-σ_3).

    c) Increase in pore water pressure (u).

    d) Increase in axial strain (ε).

    e) Reduction in preconsolidation pressure (σ_p).

    f) Reduction in confining stress (σ_3).

    g) Increase in natural water content (w).

    h) Increase in liquid limit (LL).

    i) Decrease in plastic limit (PL).

    j) Decrease in plasticity index (I_P).

    k) Increase in initial degree of saturation (S).

6. Sand columns, geo-textiles and sheet piles can be recommended to speed up the consolidation process and accordingly reduce the undrained period.
7. The liquidity index reflects the combined effect of water content (w), liquid limit (LL), plastic limit (PL), plasticity index (I_P), sensitivity (S_t), constant of variation in sensitivity (k) and initial degree of saturation (S)
8. The variation in sensitivity due to the increase in liquidity index can be expressed by the constant of variation in sensitivity, k.
9. A value of 2 for the constant of variation in sensitivity (k) obeys the relationship given by Bejerrum (1954) for clays of medium to high sensitivity. For sensitive

clays with low liquidity index the values of k = 3 or 4 governs the relationship between the sensitivity (S_t) and the liquidity index (I_L).

10. Based on the results of this study, it is concluded, that by fixing the range of preconsolidation pressure, a realistic relationship among the shear strength, sensitivity and liquidity index can be established.
11. The Modified Cam Clay Model cannot take into account the behavior of sensitive clay subjected to variations during cyclic of loading in; number of cycles, level of cyclic deviator stress, axial strain and pore water pressure, and therefore is not capable of estimating cyclic shear strength during the cyclic loading process. However, it can be used to determine the cyclic strength at the end of the cyclic loading by taking into account initial and final values of above mentioned parameters.
12. In the case of sands, drainage is likely to occur during the design storm; so it is necessary to analyze pore pressure behavior more critically in order to have feasible values for cyclic shear strength. Since proper drainage does not take place in clays, it is therefore, preferable to use the shear strain to determine the cyclic shear strength for clays. Specifically for situations where the cyclic shear strength and the cyclic shear moduli under undrained conditions are of primary interest, the shear strain plays a role of more direct parameter than the pore water pressure.
13. For sensitive clay the relationship between peak axial strain and the peak effective stress ratio for each individual cycle can be expressed in the form of a third degree polynomial equation (equation 4.4).

Recommendations for Future Work

1. Additional laboratory tests are needed to narrow the range of preconsolidation pressures for the clay samples of varying sensitivities. This can help in establishing a mathematical model for estimating the shear strength of sensitive clay subjected to cyclic loading.

REFERENCES

Ansal, M., and Erken, A., 1989. Undrained Behavior of Clay Under Cyclic Shear Stresses. Journal of Geotechnical Engineering, Vol. 115, No. 7, pp. 968-982.

Bjerrum, L., 1954. Geotechnical Properties of Norwegian Marine Clays. Geotechnique , Vol. 4, No. 2, pp. 49-69.

Bjerrum, L., 1967. Engineering Geology of Norwegian Normally Consolidated Marine Clays as Related to Settlements of Buildings. Geotechnique, Vol. 17, No. 2, pp. 81-118.

Bjerrum, L., and Simon, N.E., 1960. "omparison of Shear Strength Charactreistics of Normally Consolidated Clay" in Proc. Research Conf. On Shear Strength of Cohesive Soils, Boulder, Colorado. (Newyork: ASCE), pp. 711-26

Bardet, J.P., 1995, Scaled Memory for Cyclic Behavior of Soils. Journal of Geotechnical Engineering, Vol. 121, No. 11, pp. 766-774.

Chagnon, J.Y., Lebuis, J., Allard, J.D., and Robert, J.M., 1979. Sensitive Clays, Unstable Slopes, Corrective works and Slides in the Quebec and Shawinigan Area. Univrsite Laval, Quebec.

Eekelen, H.A.M., 1980. Fatigue Models for Cyclic Degradation of Soils. Proc., Int. Symp. On Soils under Cyclic and Transient Loading, Netherlands, pp. 447-450

Eekelen, H.A.M., and Potts, D.M., 1978. The behavior of Drammen Clay under cyclic loading. Geotechnique 28, No. 2, 173-196

Fakher, A., Jones, C.J.F.P., and Clarke, B.G., 1999. Yield Stress of Super Soft Clays. Journal of Geotechnical and Geoenvironmental Engineering, Vol. 125, No. 6. Pp. 499-509.

France, J. W., and Sangrey, D.A., 1977. Effects of Drainage in Repeated Loading of Clays. Journal of Geotechnical Engineering, Vol. 103, No. GT7, pp. 769-785.

Hanna, A., 1979. Triaxial Test on Champlain Clay (cyclic loading tests), Unpublished data, Concordia University, Montreal, Quebec.

Hermann, H.G., and Houstan, W.N., 1978. Behavior of Seafloor Soils Subjected to Cyclic Loading. Proccedings, 8th Offshore Technology Conference at Houstan, Tex., May 1978.

Houstan, W.N., and Herrmann, H.G., 1980. Undrained Cyclic Strength of Marine Soils. Journal of Geotechnical Engineering, Vol 106, No. GT6, pp. 691-711.

Hyodo, M., Yamamoto, Y., and Sugiyama, M., 1993. Undrained cyclic shear behavior of clay with initial static shear stress. Department of Civil Engineering, Yamaguchi University. Soil Dynamics and Earthquake Engineering.

Lebuis, J., Robert, J.-M., and Rissmann, P., 1983. Regional mapping of landslide hazard in Québec. In: Proceedings of the International Symposium on slopes on soft clays, Linkoping, Swedish Geotechnical Institute Report, No. 17: 205-262.

Lefebvre, G., and LeBoeuf, D., 1987. Rate Effects and Cyclic Loading of Sensitive Clays. Journal of Geotechnical Engineering, Vol. 113, No. 5, pp. 476-489

Lefebvre, G., and Pfendler, P., 1996. Strain Rate and Preshear Effects in Cyclic Resistance of Soft Clay. Journal of Geotechnical Engineering, Vol. 122, No. 1, pp. 21-26.

Locat, J. 1995. On the development of microstructure in collapsible soils: lessons from the study of recent sediments and artificial cementation. In: E. Derbyshire et al. 9eds, Genesis and Properties of Collapsible Soils, Kluwer Academic Publisher, 93-128.

Locat, J., 1997. Normalized rheological behaviour of fine muds and their flow properties in a pseudoplactic regime. In: Proceedings the ASCE Conference on Debris-Flows Hazards Mitigation: Mechanics, Prediction, and Assessment, San Francisco, pp.: 260-269.

Leroueil, S. and Locat, J., 1998. Geotechnical characterization, risk assessment and mitigation. Proceedings of the XI Danube

Liang, R.Y., and Ma, F., 1992. Anisotropic plasticity Model for Undrained Cyclic Behavior of Clays. Journal of Geotechnical Engineering, Vol. 118, No. 2, pp. 229-243McManus, K.J., and Kulhaway, F.H., 1994. Cyclic Axial Loading of Drilled Shaft. Journal of Geotechnical Engineering, Vol. 120, pp. 1481-1497.

Miller. G.A., The, S.Y., Li, D., and Zaman, M.M., 2000 Cyclic Shear Strength of Soft Railroad Subgrade. Journal of Geotechnical and Geoenvironmental Engineering, Vol. 126. No. 2, pp. 139-147.

Procter, D.C., and Khaffaf, J.H., 1984. Weakening of Undrained Saturated Clays Under Cyclic Loading. Journal of Geotechnical Engineering, Vol. 110, No. 10, pp. 1431-1445.

Puzrin, Alexander, Frydman, S., and Talesnick, M., 1995. Normalized Nondegrading Behavior of soft Clay Under Cyclic Simple Shear Loading. Journal of Geotechnical Engineering, Vol. 121, No. 12, pp. 836-843.

Quigley, R.M., 1980. Geology, Mineralogy and geochemistry of Canadian soft soils: a geotechnical perspective. Canadian Geotechnical Journal, 17: 261-285.

Reilly, M.P.O., and Brown, S.F., 1991. Cyclic Loading of Soils. Department of Civil Engineering University of Nottingham, ISBN: 0-442-30410-2.

Sangrey, D. A., Henckel, D.J., and Esring, M.L., 1969. The Effective Stress Response of a Saturated Clay Soil to Repeated Loading. Canadian Geotechnical Engineering, Vol. 6, No. 3, pp. 241-252

Seed, H. B., and Chan, C.K., 1966. Clay Strength under Earthquake Loading Conditions. Journal of Soil Mechanics and Foundation Division, ASCE, Vol. 92, No. SM2, pp. 53-78

Skempton, A.W., and Northey, R.D., 1953. The Sensitivity of Clays. Geotechnique, Vol. 3 No. 1, pp. 30-53.

Thiers, G.R., and Seed, H.B., 1968. Strength and stress-strain characteristics of clays subjected to seismic loading conditions. ASTM Special Technical Publication 450, Vibration Effects of Earthquakes on Soils and Foundations: A symposium, American Society for Testing and Materials, San Francisco, Calif., pp. 3-56.

Wathugala, G.W., and Desai, C.S., 1993. Constitutive Model for Cyclic Behavior of Clays. Journal of Geotechnical Engineering, Vol. 119, pp. 714-747.

Wood, D.M., 1990. Soil Behavior and Critical State Soil Mechanics Cambridge University Press.